
Scrambling of Speech Signals

Signals and Systems

P4 Report
MatTek4 5.239

Aalborg University
Mathematics-Technology

Copyright © Aalborg University 2022

This report is written in the typesetting language \LaTeX using text editor Overleaf. Experiments and data processing are conducted using Python 3.8. Illustrations are created using the TikZ package in \LaTeX or Python 3.8 References are cited using the Vancouver method.



AALBORG UNIVERSITY

STUDENT REPORT

Department of Mathematical Sciences
Skjernvej 4A
DK - 9220 Aalborg
<http://www.math.aau.dk>

Title:

Scrambling of Speech Signals

Theme:

Signals and Systems

Project Period:

Spring Semester 2022

Project Group:

MatTek4 5.239

Participants:

Laurits Randers
Julie Timmermann Werge
Christian Dausel Jensen
Stine Byrjalsen
Tanja Kortsen Bugajski

Supervisors:

Peter Koch
Oliver Matte

Page Numbers: 92**Date of Completion:**

May 24, 2022

Abstract:

Formålet med dette projekt er at udvikle og implementere en effektiv og billig metode til kryptering af et talesignal. For at udvikle denne metode har vi lavet en model af et digitalt talesystem. Med udgangspunkt i teori om diskret-tids systemer, Fourier analyse og sampling vil vi implementere denne model med et sæt valgte specifikationer. Eksperimenter er blevet udført for at teste vores model. For en billig implementation har vi introduceret Fast Fourier Transformationen. Denne er blevet sammenlignet med den Diskrete Cosinus Transformation. For at kryptere vores talesignal har vi anvendt permutation. I eksperimentet har vi testet to forskellige metoder, inversion og shuffle. Vi fandt ingen signifikant forskel mellem de to transformationer, dog observerede vi en forskel på de to forskellige metoder for permutation.

Preface

This project is written by Group MatTek4 5.239 on the 4th semester 2022, studying Mathematics-Technology at the Department of Mathematical Sciences, Aalborg University. The project is written in the period February 2, 2022 - May 24, 2022. The theme of this project is signals and systems. The content of this report is approximately 1/3 Mathematics, 1/3 Technical Science, and 1/3 Engineering.

Aalborg University, May 24, 2022



Christian Dausel Jensen
cdje20@student.aau.dk



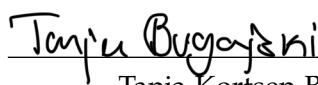
Julie Timmermann Werge
jwerge20@student.aau.dk



Laurits Randers
lrander18@student.aau.dk



Stine Byrjalsen
sbyrja@student.aau.dk



Tanja Kortsen Bugajski
tbugaj17@student.aau.dk

Contents

| | |
|--|------------|
| Preface | iii |
| 1 Introduction | 1 |
| 1.1 Sound | 1 |
| 1.2 Speech and Hearing | 2 |
| 1.3 Wireless Communication | 5 |
| 1.4 Problem Statement | 7 |
| 1.5 System Description | 7 |
| 2 Discrete-Time Signals and Systems | 8 |
| 2.1 Sequences | 8 |
| 2.2 Sequence Spaces | 9 |
| 2.3 Discrete-Time Signals | 11 |
| 2.4 Important Discrete-Time Signals | 11 |
| 2.5 Discrete-Time Systems and their Properties | 13 |
| 2.6 LTI Systems | 16 |
| 2.7 Frequency-domain Representation of Discrete-time Systems and Signals . . | 22 |
| 3 Fourier Analysis | 25 |
| 3.1 Fourier Series | 25 |
| 3.2 Function Spaces | 32 |
| 3.3 The Fourier Transform | 34 |
| 3.4 Discrete-Time Fourier Transform | 35 |
| 3.5 The Discrete Fourier Transform | 38 |
| 3.6 The Fast Fourier Transform | 42 |
| 3.7 The Discrete Cosine Transform | 47 |
| 4 Sampling | 49 |
| 4.1 Analog-To-Digital Converter | 51 |
| 5 Filter Theory | 54 |
| 5.1 Digital Filters | 54 |
| 5.2 Generalised Linear Phase | 55 |
| 5.3 The Window Method | 59 |
| 6 Application of The Short-Time Fourier Transform | 65 |
| 6.1 The Short-Time Fourier Transform | 65 |
| 6.2 Spectrograms | 66 |
| 6.3 Heisenberg's Uncertainty Principle | 69 |
| 7 Implementation | 74 |

Contents

| | | |
|-----------|-------------------------------------|-----------|
| 7.1 | System Specification | 74 |
| 7.2 | Filter | 75 |
| 7.3 | Transforms and Scrambling | 79 |
| 8 | Experiment | 82 |
| 8.1 | Test Setup | 82 |
| 8.2 | Results | 82 |
| 8.3 | Sources of Errors | 83 |
| 9 | Discussion | 84 |
| 10 | Conclusion | 85 |
| | Bibliography | 86 |
| A | Permutation | 87 |
| B | Result from experiment | 91 |

1 Introduction

In the modern world, communication is important. One way to communicate over large distances is by using wireless communication. This is possible by using a simple, analogue, wireless communication device, such as a walkie-talkie. The device transmits speech through the air as radio waves. However, with the right equipment these radio waves can be obtained by anyone. This is problematic, if the information is classified by the government or police and is deemed to be sensitive information. One way to increase the security of the information is with encryption, which distorts the signal such that the information is unidentifiable. This is referred to as locking the information. The intended recipient must thereby decrypt the encrypted signal by using a key, hence the data transfer is protected from anyone without the key. Nonetheless, not all establishments and organisations can afford an advanced encryption to complement an advanced communication system. As a result, it is interesting to explore the balance between encryption systems that are robust enough and have a low implementation cost. In this report we will focus on designing an efficient and simple digital encryption system for speech via radio communication. This leads to the initiating problem statement:

How can speech signals be easy and efficient encrypted, when using wireless communication? In order to describe speech signals a basic understanding of the physics of sound waves is needed.

1.1 Sound

When an object vibrates in the air the density of the air around it changes. This results in a change in the air pressure, which propagates through the air. This is called a sound wave. The individual particles in the air do not vibrate, instead sound waves propagate more like waves on water. A representation of sound waves propagating through air can be seen on Figure 1.1, where the air particles are illustrated on top of the sinusoidal wave.

1.2. Speech and Hearing

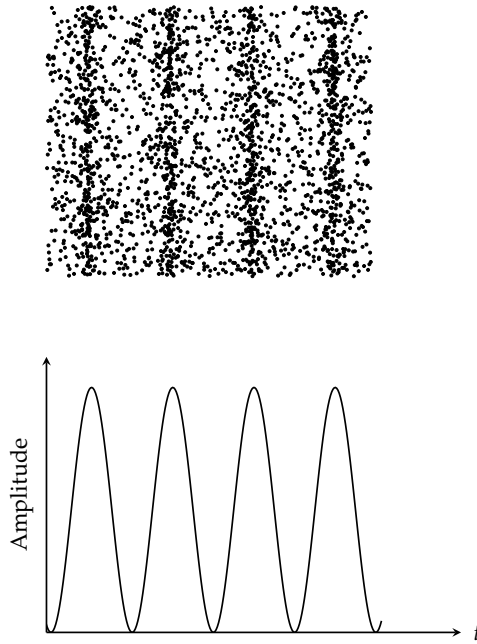


Figure 1.1: Representation of sound waves propagating through air.

When the pressure is high the particles compresses which can be seen as a maximum in amplitude. On the contrary, when the pressure is low the particles move apart which can be seen as a minimum in amplitude. Sound is measured as pressure over time. Mathematically a pure tone is represented by a sinusoidal waveform, which can be described as

$$f(t) = A \sin(2\pi ft + \phi) = A \sin(\Omega t + \phi),$$

where A is the amplitude, f is the frequency in Hertz (Hz), ϕ is the phase, and $\Omega = 2\pi f$ is the angular frequency of the wave measured in radians pr. seconds. The time it takes to complete one cycle is called the period (T) and its reciprocal is the frequency, thus $f = \frac{1}{T}$. The frequency of the sinusoidal determines the pitch of the sound. A high frequency results in a high pitch and low frequency results in a low pitch [11, pp. 527–531]. With the knowledge of sound the physiology of human speech can be introduced.

1.2 Speech and Hearing

Human speech can be composed into the subglottal system, larynx, and supralaryngeal vocal tract. The components can be seen on Figure 1.2. The process starts at the subglottal system.

1.2. Speech and Hearing

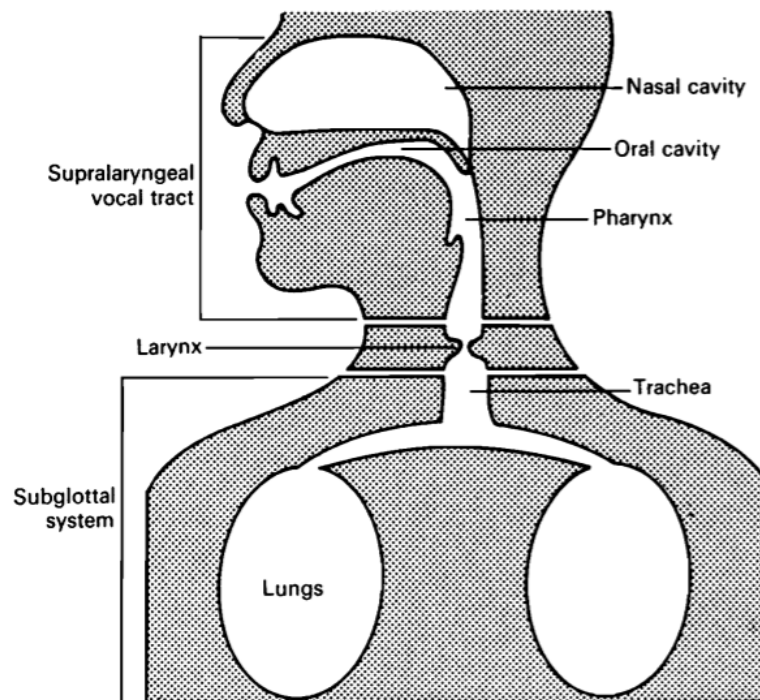


Figure 1.2: An idealised presentation of the three components for speech production [6, p. 4].

To power the air pressure towards generating a speech signal, the subglottal system utilises the lungs and leads air through the mouth and into the trachea, directing air into each lung. A pressure is released, and a steady flow of air moves towards the larynx. The larynx converts the flow of air into a series of quasi-periodic streams of air. In this case, quasi refers to almost or irregularly periodic streams of air, hence the shape and period of the signal is almost repeating itself. The vocal cords are actively used during pronunciation of all vowels in English such as "a" and "i", but also to a few consonants such as "m" and "v". When actively using the folds to pronounce a vowel, the folds rapidly expand and reduce the size of the volume of air in between, generating a frequency. The folds remain relaxed regarding consonants with some exceptions. Therefore, producing a sentence means to vary in between relaxing and actively using the folds.

The opening between the folds is called the glottis. The air flow out of the lungs shoves the folds apart, generating a force in the glottis. The folds are then pulled together by the elastic properties of their stretched tissue, generating the periodic streams of air accordingly to their movement. Lastly, the periodic air stream enters the supralaryngeal vocal tract before it leaves the lips. The air stream is guided, using the pharynx, into the oral- and nasal cavity. In the oral cavity, the positioning of the tongue, teeth, lips, and jaw helps generating specific sounds. One example is when the speakers tongue tip moves away from the teeth, it produces the sound "t". Another example is tensing the lips to be circular and slowly closing them in the event of producing the sound "u". Therefore, combining the properties in the oral cavity in various ways can create a desired stream of air. This makes the supralaryngeal vocal tract act as an acoustic filter, changing the shape

1.2. Speech and Hearing

of the speech as it leaves the body [6, pp. 3–6, 10–14]. The stream of air causes vibrations creating sound waves, when leaving the human body. The sound waves travel through the air until it is received by our ears. An illustration of the human ear can be seen on Figure 1.3.

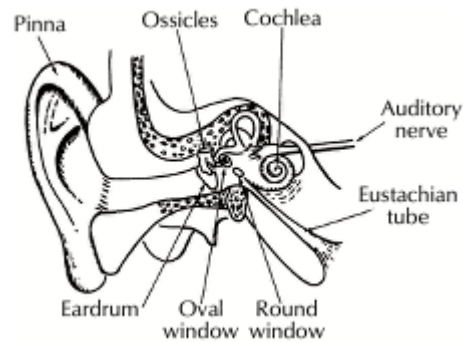


Figure 1.3: Diagram of the human ear [2, p. 57].

The sound wave is received by the pinna, guiding it towards the eardrum. The eardrum oscillates back and forth, based on the equivalent vibration, causing the ossicles to oscillate. The ossicles are small bones fastened to the eardrum. The oscillation of the ossicles is transferred to the water-like fluid within the cochlea, causing the fluid to move. Small hair cells in the fluid start bending which is then converted into nerve impulses, transmitted to the brain, recognizing that a sound is present [11, p. 530]. The Human ear is sensitive to waves in the audible range, which is located in the range of 20 - 20,000 Hz [11, p. 527]. The physical characteristics of a sound wave can be directly related to the human perception of sound. Thus, remembering Figure 1.1 the higher the pressure the louder a sound is perceived [11, p. 531].

Mathematically sounds can be analysed in the frequency domain. A plot of a speech signal and the amplitude spectrum is shown on Figure 1.4 visualizing the speech signal.

1.3. Wireless Communication

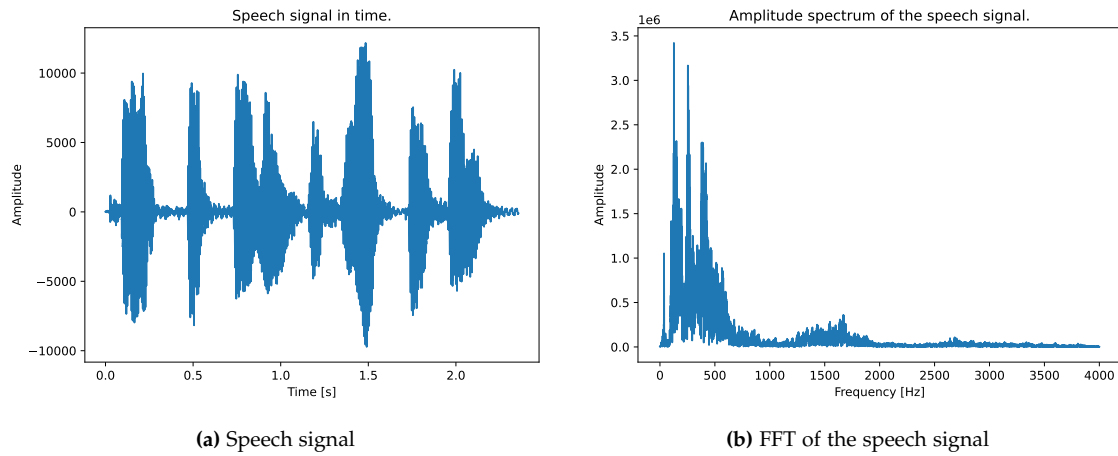


Figure 1.4: (a) A speech signal of a male speaking the sentence "Two plus seven is less than ten". (b) A plot of the amplitude spectrum of the speech signal.

It can be seen on Figure 1.4b that most of the speech signal frequency content is below 2000 Hz. For adult males, the range of frequency that can be reached lies between 80 and 300 Hz, this is due to the vocal cords of males usually are longer than females and children's. Adult females and children generally obtain a range from 80 to 500 Hz, hence short folds yield a higher range of frequencies [6, p. 37].

1.3 Wireless Communication

Communication systems transmits information from a transmitter to a receiver. With wireless communication the transmitter and receiver can be placed with a distance anywhere between a few meters to thousands of kilometers. This is possible since the signal propagates through space. This is accomplished with antennas, which transforms the electrical signals to radio signals in the form of electromagnetic (EM) waves and vice versa. Hence, both transmitter and receiver consists of an antenna, see Figure 1.5.

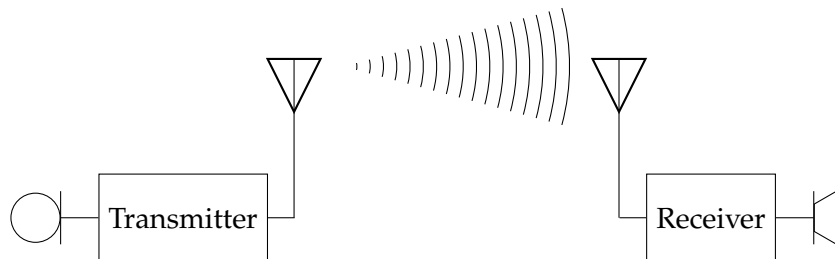


Figure 1.5: A wireless communication.

EM waves are created when a change in an electric field produces a magnetic field and vice versa. EM waves can be divided into a spectrum depending on frequency and wavelength. Since EM waves travel at the speed of light, $c \approx 3 \cdot 10^8$ m/s, the wavelengths

1.3. Wireless Communication

can be calculated from the following equation:

$$\lambda = \frac{c}{f},$$

where λ is the wavelength measured in meters (m), c is the speed of the EM waves in m/s and f is the frequency measured in 1/s. Therefore, radio waves have frequencies from 3000 Hz to 300 GHz and wavelengths from 1 mm to 100 km. Due to their large wavelength, they are widely used for communication, broadcasting and radar [11, pp. 1101–1102]. In order to transmit EM waves of a given wavelength, an antenna with the same length as the wavelength is needed. Therefore, the frequency of the input signal has to be increased in order to obtain an antenna with a feasible length. This can be done by varying one or more properties of a carrier signal which is a high frequency waveform. This process is called modulation. How the waveform is varied depends on the used modulation technique. In radio broadcasting the two most used modulations are frequency modulation (FM) and amplitude modulation (AM). AM is variations in the amplitude of the carrier signal varied by the input signal. FM is when the frequency of the carrier signal is varied by the input signal. See Figure 1.6.

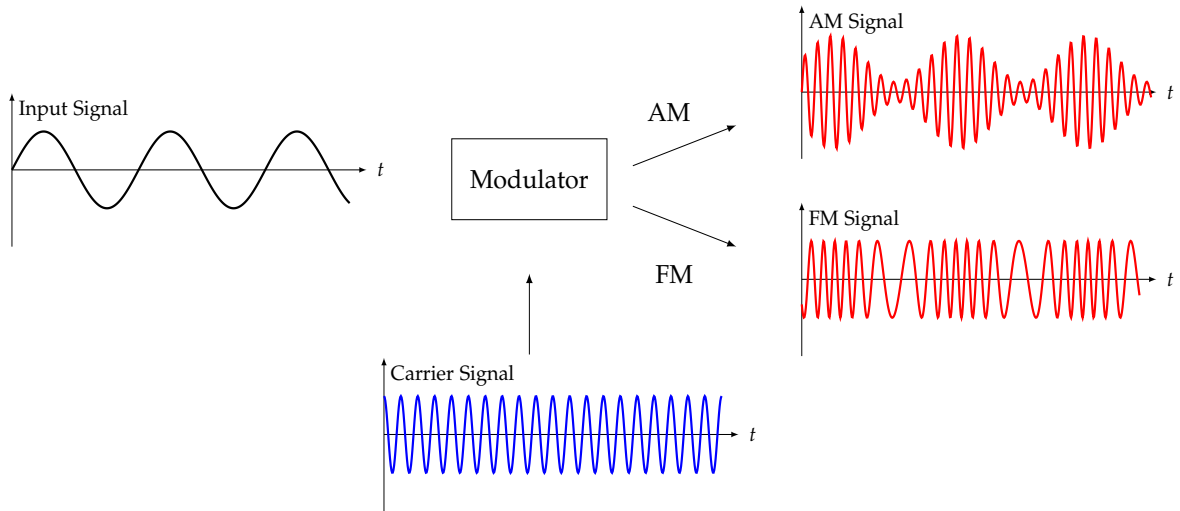


Figure 1.6: Amplitude and frequency modulation.

The device that performs the modulation is called a modulator and the inverse modulation is a demodulator [3, pp. 1–3].

With a basic knowledge of the physics of speech signals and wireless communication, this leads to the following problem statement:

1.4 Problem Statement

How can we implement a system with the ability to scramble and descramble a speech signal, while preserving the intelligibility of the speech?

Our considerations related to the system description are specified in the following section.

1.5 System Description

A block diagram of the system is illustrated in Figure 1.7. The system is separated into two parts, a transmitter that scrambles the speech signal, and a receiver which descrambles the signal. The transmitter consists of six blocks, where the first component is the **ADC**, which converts the analog signal with continuous values to a digital signal. The next block contains a **Filter**, chosen to fulfill a set of specifications. After the signal has been filtered the signal is transformed, to the frequency domain, by a transformation (T). Next the signal is scrambled (S) by permutation to make it unrecognisable. The signal is then transformed back to the time domain by the inverse transformation (T^{-1}). The process is illustrated in the following block diagram.

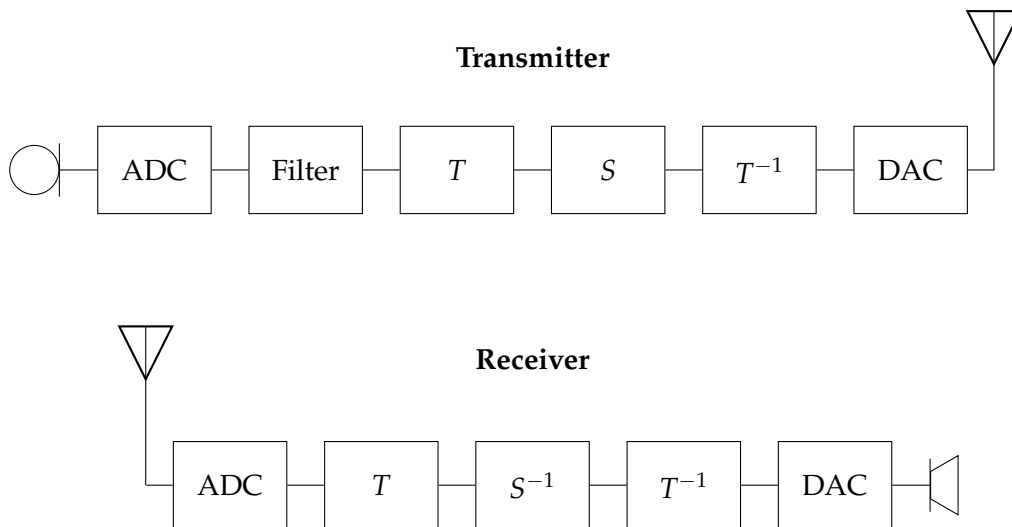


Figure 1.7: A block diagram of the system, where T is the transformation, T^{-1} the inverse, S the scrambler and S^{-1} the descrambler.

At the receiver's end the process is reversed and the signal is descrambled, with the goal of making the speech signal recognisable again. In order to create a system, as depicted in Figure 1.7, a general knowledge of discrete-time signals and systems is required.

2 Discrete-Time Signals and Systems

The term signal often applies to something that conveys information. Mathematically signals are represented as functions of one or more independent variables. The independent variables may be either continuous or discrete and the variable is commonly referred to as time. Thus, continuous-time signals are represented along a continuum of time with continuous independent variables and discrete-time signals are defined at discrete-time where the independent variables have discrete values represented as sequences of numbers. In this chapter we will focus on discrete-time signals.

2.1 Sequences

Discrete-time signals are represented as a sequence of numbers. These sequences can be classified as finite or infinite. The infinite sequence is defined as follows.

Definition 2.1 (Infinite Sequence)

The infinite sequence is defined as

$$x = \{x[n]\}_{n=-\infty}^{\infty} \in \mathbb{C}^{\mathbb{Z}}.$$

[10, p. 183]

In practice computations are always done on finite length inputs. Thus, we define the finite sequence as follows.

Definition 2.2 (Sequence of length N)

The finite sequence of length N is defined as

$$x = \{x[n]\}_{n=0}^{N-1} \in \mathbb{C}^N,$$

where $N \in \mathbb{N}$.

[10, p. 183]

For mathematical convenience we often consider sequences of infinite length, omitting the concerns of considering the boundaries [10, pp. 182–183]. Finite sequences can be extended to infinite, using different techniques. The first technique is zero-padding. For a finite sequence $x = \{x[n]\}_{n=0}^{N-1}$ we embed zeroes such that

$$\tilde{x} = \{\tilde{x}[n]\}_{n=-\infty}^{\infty} \quad \text{where } \tilde{x}[n] = \begin{cases} x[n], & \text{for } n = 0, 1, \dots, N-1 \\ 0, & \text{otherwise} \end{cases}.$$

2.2. Sequence Spaces

This is equivalent to omitting all unnecessary observations outside the interval. Another technique is extending the sequence by circular extension. This is done by considering the finite-length sequence as one period of a periodic sequence of period $N \in \mathbb{N}$ [10, p. 183]. In vector notation this yields the infinite sequence

$$x = [\dots, x[N-1], \underbrace{x[0], x[1], \dots, x[N-1]}_{\text{one period}}, x[0], x[1], \dots]^T.$$

To outline some important properties, any sum and product of two sequences x and y can be defined as the sample-by-sample sum and product, respectively. Multiplication of x by an arbitrary constant a is defined as the multiplication of each sample value by a . Lastly, any sequence x can be shifted by a constant m , where n is a fixed positive integer, to obtain a new version y , hence

$$y[n] = x[n - m]$$

shifts the input sequence to the right by m samples, resulting in a time delay. This also implies in the opposite direction for a fixed negative integer m resulting in a corresponding advance in time by $|m|$ samples [1, p. 19].

2.2 Sequence Spaces

For infinite-length sequences it is important to consider their domain, therefore some important vectorspaces will be introduced.

Definition 2.3 (Space of Absolutely Summable Spaces ($\ell^1(\mathbb{Z})$))

The vectorspace $\ell^1(\mathbb{Z})$ is defined by

$$\ell^1(\mathbb{Z}) = \left\{ x = \{x[n]\} \mid x \in \mathbb{C}^{\mathbb{Z}} : \|x\|_1 := \sum_{n=-\infty}^{\infty} |x[n]| < \infty \right\}.$$

[10, p. 194]

The space of absolutely summable sequences consists of all sequences with finite ℓ^1 norm [10, p.186].

Definition 2.4 (Space of Square-summable Sequences ($\ell^2(\mathbb{Z})$))

The vectorspace $\ell^2(\mathbb{Z})$ is defined by

$$\ell^2(\mathbb{Z}) = \left\{ x = \{x[n]\} \mid x \in \mathbb{C}^{\mathbb{Z}} : \|x\|_2 := \left(\sum_{n=-\infty}^{\infty} |x[n]|^2 \right)^{\frac{1}{2}} < \infty \right\}.$$

[10, p. 194]

2.2. Sequence Spaces

In fact, $(\ell^2(\mathbb{Z}))$ is an inner product space with inner product

$$\langle x, y \rangle := \sum_{n=-\infty}^{\infty} x[n]y^*[n], \quad x, y \in \ell^2(\mathbb{Z}).$$

The $\|x\|_2$ can be expressed using the inner product

$$\|x\|_2 = \sqrt{\langle x, x \rangle} = \left(\sum_{n=-\infty}^{\infty} |x[n]|^2 \right)^{\frac{1}{2}}.$$

Definition 2.5 (Space of Bounded Sequences $(\ell^\infty(\mathbb{Z}))$)

The vectorspace $\ell^\infty(\mathbb{Z})$ is defined by

$$\ell^\infty(\mathbb{Z}) = \left\{ x = \{x[n]\} \mid x \in \mathbb{C}^{\mathbb{Z}} : \|x\|_\infty := \sup |x[n]| < \infty \right\}.$$

[10, p. 194]

The space of bounded sequences contains all sequences x limited by some finite M equivalent to $|x[n]| \leq M, \forall n \in \mathbb{Z}$ [10, p.186]. To illustrate the definitions above an example is provided.

Example 2.6 (Sequence Spaces)

For $\alpha \in \mathbb{R}$ consider the geometric sequence defined by

$$x[n] = \begin{cases} \alpha^n, & \text{for } n \geq 0 \\ 0, & \text{otherwise} \end{cases}.$$

To show that $x \in \ell^1(\mathbb{Z})$

$$\|x\|_1 = \sum_{n=0}^{\infty} |\alpha^n| = \sum_{n=0}^{\infty} |\alpha|^n = \frac{1}{1-\alpha} < \infty \quad \text{for } |\alpha| < 1.$$

To show that $x \in \ell^2(\mathbb{Z})$

$$\|x\|_2 = \sqrt{\langle x, x \rangle} = \sqrt{\sum_{n=0}^{\infty} \alpha^n \alpha^n} = \sqrt{\sum_{n=0}^{\infty} (\alpha^2)^n} = \sqrt{\frac{1}{1-\alpha^2}} < \infty \quad \text{for } |\alpha| < 1.$$

To show that $x \in \ell^\infty(\mathbb{Z})$. For $|\alpha| \leq 1$ we have

$$|x[n]| \leq \begin{cases} 1, & \text{for } n \geq 0 \\ 0, & \text{otherwise} \end{cases},$$

2.3. Discrete-Time Signals

hence $\sup |x| = 1$ resulting in $x \in \ell^\infty(\mathbb{Z})$.

On the other hand, if $|\alpha| > 1$, then $|x[n]| \rightarrow \infty$ for $n \rightarrow \infty$ which implies that none of the norms are finite. Thus, x is not in any of the vector spaces for $|\alpha| > 1$.

Having defined some important sequence spaces, discrete-time signals will be introduced.

2.3 Discrete-Time Signals

Discrete-time signals are often derived by processing a continuous-time signal. The numeric value of the n th number in the sequence is equal to the continuous-time signal $x_c(t)$ at time $t = nT$ i.e.,

$$x[n] = x_c(nT) \quad \text{for } n \in \mathbb{Z},$$

where T is the distance between each point in the sequence. Discrete-time signals are depicted graphically by a stem-plot. An example is illustrated in Figure 2.1.

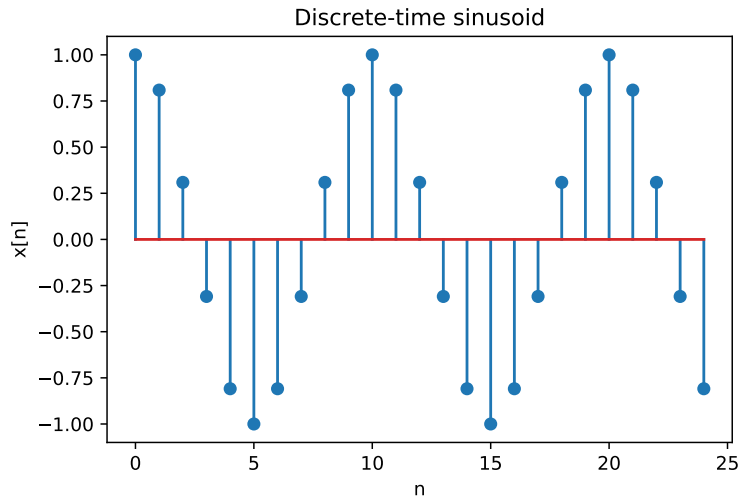


Figure 2.1: Stem-plot of $x[n] = \sin(2\pi 0.1n)$.

It is important to denote that $x[n]$ is only defined for integer values of n , equivalent to equidistantly separated points in time.

2.4 Important Discrete-Time Signals

One of the most important sequences in discrete-time signal theory is the unit impulse sequence also known as the Kronecker delta sequence.

2.4. Important Discrete-Time Signals

Definition 2.7 (The Kronecker Delta Sequence)

The Kronecker delta sequence is defined as

$$\delta[n] = \begin{cases} 1, & \text{if } n = 0 \\ 0, & \text{if } n \neq 0 \end{cases},$$

where $n \in \mathbb{Z}$.

[1, p. 14]

The importance of the unit impulse sequence, results from the fact that any discrete-time signal can be represented as a linear combination of scaled and delayed impulses. This can be written as

$$x[n] = \sum_{k=-\infty}^{\infty} x[k]\delta[n-k]. \quad (2.1)$$

The impulse sequence is also related to another sequence, the unit step function, written as

$$u[n] = \sum_{k=-\infty}^n \delta[k].$$

The unit step function can be defined independently of the impulse sequence as follows.

Definition 2.8 (The Unit Step Function)

The unit step function is defined as

$$u[n] = \begin{cases} 1, & \text{if } n \geq 0 \\ 0, & \text{if } n < 0 \end{cases},$$

where $n \in \mathbb{Z}$.

[1, p. 15]

The unit impulse sequence and the unit step function are depicted in Figure 2.2

2.5. Discrete-Time Systems and their Properties

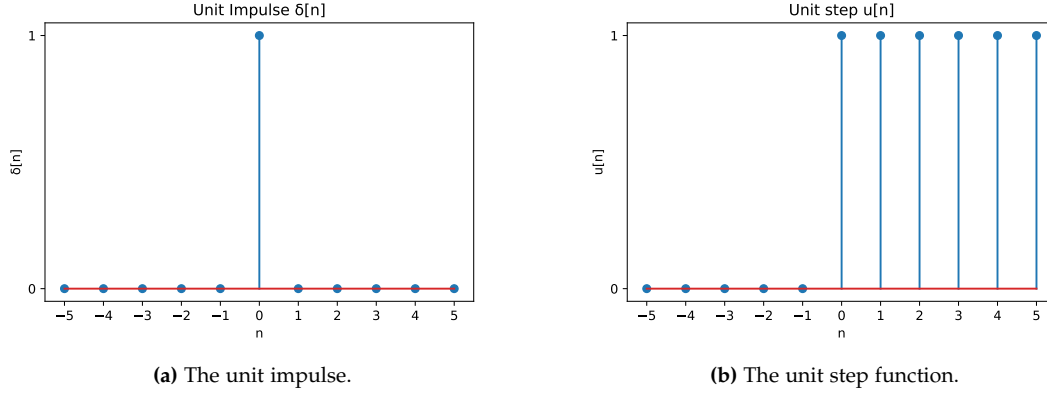


Figure 2.2: Stem-plots of the impulse sequence and unit step function respectively.

Having defined two important sequences, discrete-time systems and some of their key properties will be introduced.

2.5 Discrete-Time Systems and their Properties

Discrete-time systems, henceforth referred to as DTS, take a sequence of discrete values $x[n]$ as input, and produce a sequence with values $y[n]$ as output. Mathematically this can be defined as an operator T that maps an input $x \in V$ into an output $y \in \mathbb{C}^{\mathbb{Z}}$.

Definition 2.9 (Discrete-Time Systems)

A discrete-time system on V is an operator

$$T : V \rightarrow \mathbb{C}^{\mathbb{Z}}$$

where V is a subset of $\mathbb{C}^{\mathbb{Z}}$.

[10, p. 195]

For an input signal $x[n]$ the output $y[n] = T\{x\}[n]$ can be illustrated as in Figure 2.3.

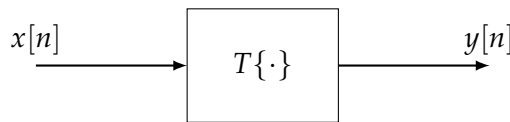


Figure 2.3: Discrete-time System.

The system is linear if it obeys the principle of superposition. The definition combines the properties of additivity and scaling and is defined as follows.

2.5. Discrete-Time Systems and their Properties

Definition 2.10 (Linear System)

A discrete-time system $y = T\{x\}$ is called linear if V is a vector space and

$$T\{\alpha x_1 + \beta x_2\}[n] = \alpha T\{x_1\}[n] + \beta T\{x_2\}[n] \quad \forall \alpha, \beta \in \mathbb{C},$$

where $x_1, x_2 \in V$.

[10, p.195]

If Definition 2.10 is fulfilled, the function T is a linear operator. Example 2.11 is an example of an operator which fails to fulfill Definition 2.10.

Example 2.11 (Linearity)

Consider an operator $T\{x\} = x^2$. For any sequence x and any arbitrary constant $\alpha \in \mathbb{R}$ we have

$$T\{\alpha x\}[n] = (\alpha x[n])^2 = \alpha^2 x[n]^2.$$

Thus, T is not linear, since Definition 2.10 is only fulfilled for $\alpha = 1$.

Another key property is time-invariance. In a time-invariant system, any time-shift in input results in a corresponding time-shift in the output. This leads to the following definition.

Definition 2.12 (Time-Invariant System)

A discrete-time system T is called time-invariant if

$$y[n] = T\{x\}[n] \Rightarrow y'[n] = T\{x'\}[n], \quad \text{where } \begin{cases} x'[n] = x[n-m] \\ y'[n] = y[n-m] \end{cases} \quad \forall m \in \mathbb{Z}.$$

[10, p.197]

Henceforth we will use the notation LTI for linear time-invariant systems. The next property to be defined is causality. A DTS is causal if the output $y[n]$ at time k is only dependent on the present and no future inputs up to time k . This can be defined as follows.

Definition 2.13 (Causality)

A discrete-time system T is called causal when, for any integer n_0 and inputs x_1 and x_2 ,

$$x_1[n] = x_2[n], \quad \forall n < n_0,$$

2.5. Discrete-Time Systems and their Properties

satisfies the corresponding output

$$T\{x_1\}[n] = T\{x_2\}[n], \quad \forall n < n_0.$$

[10, p. 197]

In other words, any system is causal if for any n_0 the output sequence value at time $n = n_0$ is only dependent on the input sequence values for $n \leq n_0$.

Example 2.14 (Forward Difference System)

Consider the forward difference system defined by

$$y[n] = x[n+1] - x[n],$$

where x is any arbitrary sequence and $n \in \mathbb{Z}$. This system is not causal since the output is dependent on future values of the input.

Causality is independent of linearity and time-invariance. Consider the operator from Example 2.11, if $x[n] = 0$ the output $y[n] = 0$, thus the non-linear operator T is causal. The last important property to be introduced is stability. We define bounded-input, bounded-output stability, henceforth referred to as BIBO, by the following definition.

Definition 2.15 (BIBO Stability)

A discrete-time system T is called BIBO stable if

$$x \in \ell^\infty(\mathbb{Z}) \Rightarrow y = T\{x\}[n] \in \ell^\infty(\mathbb{Z}),$$

for $n \in \mathbb{Z}$.

[10, p.198]

In other words, T is called BIBO stable when a bounded input results in a bounded output. To illustrate the previous definitions an example with the moving averaging operator is provided.

Example 2.16 (Moving Average Operator)

Consider the moving averaging operator T given by

$$y[n] = T\{x\}[n] = \frac{1}{N} \sum_{k=-(N-1)/2}^{(N-1)/2} x[n-k], \quad \text{for } n \in \mathbb{Z},$$

2.6. LTI Systems

where N is a odd positive integer. To show that T is linear, observe that

$$\begin{aligned} T\{\alpha x_1 + \beta x_2\}[n] &= \frac{1}{N} \sum_{k=-(N-1)/2}^{(N-1)/2} (\alpha x_1 + \beta x_2)[n-k] \\ &= \alpha \frac{1}{N} \sum_{k=-(N-1)/2}^{(N-1)/2} x_1[n-k] + \beta \frac{1}{N} \sum_{k=-(N-1)/2}^{(N-1)/2} x_2[n-k] \\ &= \alpha T\{x_1\}[n] + \beta T\{x_2\}[n]. \end{aligned}$$

Thus, T fulfils Definition 2.10 of a linear operator. To show that T is time-invariant, observe that

$$T\{x\}[n-m] = \frac{1}{N} \sum_{k=-(N-1)/2}^{(N-1)/2} x[n-k-m] = y[n-m].$$

By Definition 2.12 $T\{x\}[n-m] = y[n-m]$, yielding T is time-invariant. Since T is both linear and time-invariant, T is considered an LTI system. T is not considered causal, since the output $y[n]$ is dependent on future values of inputs. Lastly, to show that T is BIBO stable, consider

$$\begin{aligned} |y[n]| = |T\{x\}[n]| &\leq \frac{1}{N} \sum_{k=-(N-1)/2}^{(N-1)/2} |x[n-k]| \\ &\leq \frac{1}{N} N \sup |x[n]| \\ &= \sup |x[n]|. \end{aligned}$$

Hence T fulfills Definition 2.15 i.e. T is BIBO stable.

With these key properties another important concept is introduced.

2.6 LTI Systems

As previously stated, LTI systems are operators which are both linear and time-invariant. An important property of LTI systems is the impulse response, which can be defined as follows.

Definition 2.17 (Impulse Response)

A sequence h is called the impulse response of a LTI discrete-time system T when input δ produces output h . [10, p. 205]

Assume that T is a linear operator. Remember from (2.1) that any arbitrary input x to an

2.6. LTI Systems

operator T can be expressed as

$$x[n] = \sum_{k=-\infty}^{\infty} x[k]\delta[n-k], \quad \forall k \in \mathbb{Z}.$$

The output is then

$$y[n] = T \left\{ \sum_{k=-\infty}^{\infty} x[k]\delta[n-k] \right\} = \sum_{k=-\infty}^{\infty} x[k]T\{\delta\}[n-k] = \sum_{k=-\infty}^{\infty} x[k]h[n-k],$$

where $h[n-k]$ is the impulse response to the input sequences $\delta[n-k]$. Assuming that T is time-invariant, from Definition 2.12 we have that $h[n]$ is the response to $\delta[n]$ and $h[n-k]$ is the response to $\delta[n-k]$. This implies that an LTI system can be completely determined by its impulse response, since the output y can be found by h for any arbitrary input x , which leads to the following definition.

Definition 2.18 (Convolution)

The convolution between x and h is defined as

$$y[n] = (h * x)[n] = \sum_{k=-\infty}^{\infty} x[k]h[n-k], \quad \text{for } k \in \mathbb{Z},$$

where $x, h \in V$.

[10, p. 206]

In this project, only LTI systems which can be expressed by Definition 2.18 is considered. Convolution satisfies the algebraic properties commutativity, associativity, and distributivity.

Lemma 2.19 (Commutativity of the Convolution)

Assume $h \in \ell^1(\mathbb{Z})$ and $x \in \ell^\infty(\mathbb{Z})$, then

$$(h * x)[n] = (x * h)[n].$$

[1, p. 32]

Proof

To prove commutativity of the convolution, we substitute $L = n - k$ such that $k = n - L$

2.6. LTI Systems

to obtain

$$\begin{aligned}
 (h * x)[n] &= \sum_{k=-\infty}^{\infty} h[k]x[n-k] \\
 &= \sum_{L=-\infty}^{\infty} h[n-L]x[L] \\
 &= \sum_{L=-\infty}^{\infty} x[L]h[n-L] \\
 &= (x * h)[n].
 \end{aligned}$$

■

Lemma 2.20 (Associativity of the Convolution)

Assume $g, h \in \ell^1(\mathbb{Z})$ and $x \in \ell^\infty(\mathbb{Z})$, then

$$((g * h) * x)[n] = (g * (h * x))[n].$$

[1, p. 32]

Proof

To prove associativity of the convolution

$$\begin{aligned}
 ((g * h) * x)[n] &= \sum_{k=-\infty}^{\infty} (g * h)[k]x[n-k] \\
 &= \sum_{k=-\infty}^{\infty} \left(\sum_{l=-\infty}^{\infty} g[l]h[k-l] \right) x[n-k] \\
 &= \sum_{k=-\infty}^{\infty} \left(\sum_{l=-\infty}^{\infty} g[l]h[k-l]x[n-k] \right) \\
 &= \sum_{l=-\infty}^{\infty} \sum_{k=-\infty}^{\infty} g[l]h[k-l]x[n-k] \\
 &= \sum_{l=-\infty}^{\infty} g[l] \sum_{k=-\infty}^{\infty} h[k-l]x[n-k].
 \end{aligned}$$

By letting $m = k - l$ we get

$$\begin{aligned}
 &= \sum_{l=-\infty}^{\infty} g[l] \sum_{m=-\infty}^{\infty} h[m]x[n-l-m] \\
 &= \sum_{l=-\infty}^{\infty} g[l](h * x)[n-l] \\
 &= (g * (h * x))[n].
 \end{aligned}$$

■

Lemma 2.21 (Distributivity of the convolution)

Assume $g, h \in \ell^1(\mathbb{Z})$ and $x \in \ell^\infty(\mathbb{Z})$, then

$$(x * (h + g))[n] = (x * h + x * g)[n]$$

[1, p. 32]

Proof

To prove distributivity of the convolution

$$\begin{aligned} (x * (h + g))[n] &= \sum_{k=-\infty}^{\infty} x[k](h[n-k] + g[n-k]) \\ &= \sum_{k=-\infty}^{\infty} x[k]h[n-k] + \sum_{k=-\infty}^{\infty} x[k]g[n-k] \\ &= (x * h + x * g)[n]. \end{aligned}$$

■

The above properties implies convergence of the convolution, which will not be discussed further in this project. We assume convergence for all convolutions. To illustrate convolution an example with the moving average operator is provided.

Example 2.22 (Convolution)

Consider the moving average operator from Example 2.16,

$$y[n] = T\{x\}[n] = \frac{1}{N} \sum_{k=-(N-1)/2}^{(N-1)/2} x[n-k], \quad \text{for } n \in \mathbb{Z}.$$

By Definition 2.18 the impulse response is then given by

$$h[n] = \begin{cases} \frac{1}{N}, & |n| \leq (N-1)/2 \\ 0, & \text{otherwise} \end{cases}.$$

The sequences $x[n]$ and $h[n]$ are depicted in Figure 2.4.

2.6. LTI Systems

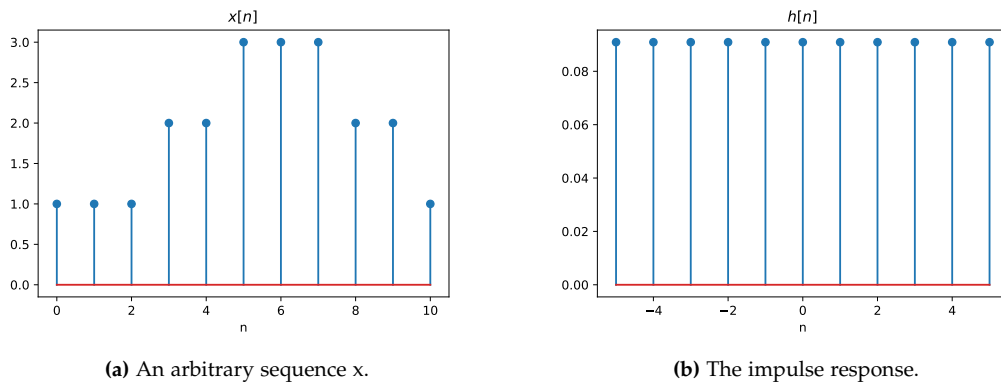


Figure 2.4: Stem-plots of the sequence $x[n]$ and the impulse response $h[n]$ respectively when $N = 11$.

Now performing the convolution $y[n] = (x * h)[n]$ yields Figure 2.5.

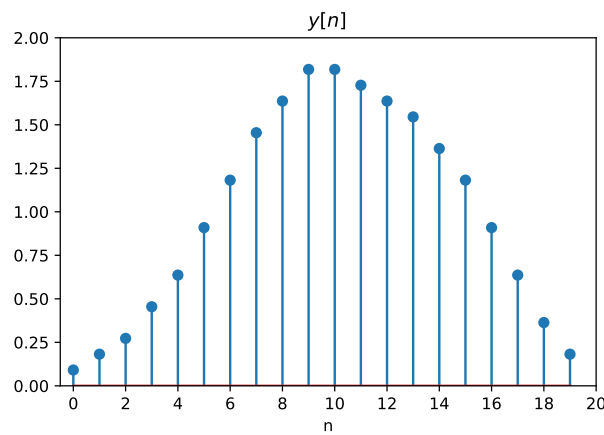


Figure 2.5: Stem-plot of the convolution between $x[n]$ and $h[n]$.

It can be seen on the output y on Figure 2.5 that the moving average operator h smooths the input signal x .

We finish this section stating the condition for stability for LTI systems and last giving an example of BIBO- and non-BIBO stable systems.

Theorem 2.23 (BIBO Stability of LTI Systems)

An LTI system is BIBO stable if its impulse response is absolutely summable.

[10, p. 208]

Proof (Theorem 2.23)

To prove absolute summability implies BIBO stability, consider an absolutely summable impulse response $h \in \ell^1(\mathbb{Z})$, such that $\|h\|_1 < \infty$ and a bounded input $x \in \ell^\infty(\mathbb{Z})$ such that $\|x\|_\infty < \infty$. The absolute value of any sample can then be bounded as follows

$$\begin{aligned}
 |y[n]| &= \left| \sum_{k=-\infty}^{\infty} h[k]x[n-k] \right| \\
 &\leq \sum_{k=-\infty}^{\infty} |h[k]| |x[n-k]| \\
 &\leq \|x\|_\infty \sum_{k=-\infty}^{\infty} |h[k]| \\
 &= \|x\|_\infty \|h\|_1 < \infty.
 \end{aligned}$$

The first inequality is obtained by the triangle inequality. The second inequality stems from bounding each $|x[n-k]|$ by $\|x\|_\infty$. Lastly applying Definition 2.3 proving that $|y[n]|$ is bounded [10, p. 209]. ■

For any LTI-system with finite impulse response h , the system is always stable. This is denoted finite impulse response, henceforth referred to as FIR systems. If the systems has infinite impulse response h , the system is stable only if the infinite sum $\sum_{n=-\infty}^{\infty} |h[n]|$ converges as $n \rightarrow \infty$. This is denoted infinite impulse response, henceforth IIR. We finish this section with an example of BIBO and non-BIBO stability.

Example 2.24 (BIBO and non-BIBO stability)

Consider an LTI system with impulse response $h_1[n] = \frac{1}{n^2}u[n-1]$. From Theorem 2.23 we know that BIBO stability is equivalent to the impulse response being absolutely summable. Thus, taking the norm $\|h[n]\|_1$ of the impulse response, we get $\sum_{n=1}^{\infty} \left| \frac{1}{n^2} \right| = \frac{\pi^2}{6}$. This implies that the norm is absolutely summable, hence the system is BIBO stable. On the contrary, suppose $h_2[n] = \frac{1}{n}u[n-1]$, the norm of this system diverges as $\sum_{n=1}^{\infty} \left| \frac{1}{n} \right| \rightarrow \infty$ which implies that the system is not BIBO stable. The two different impulse responses can be illustrated in Figure 2.6.

2.7. Frequency-domain Representation of Discrete-time Systems and Signals

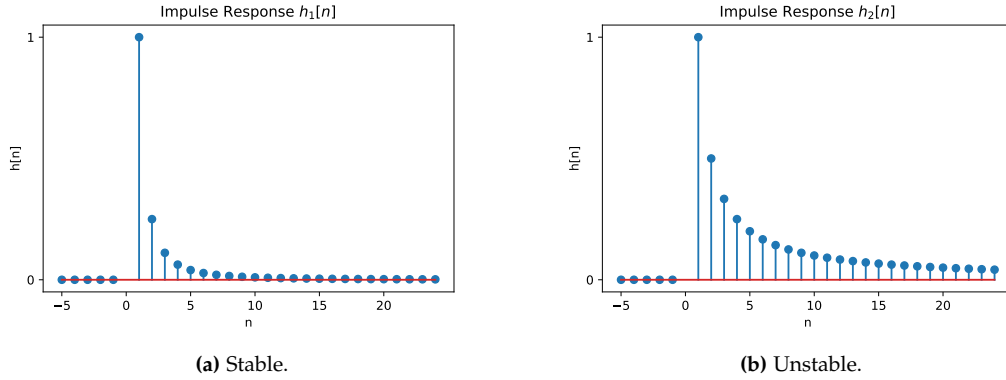


Figure 2.6: Stem-plots of a stable and unstable impulse response $h_1[n]$ and $h_2[n]$ respectively.

2.7 Frequency-domain Representation of Discrete-time Systems and Signals

Performing mathematical operations, systems and signals can be converted between the time and the frequency domain. In the frequency domain we study the amplitude and phase. Consider the impulse response h of a LTI discrete-time system. The output y of a system is given by Definition 2.18 i.e.,

$$y[n] = (x * h)[n] = \sum_{k=-\infty}^{\infty} h[k]x[n-k].$$

Applying the complex exponential as input to the system, such that $x[n] = e^{j\omega n}$ for $n \in \mathbb{Z}$, we obtain

$$\begin{aligned} y[n] &= \sum_{k=-\infty}^{\infty} h[k]e^{j\omega(n-k)} \\ &= e^{j\omega n} \sum_{k=-\infty}^{\infty} h[k]e^{-j\omega k} \\ &= H(e^{j\omega})e^{j\omega n}. \end{aligned} \tag{2.2}$$

$H(e^{j\omega})$ is denoted the frequency response of the system.

Since H is a complex quantity we have

$$H(e^{j\omega}) = H_R(e^{j\omega}) + jH_I(e^{j\omega}) = |H(e^{j\omega})|e^{j\angle H(e^{j\omega})},$$

where $|H(e^{j\omega})|$ is the magnitude and $\angle H(e^{j\omega})$ is the phase. From (2.2) it can be seen that H modifies the input x in complex amplitude and phase as a function of ω [1, pp. 42–43].

2.7. Frequency-domain Representation of Discrete-time Systems and Signals

Properties of the Frequency Response

The frequency response applies in both discrete- and continuous-time systems, however the distinction is that in LTI discrete-time systems H is always a 2π -periodic function of ω . This is shown by substituting $\omega + 2\pi$ into $H(e^{j\omega})$ to obtain

$$\begin{aligned} H(e^{j(\omega+2\pi)}) &= \sum_{n=-\infty}^{\infty} h[n]e^{-j(\omega+2\pi)n} \\ &= \sum_{n=-\infty}^{\infty} h[n]e^{-j\omega n}e^{-j2\pi n} \\ &= \sum_{n=-\infty}^{\infty} h[n]e^{-j\omega n} \\ &= H(e^{j\omega}). \end{aligned}$$

Indicating that H is 2π -periodic for all ω . In consequence, the systems response is exactly the same for both inputs $x[n] = e^{j\omega n}$ and $x_1[n] = e^{j(\omega+2\pi)n}$, thus, it is only necessary to define H over an interval of length 2π e.g., $0 \leq \omega \leq 2\pi$ or $-\pi \leq \omega \leq \pi$ [1, pp. 44–45].

A sufficient condition for the existence of the frequency response is that $h \in \ell^1(\mathbb{Z})$. In other words, if the sum $\sum_{k=-\infty}^{\infty} |h[k]|$ converges, H exists. Consider

$$|H(e^{j\omega})| = \left| \sum_{k=-\infty}^{\infty} h[k]e^{-j\omega k} \right| \leq \sum_{k=-\infty}^{\infty} |h[k]e^{-j\omega k}| \leq \sum_{k=-\infty}^{\infty} |h[k]| < \infty,$$

where the last equality ensures that, if $h \in \ell^1(\mathbb{Z})$ the system is BIBO-stable i.e, showing that H exists. This implies that in the context of LTI-systems, we know from Section 2.6 that any FIR system is always stable and therefore the frequency response exists [1, p. 52].

We finish this section with an example of the frequency response.

Example 2.25 (Moving Average Frequency Response)

Consider the moving average operator from Example 2.16.

The causal impulse response of the moving average operator is given by

$$h[n] = \begin{cases} \frac{1}{N}, & \text{for } 0 \leq k \leq \frac{1}{2}(N-1), \\ 0, & \text{otherwise} \end{cases}.$$

2.7. Frequency-domain Representation of Discrete-time Systems and Signals

By (2.2) the frequency response is

$$\begin{aligned}
 H(e^{j\omega}) &= \frac{1}{N} \sum_{k=0}^{\frac{1}{2}(N-1)} e^{-j\omega k} \\
 &= \frac{1}{N} \left(\frac{1 - e^{-j\omega(\frac{1}{2}(N+1))}}{1 - e^{-j\omega}} \right) \\
 &= \frac{1}{N} \frac{(e^{j\omega(\frac{1}{2}(N+1))/2} - e^{-j\omega(\frac{1}{2}(N+1))/2}) e^{-j\omega(\frac{1}{2}(N+1))/2}}{(e^{j\omega/2} - e^{-j\omega/2}) e^{-j\omega/2}} \\
 &= \frac{1}{N} \left(\frac{\sin \omega [\frac{1}{2}(N+1)]}{\sin \frac{1}{2}\omega} \right) e^{-j\omega(\frac{1}{2}(N-1))/2}.
 \end{aligned}$$

The magnitude and phase response of the frequency response are depicted in Figure 2.7.

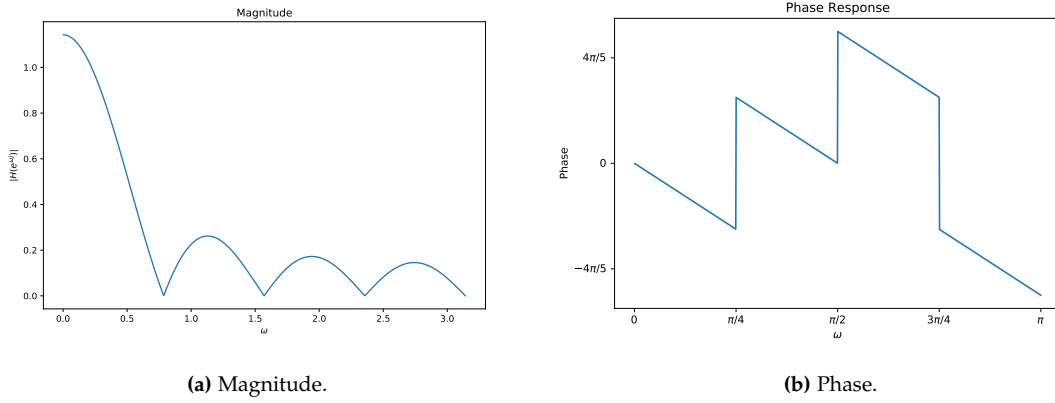


Figure 2.7: Magnitude and phase response, respectively, of the moving average operator for $N = 7$.

It can be seen that the system damps the frequency over $\pi/4$.

The relation between the impulse response h and the frequency response H can be found by Fourier analysis. This is presented in the following chapter.

3 Fourier Analysis

Signals are often analysed in the frequency domain, since several of the calculations are simplified compared to the time domain. Transforming a signal from time domain into the frequency domain can be done using the Fourier transform. To motivate the Fourier transform, Fourier series will be introduced.

3.1 Fourier Series

The purpose of this section is the introducing of the Fourier series and showing that the Fourier series of a function f converges to f under certain circumstances. The Fourier series describe periodic functions as linear combinations in terms of sines and cosines. Using the trigonometric functions the Fourier series can also be expressed in terms of the complex exponential function $e^{j\theta}$. This is sometimes more convenient since some of the calculations, are simplified compared to the corresponding sine and cosine.

Definition 3.1 (Fourier Series)

Let $f(\theta)$ be a 2π -periodic and Riemann integrable function on $[-\pi, \pi]$. Then the series

$$f(\theta) = \frac{1}{2}a_0 + \sum_{n=1}^{\infty} (a_n \cos n\theta + b_n \sin n\theta) \quad \text{or} \quad f(\theta) = \sum_{n=-\infty}^{\infty} c_n e^{jn\theta}$$

is called the Fourier series of $f(\theta)$. The corresponding Fourier coefficients of $f(\theta)$ are

$$\begin{aligned} a_n &= \frac{1}{\pi} \int_{-\pi}^{\pi} f(\theta) \cos n\theta \, d\theta, \quad n \geq 0 \\ b_n &= \frac{1}{\pi} \int_{-\pi}^{\pi} f(\theta) \sin n\theta \, d\theta, \quad n \geq 1 \\ c_n &= \frac{1}{2\pi} \int_{-\pi}^{\pi} f(\theta) e^{-jn\theta} \, d\theta, \quad n \in \mathbb{Z} \end{aligned}$$

where the relations between the coefficients are

$$c_0 = \frac{1}{2}a_0, \quad c_n = \frac{1}{2}(a_n - jb_n) \quad \text{and} \quad c_{-n} = \frac{1}{2}(a_n + jb_n) \quad \text{for } n \in \mathbb{N}.$$

[4, pp. 19–20]

The Fourier coefficients a_n and b_n can also be expressed by c_n as follows

$$a_0 = 2c_0, \quad a_n = c_n + c_{-n} \quad \text{and} \quad b_n = j(c_n - c_{-n}) \quad \text{for } n \in \mathbb{N}. \quad (3.1)$$

This is useful when introducing Bessel's inequality in terms of a_n and b_n . Bessel's inequality makes it possible to state convergence of the Fourier coefficients.

Theorem 3.2 (Bessel's Inequality)

If $f(\theta)$ is 2π -periodic and Riemann integrable on $[-\pi, \pi]$, then

$$\sum_{n=-\infty}^{\infty} |c_n|^2 \leq \frac{1}{2\pi} \int_{-\pi}^{\pi} |f(\theta)|^2 d\theta.$$

[4, p. 30]

Proof

If $z \in \mathbb{C}$ then $|z|^2 = z\bar{z}$. For $N \in \mathbb{N}$

$$\begin{aligned} 0 &\leq \left| f(\theta) - \sum_{n=-N}^N c_n e^{jn\theta} \right|^2 \\ &= \left(f(\theta) - \sum_{n=-N}^N c_n e^{jn\theta} \right) \left(\overline{f(\theta)} - \sum_{n=-N}^N \bar{c}_n e^{-jn\theta} \right) \\ &= |f(\theta)|^2 - \sum_{n=-N}^N \left(c_n \overline{f(\theta)} e^{jn\theta} + \bar{c}_n f(\theta) e^{-jn\theta} \right) + \sum_{m,n=-N}^N c_m \bar{c}_n e^{j(m-n)\theta}. \end{aligned}$$

Remember these equations

$$\frac{1}{2\pi} \int_{-\pi}^{\pi} f(\theta) e^{-jn\theta} d\theta = c_n \quad \text{and} \quad \frac{1}{2\pi} \int_{-\pi}^{\pi} e^{j(m-n)\theta} d\theta = \begin{cases} 0 & \text{if } m \neq n \\ 1 & \text{if } m = n \end{cases}.$$

Now multiply the inequality by $\frac{1}{2\pi}$ and integrate from $-\pi$ to π

$$\begin{aligned} 0 &\leq \frac{1}{2\pi} \int_{-\pi}^{\pi} \left| f(\theta) - \sum_{n=-N}^N c_n e^{jn\theta} \right|^2 d\theta \\ &= \frac{1}{2\pi} \int_{-\pi}^{\pi} |f(\theta)|^2 d\theta - \sum_{n=-N}^N (c_n \bar{c}_n + \bar{c}_n c_n) + \sum_{n=-N}^N c_n \bar{c}_n \\ &= \frac{1}{2\pi} \int_{-\pi}^{\pi} |f(\theta)|^2 d\theta - \sum_{n=-N}^N |c_n|^2. \end{aligned}$$

Adding $\sum_{n=-N}^N |c_n|^2$ to both sides of the inequality equals

$$\sum_{n=-N}^N |c_n|^2 \leq \frac{1}{2\pi} \int_{-\pi}^{\pi} |f(\theta)|^2 d\theta.$$

Let $N \rightarrow \infty$

$$\sum_{n=-\infty}^{\infty} |c_n|^2 \leq \frac{1}{2\pi} \int_{-\pi}^{\pi} |f(\theta)|^2 d\theta. \quad \blacksquare$$

3.1. Fourier Series

Bessel's inequality can also be stated using the Fourier coefficients a_n and b_n , by (3.1) for $n = 0$

$$|a_0|^2 = 4|c_0|^2.$$

For $n \geq 1$

$$\begin{aligned} |a_n|^2 + |b_n|^2 &= a_n \bar{a}_n + b_n \bar{b}_n \\ &= (c_n + c_{-n})(\bar{c}_n + \bar{c}_{-n}) + i(c_n - c_{-n})(-i)(\bar{c}_n - \bar{c}_{-n}) \\ &= 2c_n \bar{c}_n + 2c_{-n} \bar{c}_{-n} \\ &= 2(|c_n|^2 + |c_{-n}|^2). \end{aligned}$$

Which results in the following expression for Bessel's inequality

$$\frac{1}{4}|a_0|^2 + \frac{1}{2} \sum_{n=1}^{\infty} (|a_n|^2 + |b_n|^2) = \sum_{n=-\infty}^{\infty} |c_n|^2 \leq \frac{1}{2\pi} \int_{-\pi}^{\pi} |f(\theta)|^2 d\theta. \quad (3.2)$$

Equation (3.2) implies that the series $\sum |a_n|^2$, $\sum |b_n|^2$, and $\sum |c_n|^2$ are all convergent, which leads to the following corollary.

Corollary 3.3

The Fourier coefficients a_n and b_n tend to zero as $n \rightarrow \infty$. The Fourier coefficient c_n tend to zero as $n \rightarrow \pm\infty$. [4, p. 31]

Proof

$|a_n|^2$, $|b_n|^2$ and $|c_n|^2$ are the n th terms of a convergent series and thereby tend to 0 as $n \rightarrow \infty$, hence so do a_n , b_n and c_n . ■

Since the purpose of this section is to show that the Fourier series of a function f converges to f under the circumstances that f is 2π -periodic, continuous and piecewise smooth, it is necessary to define piecewise continuous and piecewise smooth functions.

Definition 3.4 (Piecewise Continuous Functions)

A function f on the interval $[a, b]$, where $-\infty < a < b < \infty$, is piecewise continuous if

1. f is continuous on the interval $[a, b]$ except perhaps at finitely many points x_1, \dots, x_k
2. the left-hand and right-hand limits of f given as

$$f(x_j-) = \lim_{\substack{h \rightarrow 0 \\ h > 0}} f(x_j - h) \quad \text{and} \quad f(x_j+) = \lim_{\substack{h \rightarrow 0 \\ h > 0}} f(x_j + h)$$

exists for $j = 1, 2, \dots, k$. If the endpoint a (or b) is one of the exceptional points x_j , only the right-hand (or left-hand) limit is required to exist.

The class of piecewise continuous functions on $[a, b]$ are denoted by $PC(a, b)$. [4, p. 32]

3.1. Fourier Series

Definition 3.5 (Piecewise Smooth Functions)

A function f on the interval $[a, b]$, where $-\infty < a < b < \infty$, is piecewise smooth if and only if, f' is defined in all but finitely many points of $[a, b]$, and f and its first derivative f' are both piecewise continuous on $[a, b]$. The class of piecewise smooth functions on $[a, b]$ are denoted by $PS(a, b)$. [4, p. 32]

A piecewise smooth function is also piecewise continuous. An example of a piecewise smooth function and a function that is not piecewise smooth can be seen on Figure 3.1.

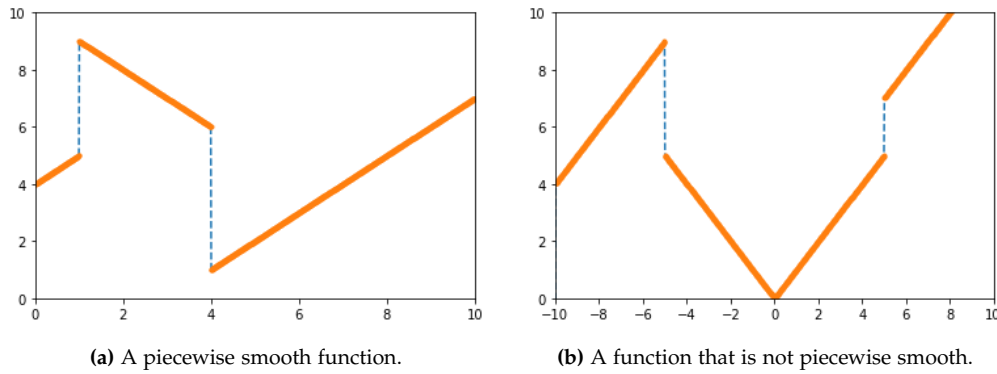


Figure 3.1: Plot of a piecewise smooth function and function that is not piecewise smooth.

It can be seen that the function in Figure 3.1b is not piecewise smooth since it is not differentiable at $x = 0$. A piecewise smooth function is a condition for pointwise convergence of the Fourier series. The N th partial sum of the Fourier series is defined with the purpose of showing that it converges to f as $N \rightarrow \infty$. The sum of any infinite series is defined as the limit of its partial sums.

Definition 3.6 (N th Partial Sum of the Fourier Series)

For a 2π -periodic and Riemann integrable function $f(\theta)$ the N th partial sum is

$$S_N^f(\theta) = \frac{1}{2}a_0 + \sum_{n=1}^N (a_n \cos n\theta + b_n \sin n\theta) = \sum_{n=-N}^N c_n e^{jn\theta},$$

where $c_n = \frac{1}{2\pi} \int_{-\pi}^{\pi} f(\psi) e^{-jn\psi} d\psi$. [4, p. 33]

A part of the N th partial sum of the Fourier series can be expressed by a function called the Dirichlet kernel, which will be useful for proving convergence of the Fourier series. To obtain that particular form of the equation, the expression for c_n is inserted into

3.1. Fourier Series

$$S_N^f(\theta)$$

$$S_N^f(\theta) = \frac{1}{2\pi} \sum_{n=-N}^N \int_{-\pi}^{\pi} f(\psi) e^{-jn\psi} e^{jn\theta} d\psi. \quad (3.3)$$

The index n in (3.3) is replaced by $-n$, which does not affect the sum since n ranges from $-N$ to N

$$S_N^f(\theta) = \frac{1}{2\pi} \sum_{n=-N}^N \int_{-\pi}^{\pi} f(\psi) e^{jn(\psi-\theta)} d\psi.$$

A change of variable $\phi = \psi - \theta$ results in the following expression for $S_N^f(\theta)$

$$S_N^f(\theta) = \frac{1}{2\pi} \sum_{n=-N}^N \int_{-\pi-\theta}^{\pi-\theta} f(\theta + \phi) e^{jn\phi} d\phi.$$

Since the integration is 2π -periodic

$$\begin{aligned} S_N^f(\theta) &= \frac{1}{2\pi} \sum_{n=-N}^N \int_{-\pi}^{\pi} f(\theta + \phi) e^{jn\phi} d\phi \\ &= \int_{-\pi}^{\pi} f(\theta + \phi) D_N(\phi) d\phi, \end{aligned}$$

where $D_N(\phi) = \frac{1}{2\pi} \sum_{n=-N}^N e^{jn\phi}$ is the Dirichlet kernel.

Definition 3.7 (Dirichlet Kernel)

The N th Dirichlet kernel function $D_N(\phi)$ is defined as

$$D_N(\phi) = \frac{1}{2\pi} \sum_{n=-N}^N e^{jn\phi}.$$

[4, p. 33]

The definition of the Dirichlet kernel can be rewritten in two specific ways. First of all it can be rewritten as an expression including cosinus

$$\begin{aligned} D_N(\phi) &= \frac{1}{2\pi} \sum_{n=-N}^N e^{jn\phi} \\ &= \frac{1}{2\pi} e^0 + \frac{1}{\pi} \sum_{n=1}^N \frac{1}{2} (e^{jn\phi} + e^{-jn\phi}) \\ &= \frac{1}{2\pi} + \frac{1}{\pi} \sum_{n=1}^N \cos(n\phi). \end{aligned} \quad (3.4)$$

3.1. Fourier Series

This rewriting is specifically useful when integrating $D_N(\phi)$. The Dirichlet kernel can also be recognized as a finite geometric progression

$$\begin{aligned} D_N(\phi) &= \frac{1}{2\pi} e^{-jN\phi} (1 + e^{j\phi} + \dots + e^{j2N\phi}) \\ &= \frac{1}{2\pi} e^{-jN\phi} \sum_{n=0}^{2N} e^{jn\phi}. \end{aligned}$$

A finite geometric progression can be rewritten by

$$\sum_{n=0}^K r^n = \frac{r^{K+1} - 1}{r - 1}, \quad \text{where } r \neq 1.$$

Rewriting the geometric progression in $D_N(\phi)$ for $\phi \neq 0$ equals

$$\begin{aligned} D_N(\phi) &= \frac{1}{2\pi} e^{-jN\phi} \frac{e^{j(2N+1)\phi} - 1}{e^{j\phi} - 1} \\ &= \frac{1}{2\pi} \frac{e^{j(N+1)\phi} - e^{jN\phi}}{e^{j\phi} - 1}. \end{aligned} \tag{3.5}$$

With the rewriting (3.4) in mind, a convenient property when integrating the Dirichlet kernel is presented in the following lemma.

Lemma 3.8

For any N

$$\int_{-\pi}^0 D_N(\theta) d\theta = \int_0^{\pi} D_N(\theta) d\theta = \frac{1}{2}.$$

[4, p. 35]

Proof

From the rewriting of $D_N(\phi)$ in (3.4)

$$D_N(\phi) = \frac{1}{2\pi} + \frac{1}{\pi} \sum_{n=1}^N \cos(n\phi).$$

Integrating from 0 to π yields

$$\int_0^{\pi} D_N(\phi) d\phi = \left[\frac{\phi}{2\pi} + \frac{1}{\pi} \sum_{n=1}^N \frac{\sin(n\phi)}{n} \right]_0^{\pi} = \frac{1}{2}.$$

Integrating from $-\pi$ to 0 leads to the same result. ■

With all the necessary conditions and properties presented, it is now possible to state and prove the main theorem of this section, which is pointwise convergence of the Fourier series.

3.1. Fourier Series

Theorem 3.9 (Pointwise Convergence of the Fourier Series)

Let $f(\theta) \in PS(\mathbb{R})$ be 2π -periodic, and have N th partial sum S_N^f , then

$$\lim_{N \rightarrow \infty} S_N^f(\theta) = \frac{1}{2} \left(f(\theta-) + f(\theta+) \right), \quad \text{for all } \theta$$

and if $f(\theta)$ is continuous, then

$$\lim_{N \rightarrow \infty} S_N^f(\theta) = f(\theta).$$

[4, p. 35]

Proof

From Lemma 3.8

$$\frac{1}{2}f(\theta-) = f(\theta-) \int_{-\pi}^0 D_N(\phi) d\phi \quad \text{and} \quad \frac{1}{2}f(\theta+) = f(\theta+) \int_0^{\pi} D_N(\phi) d\phi.$$

We need to show that the difference $S_N^f(\theta) - \frac{1}{2} \left(f(\theta-) + f(\theta+) \right)$ approaches 0 as $N \rightarrow \infty$, thus

$$\begin{aligned} S_N^f(\theta) - \frac{1}{2} \left(f(\theta-) + f(\theta+) \right) &= \int_{-\pi}^0 \left(f(\theta + \phi) - f(\theta-) \right) D_N(\phi) d\phi \\ &\quad + \int_0^{\pi} \left(f(\theta + \phi) - f(\theta+) \right) D_N(\phi) d\phi. \end{aligned} \quad (3.6)$$

Recalling the rewriting of the Dirichlet kernel from (3.5)

$$D_N(\phi) = \frac{1}{2\pi} \frac{e^{j(N+1)\phi} - e^{jN\phi}}{e^{j\phi} - 1}.$$

Equation (3.6) can be rewritten as

$$S_N^f(\theta) - \frac{1}{2} \left(f(\theta-) + f(\theta+) \right) = \frac{1}{2\pi} \int_{-\pi}^{\pi} g(\phi) (e^{j(N+1)\phi} - e^{jN\phi}) d\phi, \quad (3.7)$$

where

$$g(\phi) = \begin{cases} \frac{f(\theta+\phi) - f(\theta-)}{e^{j\phi} - 1}, & \text{if } -\pi < \phi < 0 \\ \frac{f(\theta+\phi) - f(\theta+)}{e^{j\phi} - 1}, & \text{if } 0 < \phi < \pi \end{cases}.$$

The function $g(\phi)$ is piecewise smooth for $\phi \neq 0$. By l'Hôpital's rule we have

$$\begin{aligned} \lim_{\phi \rightarrow 0+} g(\phi) &= \lim_{\phi \rightarrow 0+} \frac{f(\theta + \phi) - f(\theta+)}{e^{j\phi} - 1} \\ &= \lim_{\phi \rightarrow 0+} \frac{f'(\theta + \phi)}{je^{j\phi}} \\ &= \frac{f'(\theta+)}{j} \end{aligned}$$

3.2. Function Spaces

and

$$\begin{aligned}\lim_{\phi \rightarrow 0^-} g(\phi) &= \lim_{\phi \rightarrow 0^-} \frac{f(\theta + \phi) - f(\theta -)}{e^{j\phi} - 1} \\ &= \lim_{\phi \rightarrow 0^-} \frac{f'(\theta + \phi)}{je^{j\phi}} \\ &= \frac{f'(\theta -)}{j}.\end{aligned}$$

Hence, $g(\phi)$ is piecewise continuous and thereby Riemann-integrable on $[-\pi, \pi]$. By Corollary 3.3 the Fourier coefficients of $g(\phi)$

$$C_N = \frac{1}{2\pi} \int_{-\pi}^{\pi} g(\phi) e^{-jn\phi} d\phi, \quad (3.8)$$

tends to 0 as $N \rightarrow \pm\infty$.

The expression obtained in (3.7) can be rewritten as

$$\frac{1}{2\pi} \int_{-\pi}^{\pi} g(\phi) (e^{j(N+1)\phi} - e^{jN\phi}) d\phi = C_{-(N+1)} - C_N,$$

and like (3.8)

$$C_{-(N+1)} - C_N$$

tends to 0 as $N \rightarrow \pm\infty$. ■

To formally define the Fourier transform, the concept of function spaces is introduced.

3.2 Function Spaces

A set of functions, with addition and scalar multiplication, forms a vector space. The following three vector spaces are of interest when working with Fourier analysis.

Definition 3.10 (Space of Absolutely Integrable Functions $L^1(a, b)$)

For $a < b$

$$L^1(a, b) = \left\{ f : \int_a^b |f(x)| dx < \infty \right\}.$$

$L^1(\mathbb{R})$ denotes the space of absolutely integrable functions over \mathbb{R} . [10, p. 346]

Definition 3.11 (Space of Square-Integrable Functions $L^2(a, b)$)

For $a < b$

$$L^2(a, b) = \left\{ f : \int_a^b f^2(x) dx < \infty \right\}.$$

$L^2(\mathbb{R})$ denotes the space of square-integrable functions over \mathbb{R} . [10, p. 346]

Definition 3.12 (Space of Bounded Functions $L^\infty(\mathbb{R})$)

$$L^\infty(\mathbb{R}) = \{f : \exists M \in \mathbb{R} \forall x \in \mathbb{R} : |f(x)| \leq M\}.$$

[10, p. 346]

The following example categorises functions in $L^1(\mathbb{R})$ and $L^2(\mathbb{R})$.

Example 3.13 (Functions in $L^1(\mathbb{R})$ and $L^2(\mathbb{R})$)

Let

$$f(x) = \begin{cases} x^{-2/3}, & \text{if } 0 < x < 1 \\ 0, & \text{otherwise} \end{cases}.$$

Then

$$\int_{-\infty}^{\infty} |f(x)| dx = \int_0^1 x^{-2/3} dx = [3\sqrt[3]{x}]_0^1 = 3 < \infty.$$

Hence $f \in L^1(\mathbb{R})$. Now consider

$$\int_{-\infty}^{\infty} f^2(x) dx = \int_0^1 x^{-4/3} dx = \left[\frac{-3}{\sqrt[3]{x}} \right]_0^1.$$

This integral do not converges, hence $f \notin L^2(\mathbb{R})$.

Now consider

$$g(x) = \begin{cases} x^{-2/3}, & \text{if } x > 1 \\ 0, & \text{otherwise} \end{cases}.$$

Then

$$\int_{-\infty}^{\infty} |g(x)| dx = \int_1^{\infty} x^{-2/3} dx = [3\sqrt[3]{x}]_1^{\infty}.$$

Again this do not converges and thereby $g \notin L^1(\mathbb{R})$.

Lastly, consider

$$\int_{-\infty}^{\infty} g^2(x) dx = \int_1^{\infty} x^{-4/3} dx = \left[\frac{-3}{\sqrt[3]{x}} \right]_1^{\infty} = 3 < \infty.$$

Hence, $g \in L^2(\mathbb{R})$.

3.3. The Fourier Transform

From this example it can be seen that L^1 is not a subset of L^2 . However, for any function f in L^2 that vanishes outside an interval $[a, b]$, it can be shown that f is contained in both L^1 and L^2 . This leads to the following theorem.

Theorem 3.14

If $f \in L^2(\mathbb{R})$ and f vanishes outside a finite interval $[a, b]$, then $f \in L^1(\mathbb{R})$.

[4, p. 205]

Proof

Using that

$$\int_{-\infty}^{\infty} |f(x)| dx = \int_a^b |f(x)| dx,$$

the Cauchy-Schwarz inequality is used to get

$$\begin{aligned} &\leq \left(\int_a^b 1^2 dx \right)^{\frac{1}{2}} \left(\int_a^b |f(x)|^2 dx \right)^{\frac{1}{2}} \\ &= (b-a)^{\frac{1}{2}} \left(\int_a^b |f(x)|^2 dx \right)^{\frac{1}{2}} < \infty. \end{aligned}$$

Hence, $f \in L^1(\mathbb{R})$. ■

3.3 The Fourier Transform

Until now we have studied infinite series expansion of periodic functions. By using integral transforms, non-periodic functions on \mathbb{R} can be studied.

Definition 3.15 (The Fourier Transform)

Let x be an integrable function on \mathbb{R} . Then the Fourier transform of x is given by

$$X(\omega) = \int_{-\infty}^{\infty} x(t) e^{-j\omega t} dt.$$

[4, p. 213]

The Fourier transform maps $x \in L^2(\mathbb{R})$, to $X \in L^2(\mathbb{R})$. The proof of this will not be examined, since it is beyond the scope of this project.

The Fourier transform is invertible. Under suitable conditions it is possible to recover x from X . The procedure and conditions of the inverse Fourier transform are presented in the following theorem.

3.4. Discrete-Time Fourier Transform

Theorem 3.16 (The Fourier Inversion Theorem)

Let $x \in PC(\mathbb{R})$ be integrable and defined at the discontinuity such that $x(t) = \frac{1}{2}(x(t-) + x(t+))$. Then

$$x(t) = \lim_{\epsilon \rightarrow 0} \frac{1}{2\pi} \int_{-\infty}^{\infty} e^{-\epsilon^2 \omega^2 t} X(\omega) e^{j\omega t} d\omega = \frac{1}{2}(x(t-) + x(t+)), \quad t \in \mathbb{R}$$

and if $X \in L^1(\mathbb{R})$, then x is continuous and

$$x(t) = \frac{1}{2\pi} \int_{-\infty}^{\infty} X(\omega) e^{j\omega t} d\omega \quad t \in \mathbb{R}.$$

[4, p. 218]

The proof can be found in [4, p. 219].

3.4 Discrete-Time Fourier Transform

The discrete-time Fourier transform, henceforth referred to as DTFT, transforms discrete-time sequences into functions of continuous frequency.

Definition 3.17 (Discrete-Time Fourier Transform)

The DTFT of a sequence x is

$$X(e^{j\omega}) = \sum_{n=-\infty}^{\infty} x[n] e^{-jn\omega}$$

given that the sum converges for all $\omega \in \mathbb{R}$.

[10, p. 217]

Using $e^{-jn2\pi} = 1$ for all n it can be seen that

$$X(e^{j(\omega+2\pi)}) = \sum_{n=-\infty}^{\infty} x[n] e^{-jn(\omega+2\pi)} = \sum_{n=-\infty}^{\infty} x[n] e^{-jn\omega} e^{-jn2\pi} = X(e^{j\omega}).$$

Showing that the DTFT of a sequence is a 2π -periodic function.

The DTFT does not converge for all sequences, however it can be shown that for all sequences in $\ell^1(\mathbb{Z})$, the DTFT converges absolute.

Theorem 3.18 (DTFT of Sequences in $\ell^1(\mathbb{Z})$)

If $x \in \ell^1(\mathbb{Z})$ then the DTFT of x exists and the inverse is given by

$$x[n] = \frac{1}{2\pi} \int_{-\pi}^{\pi} X(e^{j\omega}) e^{jn\omega} d\omega, \quad \text{for } n \in \mathbb{Z}.$$

3.4. Discrete-Time Fourier Transform

The pair is denoted

$$x[n] \xleftrightarrow{DTFT} X(e^{j\omega}).$$

[10, p. 218]

Proof

Using $|e^{-jn\omega}| = 1$, we obtain

$$\sum_{n=-\infty}^{\infty} |x[n]e^{-jn\omega}| = \sum_{n=-\infty}^{\infty} |x[n]| |e^{-jn\omega}| = \sum_{n=-\infty}^{\infty} |x[n]| = \|x\|_1 < \infty.$$

Showing that Definition 3.17 is absolute convergent and thereby also convergent for all $\omega \in \mathbb{R}$ if $x \in \ell^1(\mathbb{Z})$.

To show the inverse exists notice that

$$\begin{aligned} & \frac{1}{2\pi} \int_{-\pi}^{\pi} \sum_{k=-\infty}^{\infty} x[k] e^{-jk\omega} e^{jn\omega} d\omega \\ &= \sum_{k=-\infty}^{\infty} x[k] \frac{1}{2\pi} \int_{-\pi}^{\pi} e^{j(k-n)\omega} d\omega. \end{aligned}$$

The interchange of the integral and summation is allowed since $x \in \ell^1(\mathbb{Z})$. Using that $\frac{1}{2\pi} \int_{-\pi}^{\pi} e^{j(n-k)\omega} d\omega = \delta[n-k]$ we get

$$= \sum_{k=-\infty}^{\infty} x[k] \delta[n-k] = x[n].$$

Hence the DTFT inverse exists when $x \in \ell^1(\mathbb{Z})$. ■

As a result of absolute convergence for all ω the DTFT $X(e^{j\omega})$ is a continuous function of ω if $x \in \ell^1(\mathbb{Z})$. To simplify expressions containing the DTFT some important properties are presented.

Theorem 3.19 (Linearity of DTFT)

Let x and y have the DTFT's $X(e^{j\omega})$ and $Y(e^{j\omega})$ respectively and $\alpha, \beta \in \mathbb{C}$. Then

$$\alpha x[n] + \beta y[n] \xleftrightarrow{DTFT} \alpha X(e^{j\omega}) + \beta Y(e^{j\omega}).$$

[10, p. 221]

3.4. Discrete-Time Fourier Transform

Proof

$$\begin{aligned}\sum_{n=-\infty}^{\infty} (\alpha x[n] + \beta y[n])e^{-jn\omega} &= \alpha \sum_{n=-\infty}^{\infty} x[n]e^{-jn\omega} + \beta \sum_{n=-\infty}^{\infty} y[n]e^{-jn\omega} \\ &= \alpha X(e^{j\omega}) + \beta Y(e^{j\omega}).\end{aligned}\quad \blacksquare$$

An important property is the DTFT of convolution in time.

Theorem 3.20 (DTFT of Convolution in Time)

Let $x \in \ell^1(\mathbb{Z})$ and $h \in \ell^1(\mathbb{Z})$ have the DTFT's $X(e^{j\omega})$ and $H(e^{j\omega})$ respectively. Then

$$(h * x)[n] \xleftrightarrow{DTFT} X(e^{j\omega})H(e^{j\omega}).$$

[10, p. 224]

Proof

Let $y[n] = (h * x)[n]$, then

$$\begin{aligned}Y(e^{j\omega}) &= \sum_{n=-\infty}^{\infty} y[n]e^{-jn\omega} \\ &= \sum_{n=-\infty}^{\infty} \left(\sum_{k=-\infty}^{\infty} x[k]h[n-k] \right) e^{-jn\omega},\end{aligned}$$

multiplying with $e^{-jk\omega}$ and $e^{jk\omega}$, we obtain

$$\begin{aligned}&= \sum_{n=-\infty}^{\infty} \sum_{k=-\infty}^{\infty} x[k]e^{-jk\omega} h[n-k]e^{-j(n-k)\omega} \\ &= \sum_{k=-\infty}^{\infty} x[k]e^{-jk\omega} \sum_{n=-\infty}^{\infty} h[n-k]e^{-j(n-k)\omega} = X(e^{j\omega})H(e^{j\omega}).\end{aligned}\quad \blacksquare$$

The next theorem states that multiplication in time becomes continuous circular convolution in frequency.

Theorem 3.21 (The Modulation Theorem)

Let $x \in \ell^1(\mathbb{Z})$ and $w \in \ell^1(\mathbb{Z})$ have the DTFT's $X(e^{j\omega})$ and $W(e^{j\omega})$ respectively. Then

$$x[n]w[n] \xleftrightarrow{DTFT} \frac{1}{2\pi} \int_{-\pi}^{\pi} X(e^{j\theta})W(e^{j(\omega-\theta)})d\theta.$$

[8, pp. 302–303]

3.5. The Discrete Fourier Transform

Proof

Since $x \in \ell^1(\mathbb{Z})$ by Theorem 3.18 we have that

$$x[n] = \frac{1}{2\pi} \int_{-\pi}^{\pi} X(e^{j\theta}) e^{jn\theta} d\theta, \quad \text{for } n \in \mathbb{Z}.$$

Let $y[n] = x[n]w[n]$. Then

$$\begin{aligned} Y(e^{j\omega}) &= \sum_{n=-\infty}^{\infty} y[n] e^{-jn\omega} \\ &= \sum_{n=-\infty}^{\infty} x[n] w[n] e^{-jn\omega} \\ &= \sum_{n=-\infty}^{\infty} \frac{1}{2\pi} \int_{-\pi}^{\pi} X(e^{j\theta}) e^{jn\theta} d\theta w[n] e^{-jn\omega} \\ &= \frac{1}{2\pi} \int_{-\pi}^{\pi} X(e^{j\theta}) \sum_{n=-\infty}^{\infty} w[n] e^{-jn(\omega-\theta)} d\theta \\ &= \frac{1}{2\pi} \int_{-\pi}^{\pi} X(e^{j\theta}) W(e^{j(\omega-\theta)}) d\theta. \end{aligned}$$

■

Often it is necessary to Fourier transform sequences of finite length. Therefore the DFT is introduced which can be interpreted as a tool for computing the DTFT.

3.5 The Discrete Fourier Transform

The discrete Fourier transform, henceforth referred to as DFT, transforms finite length sequences in time into finite length sequences in the frequency domain. The DFT can be interpreted as a sampled version of the DTFT of a finite length- N sequences that is zero-padded. The DTFT is 2π -periodic, hence it is only necessary to sample on the interval $[0, 2\pi]$. Let

$$\omega[k] = \frac{2\pi k}{N} \quad \text{for } k = 0, 1, \dots, N-1$$

be N uniformly distributed samples of ω on $[0, 2\pi]$. Then the DTFT is

$$\begin{aligned} X(e^{j\omega}) \Big|_{\omega=\omega[k]} &= X(e^{j\frac{2\pi k}{N}}) \\ &= \sum_{n=-\infty}^{\infty} x[n] e^{-j\frac{2\pi kn}{N}}. \end{aligned}$$

Using that x is zero-padded we get

$$= \sum_{n=0}^{N-1} x[n] e^{-j\frac{2\pi kn}{N}} = X[k],$$

3.5. The Discrete Fourier Transform

where X is called the DFT of x and formally defined as follows [10, p. 255].

Definition 3.22 (The Discrete Fourier Transform)

Let x be a length- N sequence. Then the DFT of x is given by

$$X[k] = (Fx)_k = \sum_{n=0}^{N-1} x[n] W_N^{nk} \quad \text{for } k = 0, 1, \dots, N-1,$$

where $W_N = e^{-j\frac{2\pi}{N}}$.

[10, pp. 253–254]

Notice that

$$\begin{aligned} X[k+N] &= \sum_{n=0}^{N-1} x[n] W_N^{n(k+N)} = \sum_{n=0}^{N-1} x[n] W_N^{nk} W_N^{nN} = \sum_{n=0}^{N-1} x[n] W_N^{nk} e^{-j\frac{2\pi Nk}{N}} \\ &= \sum_{n=0}^{N-1} x[n] W_N^{nk} e^{-j2\pi k} = \sum_{n=0}^{N-1} x[n] W_N^{nk} = X[k]. \end{aligned}$$

By this it makes sense to extend the N -point DTFT by circular extension making it a N -periodic sequence.

The transform is linear and thereby the transform can be expressed as a matrix-vector product. Let

$$F = \begin{bmatrix} 1 & 1 & 1 & \dots & 1 \\ 1 & W_N^1 & W_N^2 & \dots & W_N^{(N-1)} \\ 1 & W_N^2 & W_N^4 & \dots & W_N^{2(N-1)} \\ \vdots & \vdots & \vdots & \ddots & \vdots \\ 1 & W_N^{(N-1)} & W_N^{(N-1)^2} & \dots & W_N^{(N-1)^2} \end{bmatrix}$$

and $x \in \mathbb{C}^N$ and $X \in \mathbb{C}^N$. Then the transform can be expressed as

$$X = Fx.$$

The DFT is an invertible transform, which can be proved by the following theorem.

Theorem 3.23 (Inverse Discrete Fourier Transform)

The inverse DFT of a length- N sequence is given by

$$F^{-1} = \frac{1}{N} \bar{F}.$$

This can also be expressed as

$$x[n] = \frac{1}{N} \sum_{k=0}^{N-1} X[k] W_N^{-nk} \quad n = 0, 1, \dots, N-1.$$

[10, p. 254].

3.5. The Discrete Fourier Transform

Proof

To prove that F is invertible, it is shown that $\frac{1}{N}F\bar{F} = I_N$. Using the complex conjugate \bar{F} we have

$$\begin{aligned} \left(\frac{1}{N}F\bar{F}\right)_{mn} &= \frac{1}{N} \sum_{i=0}^{N-1} W_N^{mi} \overline{W_N^{in}} \\ &= \frac{1}{N} \sum_{i=0}^{N-1} e^{\frac{-j2\pi}{N}mi} e^{\frac{j2\pi}{N}ni} \\ &= \frac{1}{N} \sum_{i=0}^{N-1} e^{\frac{-j2\pi}{N}(m-n)i}. \end{aligned}$$

If $n = m$, then it is a sum of ones. If $n \neq m$, then the sum is a geometric sequence

$$= \begin{cases} \frac{N}{N} & \text{if } n = m \\ \frac{1}{N} \frac{1 - e^{\frac{-j2\pi}{N}(m-n)N}}{1 - e^{\frac{-j2\pi}{N}(m-n)}} & \text{if } n \neq m \end{cases}.$$

Using that $e^{-j2\pi(m-n)} = 1$, if $n \neq m$, we get

$$= \begin{cases} 1 & \text{if } n = m \\ 0 & \text{if } n \neq m \end{cases}.$$

This shows that $\frac{1}{N}F\bar{F} = I_N$ [10, p. 314]. ■

The DFT pair will be denoted as

$$x[n] \xleftrightarrow{DFT} X[k].$$

The DFT can be seen as DTFT for finite length sequences. Likewise, convolution can be modified to operate on finite length sequences using the modulo operator. This is denoted circular convolution which leads to the following definition.

Definition 3.24 (Circular Convolution)

The circular convolution between two length- N sequences h and x is defined as

$$(h \circledast x)[n] = \sum_{k=0}^{N-1} x[k]h[(n-k) \bmod N], \quad n = 0, 1, \dots, N-1.$$

[10, p. 213]

To derive the DFT of circular convolution in time, the following theorem is needed.

3.5. The Discrete Fourier Transform

Theorem 3.25 (Circular Shift in Time)

Let $n_0 \in \mathbb{Z}$ and x be a length- N sequence, then

$$x[(n - n_0) \bmod N] \xleftrightarrow{DFT} W_N^{kn_0} X[k].$$

[10, p. 255]

Proof

Let $y[n] = x[(n - n_0) \bmod N]$, then

$$Y[k] = \sum_{n=0}^{N-1} x[(n - n_0) \bmod N] W_N^{nk}.$$

Let $m = n - n_0$

$$= \sum_{m=-n_0}^{N-1-n_0} x[m \bmod N] W_N^{(m+n_0)k}.$$

The sum is periodic and thereby the sum can be shifted by n_0 without changing its value

$$\begin{aligned} &= \sum_{m=0}^{N-1} x[m \bmod N] W_N^{(m+n_0)k} \\ &= W_N^{n_0k} \sum_{m=0}^{N-1} x[m \bmod N] W_N^{mk} \\ &= W_N^{n_0k} X[k]. \end{aligned}$$

■

Now the DFT of circular convolution can be derived. Note that this result is similar to the DTFT of convolution.

Theorem 3.26 (DFT of Circular Convolution)

Let x and h be length- N sequences, then

$$(h \circledast x)[n] \xleftrightarrow{DFT} X[k]H[k]$$

[10, p. 257]

3.6. The Fast Fourier Transform

Proof

Let $y[n] = (h \circledast x)[n]$, then

$$\begin{aligned} Y[k] &= \sum_{n=0}^{N-1} (h \circledast x)[n] W_N^{nk} \\ &= \sum_{n=0}^{N-1} \sum_{l=0}^{N-1} x[l] h[(n-l) \bmod N] W_N^{nk} \\ &= \sum_{l=0}^{N-1} x[l] \sum_{n=0}^{N-1} h[(n-l) \bmod N] W_N^{nk}. \end{aligned}$$

Using Theorem 3.25 we get

$$= \sum_{l=0}^{N-1} x[l] W_N^{kl} H[k] = X[k] H[k],$$

which concludes the proof. ■

3.6 The Fast Fourier Transform

The fast Fourier transform, henceforth referred to as FFT, is an algorithm to efficiently calculate the DFT of a sequence. First we investigate the computational cost of the DFT. Each coefficient in an N -point DFT can be computed using N multiplications and $N - 1$ additions. Meaning that in order to compute the full DFT, N^2 multiplications and $N(N - 1)$ additions are needed. Subtractions will be counted as additions. If the cost is defined to be the sum of total numbers of multiplications and additions, then the cost of computing the DFT is

$$C_{\text{DFT}} = N(N - 1) + N^2 = 2N^2 - N. \quad (3.9)$$

A more efficient way to compute DFT is the Radix-2 FFT [10, p. 304].

Theorem 3.27 (Radix-2 FFT)

Let x be a length- N sequence where N is even, x_e be the even entries of x , x_o the odd entries and X_e and X_o be $N/2$ -DFT of x_e and x_o , respectively. Then

$$\begin{aligned} X[k] &= X_e[k] + W_N^k X_o[k] \quad k = 0, 1, \dots, \frac{N}{2} - 1 \\ X\left[k + \frac{N}{2}\right] &= X_e[k] - W_N^k X_o[k] \quad k = 0, 1, \dots, \frac{N}{2} - 1. \end{aligned}$$

[1, pp. 757–758]

3.6. The Fast Fourier Transform

Proof

It is first noted that

$$W_N^{2n} = e^{-j\frac{2\pi 2n}{N}} = e^{-j\frac{2\pi n}{N/2}} = W_{N/2}^n \quad (3.10)$$

$$W_N^{N/2} = e^{-j\frac{2\pi N/2}{N}} = e^{-j\pi} = -1. \quad (3.11)$$

The DFT of x is given by

$$X[k] = \sum_{n=0}^{N-1} x[n] W_N^{nk}.$$

Splitting the sum into an odd and an even part yields

$$\begin{aligned} &= \sum_{n=0}^{N/2-1} x[2n] W_N^{k2n} + \sum_{n=0}^{N/2-1} x[2n+1] W_N^{k(2n+1)} \\ &= \sum_{n=0}^{N/2-1} x[2n] W_N^{k2n} + W_N^k \sum_{n=0}^{N/2-1} x[2n+1] W_N^{k2n}. \end{aligned}$$

Using (3.10) we obtain

$$= \sum_{n=0}^{N/2-1} x[2n] W_{N/2}^{kn} + W_N^k \sum_{n=0}^{N/2-1} x[2n+1] W_{N/2}^{kn}.$$

The two sums is the $(N/2)$ -DFT of x_e and x_o

$$= X_e[k] + W_N^k X_o[k].$$

Using (3.11) it can be seen that $W_N^{k+N/2} = W_N^k W_N^{N/2} = -W_N^k$ and that $X_e[k]$ and $X_o[k]$ is $(N/2)$ -periodic the above can be expressed as

$$\begin{aligned} X[k] &= X_e[k] + W_N^k X_o[k] \quad k = 0, 1, \dots, \frac{N}{2} - 1 \\ X\left[k + \frac{N}{2}\right] &= X_e[k] - W_N^k X_o[k] \quad k = 0, 1, \dots, \frac{N}{2} - 1. \end{aligned} \quad \blacksquare$$

From Theorem 3.27 it can be seen that computing the first $N/2$ entries of the DFT, the second half can be computed faster since $X_e[k]$ and $W_N^k X_o[k]$ are already known. This is illustrated in Figure 3.2 when $N = 8$.

3.6. The Fast Fourier Transform

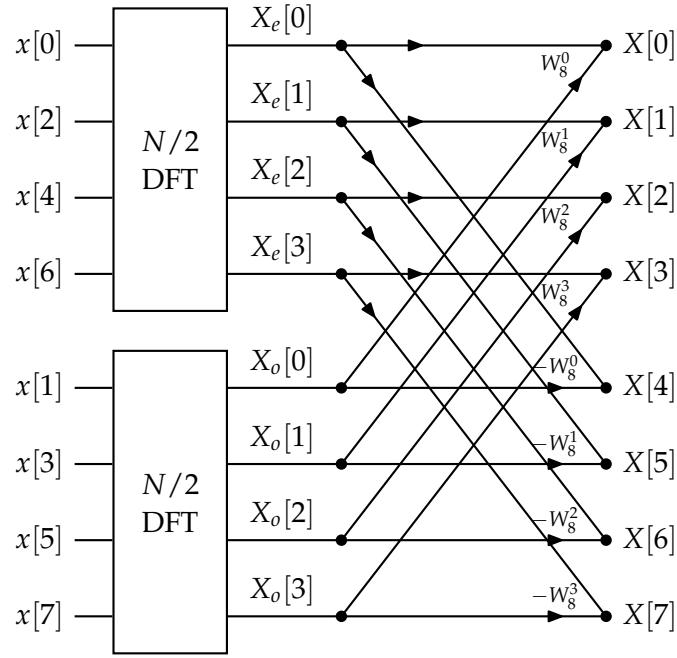


Figure 3.2: A flow graph of illustrating the Radix-2 FFT when $N = 8$.

If $N/2$ is even then the Radix-2 FFT can be applied again, this results in four $N/4$ -point DFTs. If N is limited to be on the form $N = 2^k$ where $k \in \mathbb{N}$ the Radix-2 FFT can be repeated $k = \log_2 N$ times. When finished the 2-point DFT can be computed as

$$X[0] = \sum_{n=0}^1 x[n] W_2^{n0} = x[0] + x[1]$$

$$X[1] = \sum_{n=0}^1 x[n] W_2^{n1} = x[0] + x[1] e^{-j\pi} = x[0] - x[1].$$

The negative term of $X[1]$ stems from (3.11). Therefore a 2-point DFT can be computed by adding the two points for the first coefficient and subtracting the two points for the second coefficient. To calculate the cost of the FFT let μ_N and ν_N denote the numbers of multiplications and additions of an N -point DFT, respectively. Hence $\mu_2 = 0$ and $\nu_2 = 2$. The N -point DFT can be computed as two $(N/2)$ -point DFT, $N/2$ multiplications, and N additions. Using this, the number of additions can be calculated as

$$\begin{aligned} \nu_N &= 2\nu_{N/2} + N \\ &= 2 \left(2\nu_{N/2^2} + \frac{N}{2} \right) + N = 2^2 \nu_{N/2^2} + 2N \\ &= 2^2 \left(2\nu_{N/2^3} + \frac{N}{4} \right) + 2N = 2^3 \nu_{N/2^3} + 3N \\ &\vdots \\ &= \frac{N}{2} \nu_2 + (\log_2 N - 1)N = N \log_2 N. \end{aligned}$$

3.6. The Fast Fourier Transform

The same process can be used to calculate the number of multiplications

$$\begin{aligned}
 \mu_N &= 2\mu_{N/2} + \frac{N}{2} \\
 &= 2 \left(2\mu_{N/2^2} + \frac{N}{4} \right) + \frac{N}{2} = 2^2\mu_{N/2^2} + 2\frac{N}{2} \\
 &= 2^2 \left(2\mu_{N/2^3} + \frac{N}{8} \right) + 2\frac{N}{2} = 2^3\mu_{N/2^3} + 3\frac{N}{2} \\
 &\vdots \\
 &= \frac{N}{2}\mu_2 + (\log_2 N - 1)\frac{N}{2} = \frac{N}{2}\log_2 N - \frac{N}{2}.
 \end{aligned}$$

Thereby the total cost of computing the FFT is

$$C_{\text{FFT}} = N \log_2 N + \frac{N}{2} \log_2 N - \frac{N}{2} = \frac{3N}{2} \log_2 N - \frac{N}{2}.$$

The cost of the FFT is lower than the cost of the DFT, especially when N is large [10, p. 305]. This is illustrated in the following example.

Example 3.28 (Cost of the FFT)

Let $N = 2^{10} = 1024$ then

$$\begin{aligned}
 C_{\text{DFT}} &= 2 \left(2^{10} \right)^2 - 2^{10} = 2.096.128 \\
 C_{\text{FFT}} &= \frac{3 \cdot 2^{10}}{2} \log_2 2^{10} - \frac{2^{10}}{2} = 14.848.
 \end{aligned}$$

It can be seen that the cost of the FFT is two orders of magnitude smaller than the cost of the DFT.

A plot of the cost of FFT and DFT as a function of N is shown in Figure 3.3.

3.6. The Fast Fourier Transform

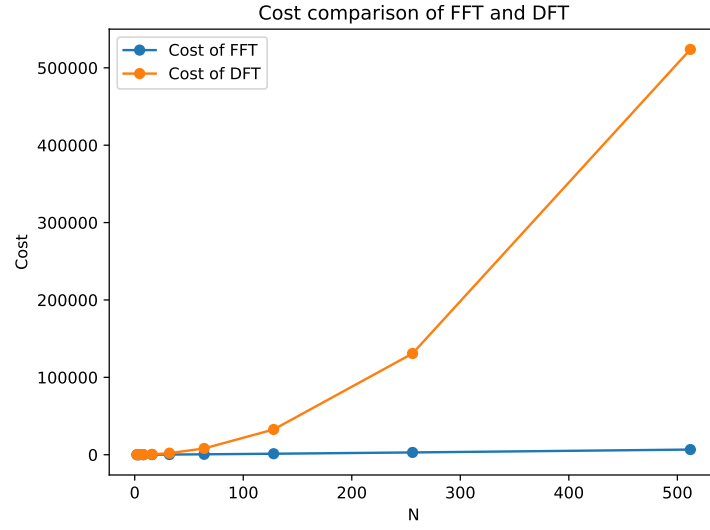


Figure 3.3: Plot of the cost of FFT and DFT as a function of $N = 2^k$ for $k = 1, 2, \dots, 9$.

Again it can be seen that the cost of the DFT grows faster than the cost of the FFT.

The inverse DFT can also be computed using the FFT algorithm. Let $X = \text{FFT}\{x\}$ represent the computation of the DFT by the FFT algorithm. Observe that

$$x = F^{-1}X = \frac{1}{N}\bar{F}X = \frac{1}{N}\bar{F}\bar{\bar{X}} = \frac{1}{N}\overline{\text{FFT}\{\bar{X}\}}.$$

Hence, the FFT algorithm can also be used to compute the inverse DFT.

Example 3.29 (Fast Fourier Transform)

Calculate the DFT of the signal $x = [1 \ -2 \ 1 \ -3]^T$ using FFT. The signal is split into even and odd entries

$$x_e = [x_0 \ x_2]^T = [1 \ 1]^T \quad \text{and} \quad x_o = [x_1 \ x_3]^T = [-2 \ -3]^T.$$

First we need to calculate F_2

$$F_2 = \begin{bmatrix} 1 & 1 \\ 1 & W_2^1 \end{bmatrix} = \begin{bmatrix} 1 & 1 \\ 1 & e^{-j2\pi/2} \end{bmatrix} = \begin{bmatrix} 1 & 1 \\ 1 & -1 \end{bmatrix}.$$

This is used to calculate X_e and X_o

$$\begin{aligned} X_e &= F_2 x_e = \begin{bmatrix} 1 & 1 \\ 1 & -1 \end{bmatrix} \begin{bmatrix} 1 \\ 1 \end{bmatrix} = \begin{bmatrix} 2 \\ 0 \end{bmatrix} \\ X_o &= F_2 x_o = \begin{bmatrix} 1 & 1 \\ 1 & -1 \end{bmatrix} \begin{bmatrix} -2 \\ -3 \end{bmatrix} = \begin{bmatrix} -5 \\ 1 \end{bmatrix}. \end{aligned}$$

3.7. The Discrete Cosine Transform

Now F_4 is calculated

$$\begin{aligned}
 F_4 &= \begin{bmatrix} 1 & 1 & 1 & 1 \\ 1 & W_4^1 & W_4^2 & W_4^3 \\ 1 & W_4^2 & W_4^4 & W_4^6 \\ 1 & W_4^3 & W_4^6 & W_4^9 \end{bmatrix} \\
 &= \begin{bmatrix} 1 & 1 & 1 & 1 \\ 1 & e^{-j2\pi/4} & (e^{-j2\pi/4})^2 & (e^{-j2\pi/4})^3 \\ 1 & (e^{-j2\pi/4})^2 & (e^{-j2\pi/4})^4 & (e^{-j2\pi/4})^6 \\ 1 & (e^{-j2\pi/4})^3 & (e^{-j2\pi/4})^6 & (e^{-j2\pi/4})^9 \end{bmatrix} \\
 &= \begin{bmatrix} 1 & 1 & 1 & 1 \\ 1 & -j & -1 & j \\ 1 & -1 & 1 & -1 \\ 1 & j & -1 & -j \end{bmatrix}.
 \end{aligned}$$

The entries of X can be calculated as

$$\begin{aligned}
 X[0] &= X_e[0] + W_4^0 X_o[0] = 2 + 1(-5) = -3 \\
 X[1] &= X_e[1] + W_4^1 X_o[1] = 0 - j(1) = -j \\
 X[2] &= X_e[0] - W_4^0 X_o[0] = 2 - (-5) = 7 \\
 X[3] &= X_e[1] - W_4^1 X_o[1] = 0 - (-j) = j.
 \end{aligned}$$

The resulting FFT signal is

$$X = [-3 \quad -j \quad 7 \quad j]^T.$$

3.7 The Discrete Cosine Transform

The discrete cosine transform, henceforth denoted DCT, is a transform similar to the DFT. However, instead of mapping a complex sequence to a complex sequence, such as the DFT, the DCT maps a real sequence to a real sequence. The DCT is defined in the following definition.

Definition 3.30 (The Discrete Cosine Transform)

The DCT of a real length- N sequence x is given by

$$X[k] = 2 \sum_{n=0}^{N-1} x[n] \cos\left(\frac{\pi k(2n+1)}{2N}\right) \quad \text{for } k = 0, 1, \dots, N-1.$$

[1, p. 703]

3.7. The Discrete Cosine Transform

The DCT is invertible and the inverse is given by the following theorem.

Theorem 3.31 (The Inverse Discrete Cosine Transform)

The inverse DCT of a real length- N sequence X is given by

$$x[n] = \frac{1}{2N}X[0] + \frac{1}{N} \sum_{k=1}^{N-1} X[k] \cos\left(\frac{\pi k(2n+1)}{2N}\right) \quad \text{for } n = 0, 1, \dots, N-1.$$

[1, p. 703]

Theorem 3.31 is stated without proof.

The computational cost of the DCT, of an input signal x , requires N^2 multiplications and $N(N-1)$ additions. The sum of total numbers of multiplications and additions then yields

$$C_{DCT} = N(N-1) + N^2 = 2N^2 - N.$$

Thus, compared to (3.9) and by Example 3.28 we find that the computational cost of the DCT is the same as for the DFT, when we count the cost of complex arithmetic the same as for real numbers.

4 Sampling

Sampling is the process of converting a continuous-time signal to a discrete-time signal. This is done by discretising a continuous-time signal to the times $t = nT$ for $n \in \mathbb{Z}$. Hence, the sampling sequence $x[n]$ can be expressed as

$$x[n] = x_c(nT) \quad \text{for } n \in \mathbb{Z},$$

where T is the sampling period, which is the time between two consecutive samples. The number of samples obtained per second is called the sampling frequency and is given by $f_s = \frac{1}{T}$. It is important to choose a sufficient sampling frequency to obtain $x[n]$. A visual representation of sampling with an insufficient sampling frequency can be seen on Figure 4.1.

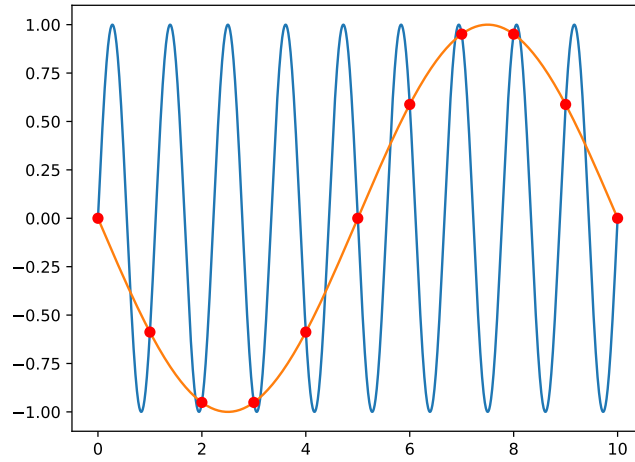


Figure 4.1: The blue curve is a sine wave with an angular frequency of 0.9 Hz and the orange curve is a sine wave with an angular frequency of 0.1 Hz. The red dots are samples of the blue curve at 1 Hz.

On the figure the red dots are samples of the blue sine wave. The orange sine wave pass through all the red dots, which means that the blue sine wave is not uniquely determined by the samples. This phenomena is called aliasing. To avoid aliasing, a sufficient sampling frequency is required. This can be determined by the Nyquist–Shannon sampling theorem [1, pp. 163–164].

Theorem 4.1 (The Nyquist–Shannon Sampling Theorem)

Let $x(t) \in L^2(\mathbb{R})$ and let the Fourier transform of x , be $X(\omega) = 0$ for $|\omega| \geq B$. If the sampling frequency is

$$\omega_s = \frac{2\pi}{T} \geq 2B,$$

where B is the Nyquist frequency and $2B$ is the Nyquist rate, then the signal $x(t)$ is uniquely determined by its samples $x[n] = x(nT)$, where $n \in \mathbb{Z}$. Furthermore,

$$x(t) = \sum_{n=-\infty}^{\infty} x\left(\frac{n\pi}{B}\right) \frac{\sin(Bt - n\pi)}{Bt - n\pi}.$$

[1, p. 170][4, pp. 230–231]

Proof

We start by expanding X according to its Fourier series on the interval $[-B, B]$, and we will replace n with $-n$ for later convenience

$$X(\omega) = \sum_{n=-\infty}^{\infty} c_{-n} e^{-\frac{j\pi n\omega}{B}}, \quad |\omega| \leq B.$$

The coefficients c_{-n} are given by Definition 3.1

$$c_{-n} = \frac{1}{2B} \int_{-B}^B X(\omega) e^{\frac{j\pi n\omega}{B}} d\omega.$$

Since the function is non-zero within $[-B, B]$ and zero otherwise, the integration limits can be expanded to \mathbb{R}

$$= \frac{1}{2B} \int_{-\infty}^{\infty} X(\omega) e^{\frac{j\pi n\omega}{B}} d\omega.$$

The Fourier inversion formula, from Theorem 3.16, then yields

$$= \frac{\pi}{B} x\left(\frac{n\pi}{B}\right).$$

Therefore the Fourier series for X is

$$X(\omega) = \sum_{n=-\infty}^{\infty} \frac{\pi}{B} x\left(\frac{n\pi}{B}\right) e^{-\frac{j\pi n\omega}{B}}, \quad |\omega| \leq B.$$

Since $x \in L^2(\mathbb{R})$ from the note under Definition 3.15 $X \in L^2(\mathbb{R})$. Furthermore since X vanishes outside a finite interval Theorem 3.14 shows that $X \in L^1(\mathbb{R})$ hence, Theorem 3.16 holds and X is given by

$$x(t) = \frac{1}{2\pi} \int_{-B}^B X(\omega) e^{j\omega t} d\omega = \frac{1}{2\pi} \int_{-B}^B \sum_{n=-\infty}^{\infty} \frac{\pi}{B} x\left(\frac{n\pi}{B}\right) e^{-\frac{j\pi n\omega}{B}} e^{j\omega t} d\omega.$$

4.1. Analog-To-Digital Converter

The interchange of the sum from the integral is permitted because the Fourier series of X converges in $L^2(-B, B)$

$$\begin{aligned}
&= \frac{1}{2\pi} \sum_{n=-\infty}^{\infty} \frac{\pi}{B} x\left(\frac{n\pi}{B}\right) \int_{-B}^B e^{-\frac{j\pi n\omega}{B}} e^{j\omega t} d\omega \\
&= \frac{1}{2\pi} \sum_{n=-\infty}^{\infty} \frac{\pi}{B} x\left(\frac{n\pi}{B}\right) \int_{-B}^B e^{j\left(t-\frac{\pi n}{B}\right)\omega} d\omega \\
&= \frac{1}{2\pi} \sum_{n=-\infty}^{\infty} \frac{\pi}{B} x\left(\frac{n\pi}{B}\right) \left[\frac{e^{j\left(t-\frac{\pi n}{B}\right)\omega}}{j\left(t-\frac{\pi n}{B}\right)} \right]_{-B}^B \\
&= \frac{1}{2\pi} \sum_{n=-\infty}^{\infty} \frac{\pi}{B} x\left(\frac{n\pi}{B}\right) \frac{e^{j\left(t-\frac{\pi n}{B}\right)B} - e^{-j\left(t-\frac{\pi n}{B}\right)B}}{j\left(t-\frac{\pi n}{B}\right)} \\
&= \sum_{n=-\infty}^{\infty} x\left(\frac{n\pi}{B}\right) \frac{1}{2B} \frac{e^{j\left(t-\frac{\pi n}{B}\right)B} - e^{-j\left(t-\frac{\pi n}{B}\right)B}}{j\left(t-\frac{\pi n}{B}\right)} \\
&= \sum_{n=-\infty}^{\infty} x\left(\frac{n\pi}{B}\right) \frac{1}{B\left(t-\frac{\pi n}{B}\right)} \frac{e^{j\left(t-\frac{\pi n}{B}\right)B} - e^{-j\left(t-\frac{\pi n}{B}\right)B}}{2j}
\end{aligned}$$

Euler's identity is used

$$\begin{aligned}
&= \sum_{n=-\infty}^{\infty} x\left(\frac{n\pi}{B}\right) \frac{\sin\left(B\left(t-\frac{\pi n}{B}\right)\right)}{B\left(t-\frac{\pi n}{B}\right)} \\
&= \sum_{n=-\infty}^{\infty} x\left(\frac{n\pi}{B}\right) \frac{\sin(Bt - n\pi)}{Bt - n\pi}.
\end{aligned}$$

From this the function $x(t)$ is uniquely determined by $\{x(\frac{n\pi}{B})\}_{n \in \mathbb{Z}}$ since it is the only variable in the sum. ■

It is determined by Theorem 3.14 that $x(t)$ is continuous in Theorem 4.1.

4.1 Analog-To-Digital Converter

In practice, sampling and analog-to-digital conversion can be performed by a single component called the ADC. However, to gain a more profound understanding these processes will be considered individually. The conversion from an analog signal to a digital signal can be divided into three steps: sample/hold (S/H), the analog-to-digital converter (ADC) and quantisation (Q) [1, p. 215]. The block diagram in Figure 4.2 shows the conversion.

4.1. Analog-To-Digital Converter



Figure 4.2: A block diagram of an analog-to-digital conversion, where $x_c(t)$ is a continuous-time signal, $x_0(t)$ is a continuous output of the S/H, $x[n]$ is a discrete-time signal and $\tilde{x}[n]$ is a quantised samples.

Sample/Hold

Sampling with a proper sampling rate Theorem 4.1 is convenient mathematically. However, in reality the sampling process can not happen instantaneous, hence, it is required to hold the computed value until the next sample value [1, p. 219]. The S/H is illustrated in Figure 4.3.

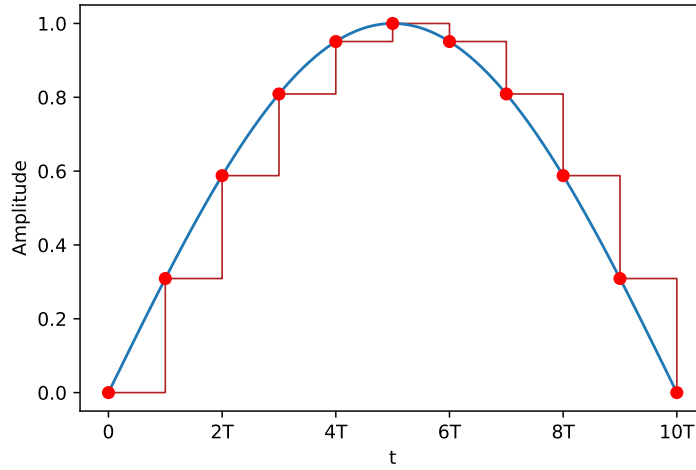


Figure 4.3: An illustration of S/H, which samples the blue analog input signal and holds the output for some length of time until the next sampled value. Every sample is marked with a red dot. This results in a red staircase wave.

Thus, the S/H process provides a signal with a finite amount of samples. These samples are discrete in time, but continuous in amplitude and must be quantised before computation.

Quantisation

Computers represent values as binary numbers. Hence, the amplitude of each sample in $x[n]$ must be approximated to a binary number. This process is called quantisation. The quantiser Q , which is an operator, divides the sample space in discrete intervals and approximates the amplitude to a binary number. Applying Q to a sequence is expressed as

$$Q(x[n]) = \tilde{x}[n].$$

4.1. Analog-To-Digital Converter

The step size is dependent on the spacing of the quantisation level, which is typically uniform and can be expressed as

$$\Delta = \frac{L_D}{2^B}.$$

The number of bits is denoted B and L_D is the length of the domain the quantiser is applied on. The step size is the smallest possible distance between two quantisation levels [1, pp. 220–222]. When converting a continuous amplitude to a binary number, information is lost as a result of the approximation. In consequence, the quantisation process is irreversible i.e. an error occurs, which can be expressed as

$$e[n] = \tilde{x}[n] - x[n].$$

Therefore, the greater the number of bits, the distance between \tilde{x} and x approaches zero. The quantised sample must obtain values at the quantisation levels, therefore the maximum value of the error will be $\frac{\Delta}{2}$ i.e.

$$-\frac{\Delta}{2} \leq e[n] < \frac{\Delta}{2}.$$

Figure 4.4 shows an example of quantisation to 3-bit, where the green dots represent the actual values of the signal, and the red circles represent the quantised values.

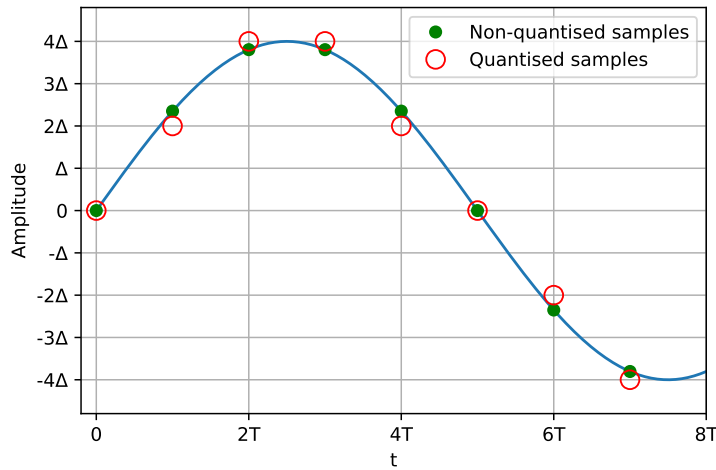


Figure 4.4: Quantised samples, non-quantised samples, and the error of a 3-bit quantiser.

As seen on the figure, the red circles deviate from the original value. This is due to the error that occurs [1, pp. 224–226].

5 Filter Theory

In discrete-time signal processing, a signal can have unwanted or irrelevant frequencies that we want to attenuate. This can be done by a digital filter.

5.1 Digital Filters

Generally, there are four basic filter types: low-pass, high-pass, band-pass and band-stop. The low-pass filter does not effect low frequencies but attenuate high frequencies, whereas the high-pass filter attenuates the low frequencies and passes the high frequencies. The band-pass filter passes only frequencies in a specific band, and the band-stop filter only attenuates frequencies in a specific band. The area where the frequencies is allowed to pass is called the passband, and the area where the frequencies is attenuated is called the stopband. The abrupt transition from the passband to the stopband is the cut-off frequency. These four filters are visualised on Figure 5.1.

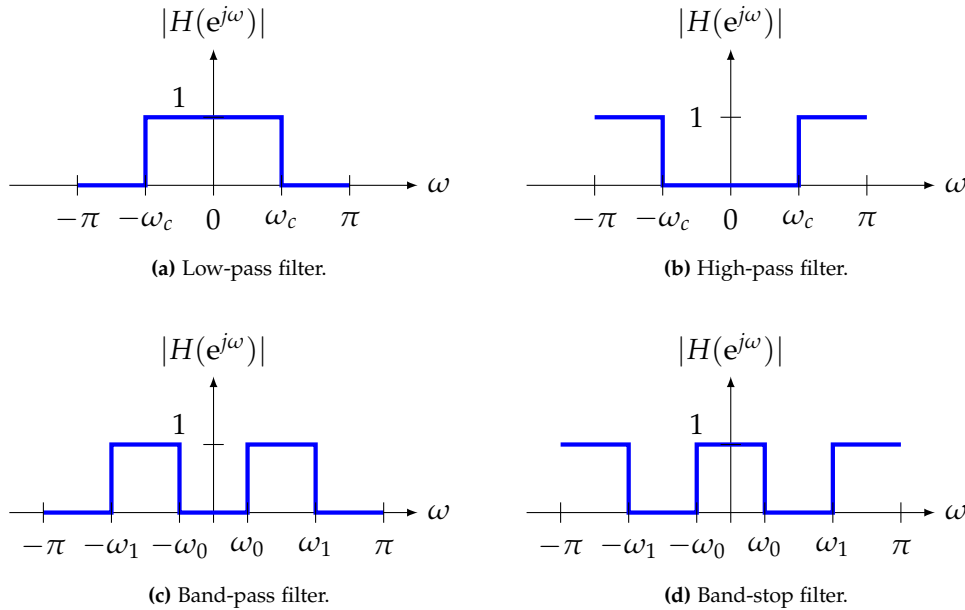


Figure 5.1: Representation of the magnitude of the four types of filters, where $\pm\omega_c$ is the cut-off frequency for the low-pass and high-pass filter and $\pm\omega_0$ and $\pm\omega_1$ is the boundaries of the passband for the band-pass and band-stop filter.

These filters are all ideal filters, meaning the gain is 1 in the passband and 0 in the stopband, and the transition from the passband to the stopband occurs abrupt [8, p. 313]. However, in practical settings the abrupt transition is not realisable. Therefore, a transition band between the passband and stopband is allowed consequently the attenuation increases monotonically. A representation of the tolerance limits of a low-pass filter can be seen on Figure 5.2.

5.2. Generalised Linear Phase

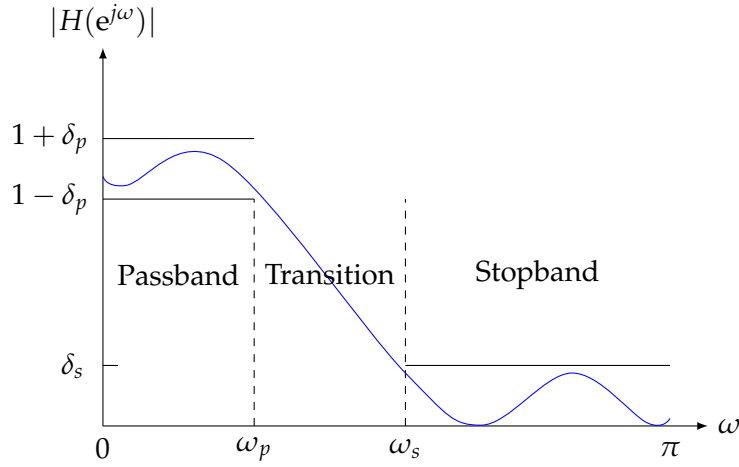


Figure 5.2: A tolerance scheme of a low-pass filter.

As shown on Figure 5.2, ω_p is the passband edge frequency and ω_s is the stopband edge frequency. The tolerance limits, denoted δ_p and δ_s , are the tolerance limits on the passband and the stopband, respectively [1, pp. 518–519].

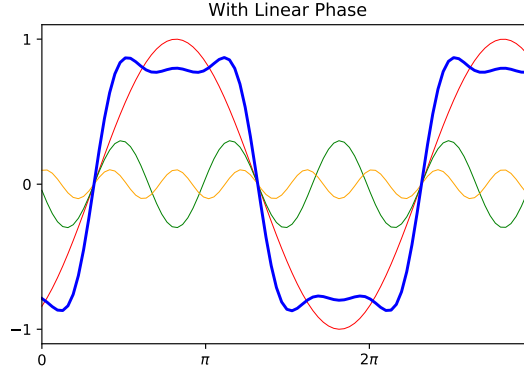
To further categorise, digital filters can be divided into two groups, IIR and FIR filters. The IIR filter has the advantage of a lower implementation cost, due to a fewer numbers of arithmetic operations compared to the FIR filter. FIR filters are always stable by Theorem 2.23, while IIR filters are potentially unstable. The most significant difference is that FIR filters can be designed with linear phase. A system with linear phase is beneficial when the frequency content of a signal is modified, where the goal is to maintain the waveform as close to the original signal as possible. With zero phase it is possible to maintain the original waveform completely, however, for causal systems zero phase is not attainable. Zero phase leads to left-right symmetric impulse response around zero and thereby leads to a non-causal system. This is problematic since half of the impulse response occurs before the time reference 0. Linear phase also leads to a left-right symmetric impulse response, however, it is delayed compared to systems with zero phase, excluding negative indices when the impulse response is truncated. This results in an identical delay in the output signal. Linear phase ensures that at every frequency the signal is equally delayed. This phenomena is referred to as group delay [1, p. 336].

5.2 Generalised Linear Phase

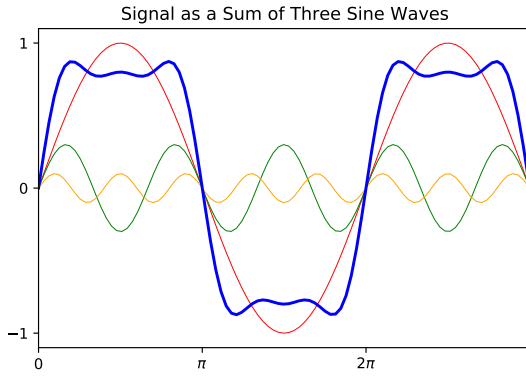
Linear phase ensures a constant group delay in contrast to systems with non-linear phase which potentially leads to major distortions of the waveform in the signal. The importance of linear phase and group delay is illustrated in Figure 5.3 where the resulting signal of three sine waves is input to a LTI system with linear phase. Group delay will result in a new signal with approximately the same waveform as the input. If the same signal is input to a LTI system with non-linear phase, the components will be delayed

5.2. Generalised Linear Phase

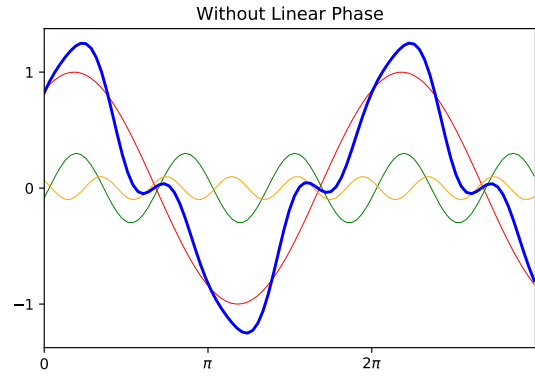
separately resulting in a waveform that differs from the original input. Note that the filter used in this illustration is an all-pass filter and therefore the output is not scaled, which could be the case if a different filter was used.



(a) A signal, blue graph, as a sum of three sine waves.



(b) Output of an LTI system with linear phase.



(c) Output of an LTI system without linear phase.

Figure 5.3: The blue graph represents a signal which is the sum of three sine waves plotted as green, orange and red. The plots (b) and (c) shows the resulting output signal of LTI systems with linear and non-linear phase, respectively.

A system with linear phase can be characterised by constant group delay.

This type of system can be designed with frequency response as expressed in the following definition.

Definition 5.1 (Frequency Response for Generalised Linear Phase Systems)

A generalised linear phase system has frequency response

$$H(e^{j\omega}) = A(e^{j\omega})e^{-j(\alpha\omega - \beta)},$$

where $\alpha, \beta \in \mathbb{R}$ and $A(e^{j\omega})$ is a real function.

[1, p. 340]

5.2. Generalised Linear Phase

The magnitude for a system with linear phase is

$$|H(e^{j\omega})| = |A(e^{j\omega})||e^{-j(\alpha\omega - \beta)}| = |A(e^{j\omega})|.$$

The phase is

$$\begin{aligned}\angle H(e^{j\omega}) &= \arg\{A(e^{j\omega})[\cos(\alpha\omega - \beta) - j\sin(\alpha\omega - \beta)]\} \\ &= \arg\{A(e^{j\omega})\} + \arctan\left(\frac{-\sin(\alpha\omega - \beta)}{\cos(\alpha\omega - \beta)}\right) \\ &= \begin{cases} -(\alpha\omega - \beta) & \text{if } A(e^{j\omega}) \geq 0 \\ -(\alpha\omega - \beta) - \pi & \text{if } A(e^{j\omega}) < 0 \end{cases}.\end{aligned}$$

Thus, the phase is the equation for a straight line resulting in linear phase.

The phase is used when calculating the group delay

$$G(e^{j\omega}) = -\frac{d}{d\omega}\angle H(e^{j\omega}) = \alpha.$$

When the group delay equals a constant it ensures that every frequency ω is delayed equally [1, p.341]. A necessary, however not sufficient, condition for linear phase is stated in the following theorem.

Theorem 5.2 (Condition for Linear Phase)

For systems with linear phase the condition

$$\sum_{n=-\infty}^{\infty} h[n] \sin[\omega(n - \alpha) + \beta] = 0$$

must be valid for all ω .

[1, p. 341]

Proof

The frequency response for a linear phase system can be expressed as

$$\begin{aligned}H(e^{j\omega}) &= A(e^{j\omega})e^{-j(\alpha\omega - \beta)} \\ &= A(e^{j\omega})\cos(\beta - \alpha\omega) + A(e^{j\omega})j\sin(\beta - \alpha\omega)\end{aligned}\tag{5.1}$$

or equivalently

$$\begin{aligned}H(e^{j\omega}) &= \sum_{n=-\infty}^{\infty} h[n]e^{-jn\omega} \\ &= \sum_{n=-\infty}^{\infty} h[n]\cos(\omega n) - j \sum_{n=-\infty}^{\infty} h[n]\sin(\omega n).\end{aligned}\tag{5.2}$$

The phase is calculated for the two expressions. First the phase of (5.1)

$$\angle H(e^{j\omega}) = \arctan\left(\frac{\sin(\beta - \alpha\omega)}{\cos(\beta - \alpha\omega)}\right).\tag{5.3}$$

5.2. Generalised Linear Phase

Then the phase of (5.2)

$$\angle H(e^{j\omega}) = \arctan \left(\frac{-\sum_{n=-\infty}^{\infty} h[n] \sin(\omega n)}{\sum_{n=-\infty}^{\infty} h[n] \cos(\omega n)} \right). \quad (5.4)$$

Since the left hand side is identical in (5.3) and (5.4), then

$$\arctan \left(\frac{\sin(\beta - \alpha\omega)}{\cos(\beta - \alpha\omega)} \right) = \arctan \left(\frac{-\sum_{n=-\infty}^{\infty} h[n] \sin(\omega n)}{\sum_{n=-\infty}^{\infty} h[n] \cos(\omega n)} \right)$$

and thereby

$$\frac{\sin(\beta - \alpha\omega)}{\cos(\beta - \alpha\omega)} = \frac{-\sum_{n=-\infty}^{\infty} h[n] \sin(\omega n)}{\sum_{n=-\infty}^{\infty} h[n] \cos(\omega n)}.$$

Cross multiplying leads to the expression

$$\sum_{n=-\infty}^{\infty} h[n] \cos(\omega n) \sin(\beta - \alpha\omega) = - \sum_{n=-\infty}^{\infty} h[n] \sin(\omega n) \cos(\beta - \alpha\omega).$$

Adding the right hand side term on both sides

$$\sum_{n=-\infty}^{\infty} h[n] (\cos(\omega n) \sin(\beta - \alpha\omega) + \sin(\omega n) \cos(\beta - \alpha\omega)) = 0.$$

Using the trigonometric identity $\sin(a + b) = \sin(a) \cos(b) + \cos(a) \sin(b)$ yields

$$\sum_{n=-\infty}^{\infty} h[n] \sin[\omega(n - \alpha) + \beta] = 0,$$

which is the desired result. ■

Some general values that fulfills the condition in Theorem 5.2 are

$$\begin{aligned} \beta &= 0 \quad \text{or} \quad \pi, \\ 2\alpha &= M, \quad \text{where } M \text{ is an integer,} \\ h[M - n] &= h[n] \quad \text{for } n = 0, 1, \dots, M. \end{aligned}$$

With the above values for β, α and h , the impulse response will be symmetric around $\alpha = \frac{M}{2}$ [1, pp. 341–342]. Another set of sufficient values to fulfill the condition in Theorem 5.2 are

$$\begin{aligned} \beta &= \frac{\pi}{2} \quad \text{or} \quad \frac{3\pi}{2}, \\ 2\alpha &= M, \quad \text{where } M \text{ is an integer,} \\ h[M - n] &= -h[n] \quad \text{for } n = 0, 1, \dots, M. \end{aligned}$$

In this case the impulse response is anti-symmetric [1, p.342]. This results in four different FIR filter types with generalised linear phase. The order M of the filter is either even or

5.3. The Window Method

odd and the impulse response is either symmetric or anti-symmetric around α . This can be seen on Table 5.1.

| $h[n]$ \ M | Even | Odd |
|----------------|------|-----|
| Symmetric | I | II |
| Anti-symmetric | III | IV |

Table 5.1: The different types of FIR filters.

The type I FIR filter has a symmetric impulse response around $\alpha = \frac{M}{2}$

$$h[n] = h[M - n], \quad 0 \leq n \leq M,$$

and with M even. The frequency response is given by

$$H(e^{j\omega}) = e^{-j\omega M/2} \left(\sum_{k=0}^{M/2} a[k] \cos(\omega k) \right),$$

where

$$\begin{aligned} a[0] &= h[M/2], \\ a[k] &= 2h[(M/2) - k], \quad k = 1, 2, \dots, M/2 \end{aligned}$$

[1, p. 343]. The frequency response is used in a method to design FIR filters with generalised linear phase. Therefore the following method needs to be introduced.

5.3 The Window Method

The design techniques for FIR filters are based upon approximating the desired frequency response or impulse response of the discrete-time system. A simple design approach is called the window method, commonly referred to as windowing.

The method begins with the ideal desired frequency response, represented by the Fourier series as

$$H_d(e^{j\omega}) = \sum_{n=-\infty}^{\infty} h_d[n] e^{-jn\omega}, \quad \text{for } n \in \mathbb{Z},$$

where the Fourier coefficients are expressed by the inverse DTFT as

$$h_d[n] = \frac{1}{2\pi} \int_{-\pi}^{\pi} H_d(e^{j\omega}) e^{jn\omega} d\omega. \quad (5.5)$$

Given H_d the impulse response can be determined when evaluating the integral in (5.5). In general h_d becomes noncausal and infinitely. Thus, in order to implement h_d it must be

5.3. The Window Method

truncated at some point $n = M$, to yield a causal FIR filter of length $M + 1$. The truncation can be done by the window method. Theoretically, the method consists of windowing the ideal impulse response by a chosen rectangular window function w defined as

Definition 5.3 (The Rectangular Window)

$$w[n] = \begin{cases} 1, & 0 \leq n \leq M, \\ 0, & \text{otherwise} \end{cases}.$$

[1, p. 558]

Hence, the new impulse response of the FIR filter becomes

$$\begin{aligned} h[n] &= w[n]h_d[n] \\ &= \begin{cases} h_d[n], & 0 \leq n \leq M, \\ 0, & \text{otherwise} \end{cases}, \end{aligned}$$

which is finite in duration and causal [1, pp. 557–558]. Studying the effects of the window method, we remember from Theorem 3.21 that multiplication of w with h_d is equivalent to convolution of H_d with the Fourier transformed window W i.e.

$$W(e^{j\omega}) = \sum_{n=0}^M w[n]e^{-jn\omega}.$$

The convolution yields the frequency response of the truncated FIR filter, hence

$$H(e^{j\omega}) = \frac{1}{2\pi} \int_{-\pi}^{\pi} H_d(e^{j\theta})W(e^{j(\omega-\theta)})d\theta.$$

Thus, $H(e^{j\omega})$ becomes an approximated version of the desired $H_d(e^{j\omega})$. If $w[n] = 1$ for all n , then $W(e^{j\omega})$ is a 2π -periodic, in consequence $H(e^{j\omega}) = H_d(j\omega)$. The Fourier transform of the rectangular window is

$$\begin{aligned} W(e^{j\omega}) &= \sum_{n=0}^M e^{-jn\omega} \\ &= \frac{1 - e^{-j(M+1)\omega}}{1 - e^{-j\omega}} = e^{-j\omega M/2} \frac{\sin[\omega(M+1)/2]}{\sin(\omega/2)}. \end{aligned}$$

Where the magnitude is given by

$$|W(e^{j\omega})| = \frac{|\sin[\omega(M+1)/2]|}{|\sin(\omega/2)|}, \quad \text{for } |\omega| \leq \pi. \quad (5.6)$$

The magnitude of (5.6) for $M = 25$ and $M = 50$ is depicted in Figure 5.4

5.3. The Window Method

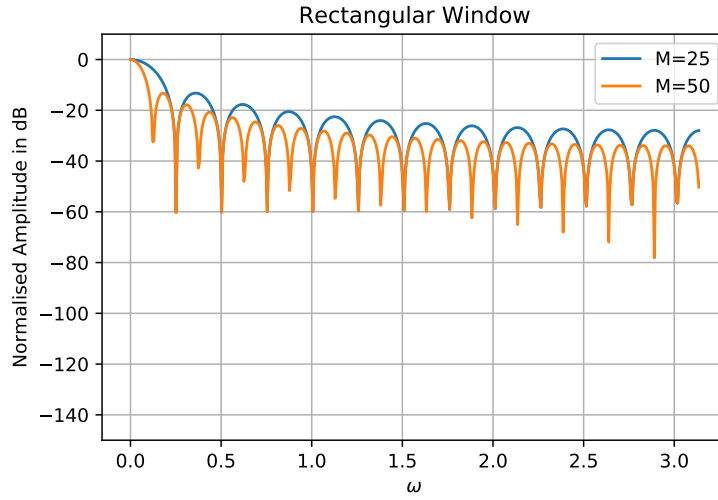


Figure 5.4: Magnitude of the rectangular window for $M = 25$ and $M = 50$.

The width of the main lobe is measured to the first zero of W on both sides, and it determines the length of the transition band given by a function of ω , as illustrated in Figure 5.2. As M increases, the width of the main lobe decreases, resulting in a narrow transition band. However, the width and the height of each sidelobe extend in such a way that the area under each sidelobe remains invariant to any change in M . These characteristics are significant when determining the frequency response of the truncated FIR filter. The discontinuity of H_d results in oscillating behavior, when each sidelobe moves past the discontinuities, since the area under each sidelobe remains unchanged the oscillations occurs more rapidly. This behavior is known as Gibbs phenomena. Gibbs phenomena is characterised by high frequency oscillating behavior near points of discontinuities resulting in a overshoot and undershoot [1, p. 558]. This is illustrated on Figure 5.5.

5.3. The Window Method

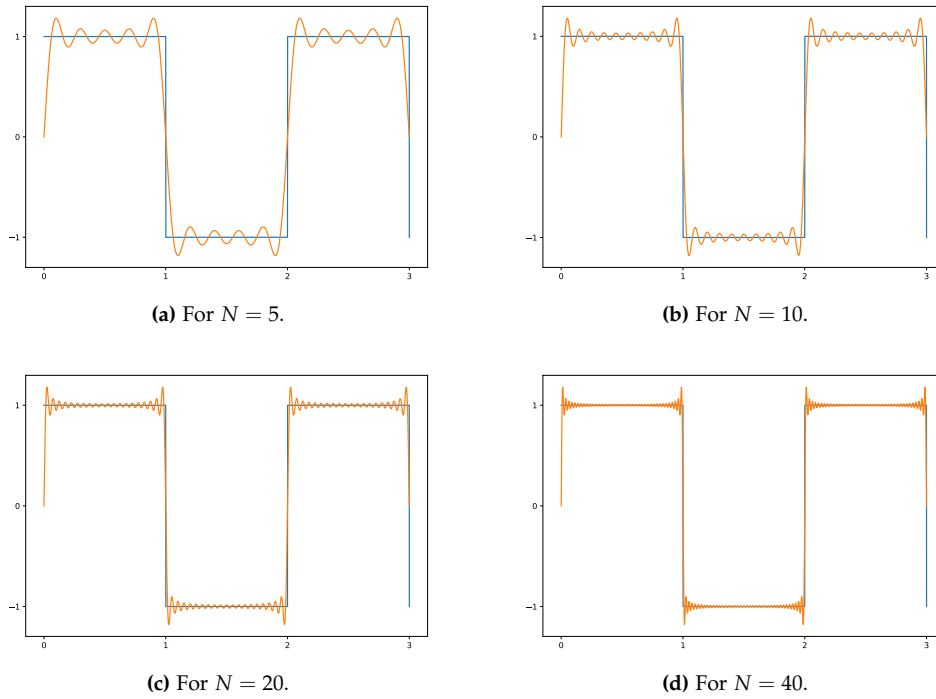


Figure 5.5: Representation of Gibbs phenomena for the squared wave $\frac{4}{\pi} \sum_1^N \frac{\sin(n\pi x)}{n}$.

The phenomena can be moderated by choosing windows without abrupt discontinuities in their time domain. Figure 5.6 illustrates three commonly used windows in their time domain.

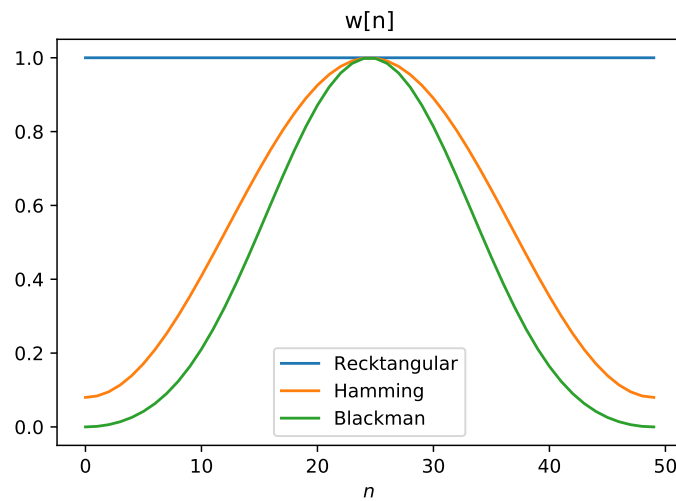


Figure 5.6: The rectangular, Hamming and Blackman windows plotted for $M = 50$.

The Hamming window and Blackman window can be formally defined as follows.

Definition 5.4 (The Hamming Window)

$$w[n] = \begin{cases} 0.54 - 0.46 \cos(2\pi n/M), & 0 \leq n \leq M, \\ 0, & \text{otherwise} \end{cases}.$$

[1, p. 560]

The magnitude of the Hamming window is depicted in Figure 5.7.

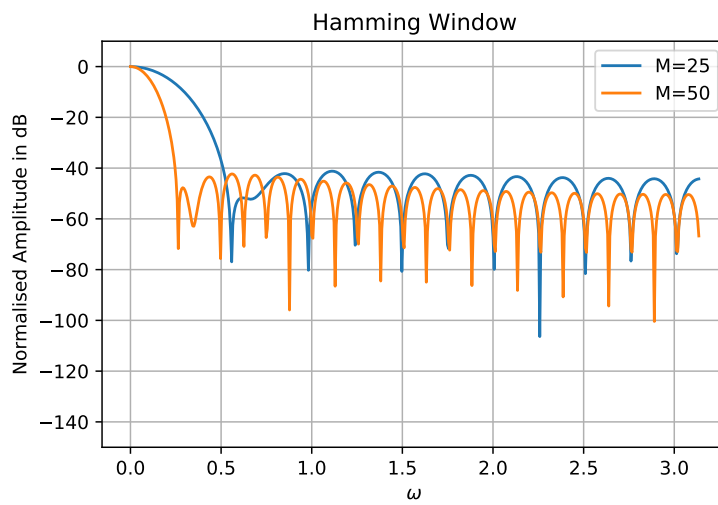


Figure 5.7: Magnitude of the Hamming window for $M = 25$ and $M = 50$.

Definition 5.5 (The Blackman Window)

$$w[n] = \begin{cases} 0.42 - 0.5 \cos(2\pi n/M) + 0.08 \cos(4\pi n/M), & 0 \leq n \leq M, \\ 0, & \text{otherwise} \end{cases}.$$

[1, p. 560]

The magnitude of the Blackman window is depicted in Figure 5.8.

5.3. The Window Method

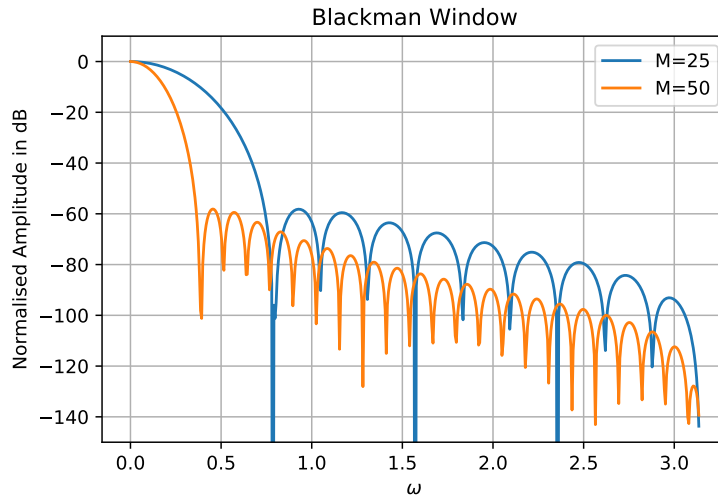


Figure 5.8: Magnitude of the Blackman window for $M = 25$ and $M = 50$.

Figure 5.6 depicts the windows defined above. Both the Hamming window and the Blackman window have significantly lower sidelobes than the rectangular window. Meanwhile, the main lobe is wider for both windows. In consequent, performing the convolution, the window functions provide more smoothing in the frequency domain, contrariwise, this results in a wider transition window [1, p. 558]. These properties are listed in Table 5.2 for commonly used windows.

| Type of Window | Peak Side Lobe (dB) | Approximate Transition Width of Main Lobe |
|----------------|---------------------|---|
| Rectangular | -13 | $4\pi/M$ |
| Hamming | -41 | $8\pi/M$ |
| Blackman | -57 | $12\pi/M$ |

Table 5.2: Comparison of properties of commonly used windows.

Implementing window functions in practical settings can be done combined with the short-time Fourier transform. This is demonstrated in the following chapter where the short-time Fourier transform is introduced.

6 Application of The Short-Time Fourier Transform

The DFT is not sufficient when a signal's frequency changes with time. Instead the short-time Fourier transform, henceforth referred to as STFT, is used since it provides information of the time-dependent frequency. The benefits of the STFT will be reviewed in the following section, followed by examples of spectrograms and an application of the STFT using different window functions to demonstrate Heisenberg's uncertainty principle.

6.1 The Short-Time Fourier Transform

The STFT splits the signal into segments and then performs the DFT on each of these segments individually. The signal is split by windowing.

Definition 6.1 (The Short-Time Fourier Transform)

The short-time Fourier transform of a signal x is

$$X[n, \lambda] = \sum_{m=-\infty}^{\infty} x[n+m]w[m]e^{-j\lambda m}, \quad n \in \mathbb{Z}.$$

n is the discrete time and λ is the 2π -periodic continuous frequency.

[1, p. 846]

Computing the STFT explicit, discretisation is required since λ is an infinite set of values. This is done by sampling $X[n, \lambda]$ at N equally spaced frequencies $\lambda_k = \frac{2\pi k}{N}$ for $k = 0, \dots, N-1$, with a window w of length L [1, p. 854]. Assume that the samples begin at $m = 0$, then the window is defined as

$$w[m] = \begin{cases} w[m], & 0 \leq m \leq L-1, \\ 0, & \text{otherwise} \end{cases}.$$

This leads to the discrete STFT, henceforth referred to as DSTFT, which is a sequence of L -point DFTs of the segments

$$x_r[m] = x[rR+m]w[m], \quad r \in \mathbb{Z}, \quad m = 0, 1, \dots, L-1,$$

where R is a constant used to control the number of overlapping samples between segments. If $R < L$ the segments overlap, however if $R > L$ some of the samples of the signal is ignored resulting in a loss of information. This is due to the fact that window functions such as the Hamming window and the Blackman window, formally defined in

6.2. Spectrograms

Section 5.3, are very small, or zero, near their boundaries resulting in a loss of information. This situation can be improved implementing an overlap of segments as illustrated on Figure 6.1 [1, p. 855].

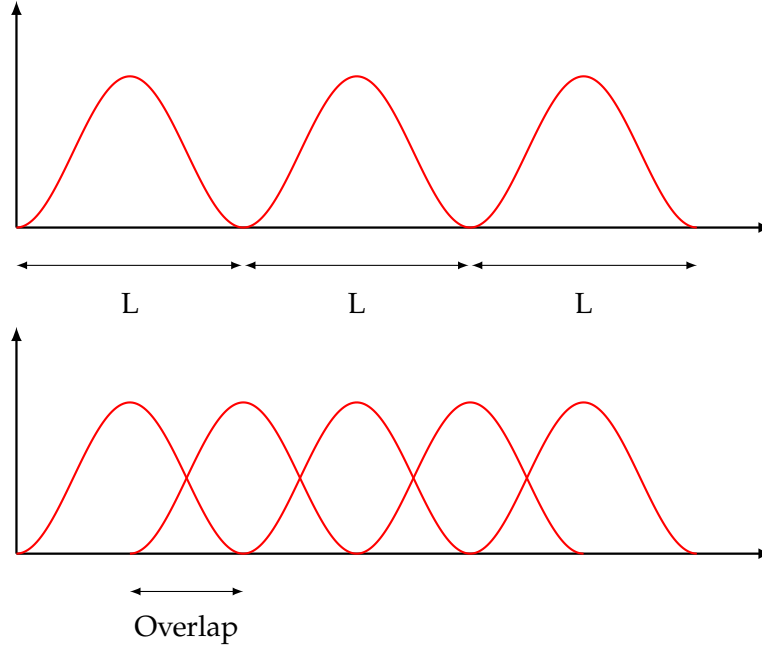


Figure 6.1: Length- L window function with and without overlap.

We finish this chapter implementing an overlap in an example, however, to continue the introduction of the DSTFT a formal definition is provided.

Definition 6.2 (The Discrete Short-Time Fourier Transform)

The discrete short-time Fourier transform is given by

$$X[rR, k] = \sum_{m=0}^{L-1} x[rR + m]w[m]e^{-j\frac{2\pi}{N}km}, \quad r \in \mathbb{Z} \quad k = 0, 1, \dots, N-1.$$

Where w is of length L .

[1, p. 855]

Studying signals where the frequency changes over time the DSTFT is efficient. The DSTFT can be visualised by a spectrogram.

6.2 Spectrograms

The DSTFT is a function of two variables i.e. the spectrogram is a three dimensional plot with time on the x -axis, frequency on the y -axis, and power on the z -axis, defined

6.2. Spectrograms

as $|X[rR, k]|^2$. The power is visualised by a colour bar on the right-hand side of the spectrogram, and the amount of power is represented by the intensity of the colours. Dark colors represent low amount of power while bright colors represent high amount of power. A plot of a spectrogram is depicted in the following example.

Example 6.3 (Spectrogram of a Function)

Let a signal be given as

$$x(t) = \cos(2\pi 1000 t^2).$$

Sampling $x(t)$ yields the discrete-time signal

$$x[n] = \cos\left(2\pi 1000 \left(\frac{n}{f_s}\right)^2\right), \quad (6.1)$$

where the sampling frequency is $f_s = 8000$ Hz. The plot of the signal can be seen on Figure 6.2.

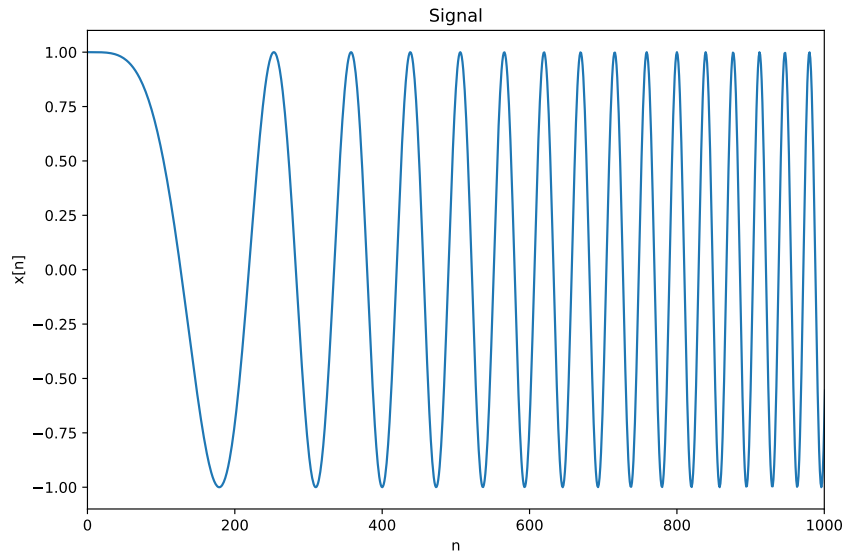


Figure 6.2: The signal $x[n]$ for $f_s = 8000$ Hz.

The spectrogram of (6.1) is then plotted.

6.2. Spectrograms

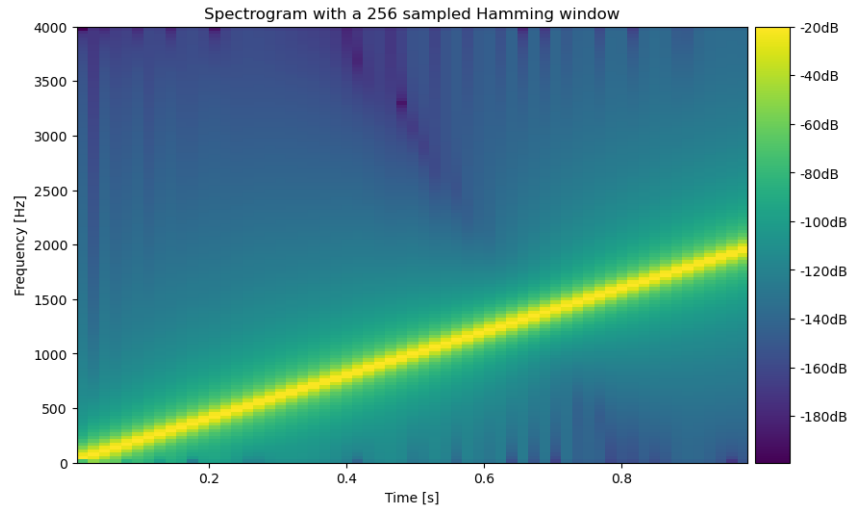


Figure 6.3: Spectrogram with a 256-length Hamming window without overlap.

On the spectrogram, a 256-length Hamming window is used. It can be seen that there is a straight yellow line from 0 Hz at $t = 0$ to 2000 Hz at $t \approx 1$. The yellow colors represent large values of the DSTFT.

To demonstrate spectrograms in a practical application, we let the signal be a speech signal of a male pronouncing the sentence *"Two plus seven is less than ten"*. A plot of the time domain representation of the speech signal and the spectrogram are depicted on Figure 6.4.

6.3. Heisenberg's Uncertainty Principle

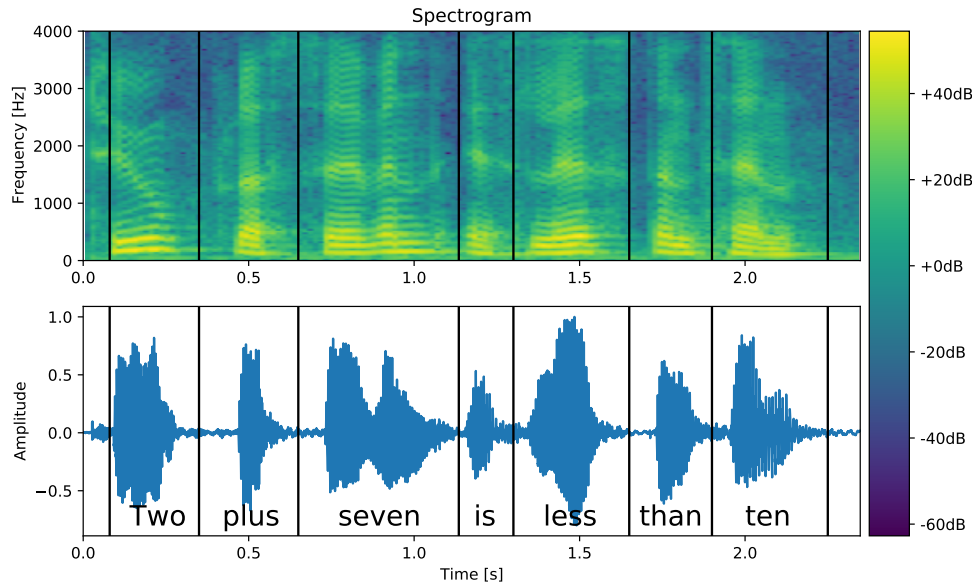


Figure 6.4: A spectrogram of a speech signal of a male pronouncing the sentence “Two plus seven is less than ten”.

It can be seen that most of the speech signal frequency content is below 3000 Hz. The parts of the signal that is over 3000 Hz stem from when the speakers pronounces an “s” sound, in the words *plus*, *seven*, *is* and *less*. In practice, speech signals band-limited to frequencies below 3000 Hz is still highly intelligible [1, p. 867].

6.3 Heisenberg's Uncertainty Principle

When working with spectrograms the goal is to obtain high resolution in both the frequency and time domain. However, this is not possible since one occur at the expense of the other. This is stated in the uncertainty principle for finite-length sequences.

Theorem 6.4 (Uncertainty Principle for Finite-Length Sequences)

Let a nonzero $x \in \mathbb{C}^N$ have N_t nonzero entries and the discrete-time Fourier transform X with N_f nonzero entries. Then,

$$N_t N_f \geq N.$$

[10, p. 637]

By Theorem 6.4 one cannot have both high resolution in time and frequency at the same time. There is a trade-off in between. This is a direct consequence of Theorem 6.4 that states that the product of the nonzero entries of x and X is bounded by a lower bound. In consequence, the fewer nonzero entries of x the more nonzero entries X must have, to satisfy the lower bound N in Theorem 6.4. We finish this section with an example of the trade-off between time and frequency.

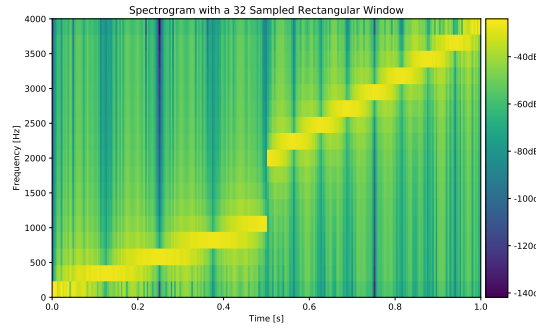
6.3. Heisenberg's Uncertainty Principle

Example 6.5 (Trade-off Between High Resolution in Time and Frequency)

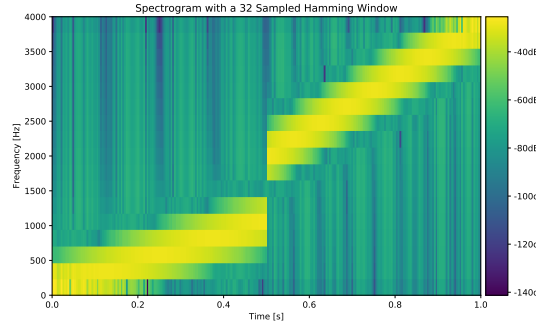
Consider the signal

$$x[n] = \begin{cases} \cos\left(2\pi 1000 \left(\frac{n}{f_s}\right)^2\right), & \text{for } n \leq 4000 \\ \cos\left(2\pi 2000 \left(\frac{n}{f_s}\right)^2\right), & \text{otherwise} \end{cases}, \quad (6.2)$$

where $f_s = 8000$ Hz. The DSTFT combined with the rectangular and Hamming window is used on the signal. This results in the following plots.



(a) The rectangular window.



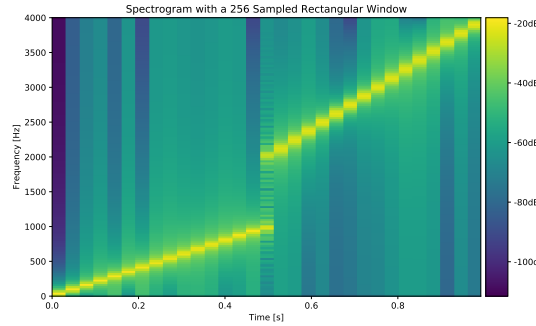
(b) The Hamming window.

Figure 6.5: Spectrograms with a 32-length window.

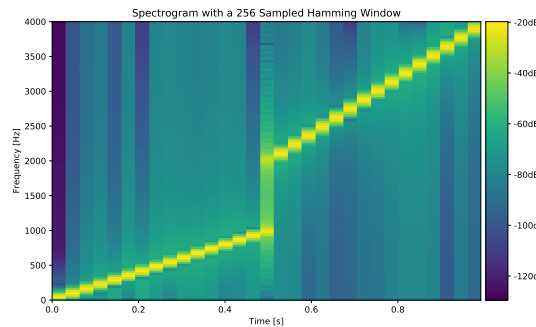
Studying Figure 6.5 we find that it is not possible to see the exact frequency that is present in the signal, whereas the time is in higher resolution. We see a change in the frequency happening abrupt, which is a consequence of a discontinuity in the function. The difference between the two windows can be found studying the characteristics of Figure 5.4 and Figure 5.7, where we see that the rectangular window has a narrow main lobe and more oscillating behavior in the sidelobes compared to the hamming window. In consequence, we see a higher intensity of power concentrated around the yellow line on Figure 6.5b compared to Figure 6.5a where the intensity of power is smeared all over

6.3. Heisenberg's Uncertainty Principle

the spectrogram. However, by increasing the window length we obtain the following spectrograms.



(a) The rectangular window.



(b) The Hamming window.

Figure 6.6

Thus, we see that the resolution in the frequency domain has improved. This occurs at the expense of a low resolution in time which demonstrates the trade-off between time and frequency. Therefore, it is important to determine a window length sufficient to provide a satisfactory resolution in time and frequency.

This chapter is finished demonstrating the effect of windowing with overlap. First the overlap for a Hamming window is illustrated on Figure 6.7.

6.3. Heisenberg's Uncertainty Principle

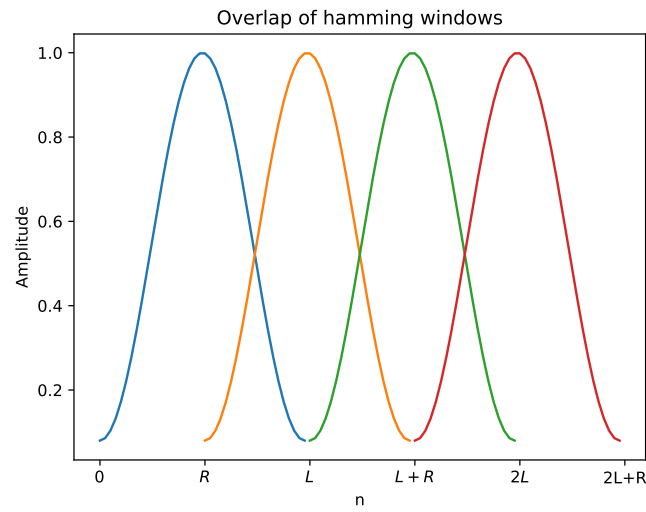


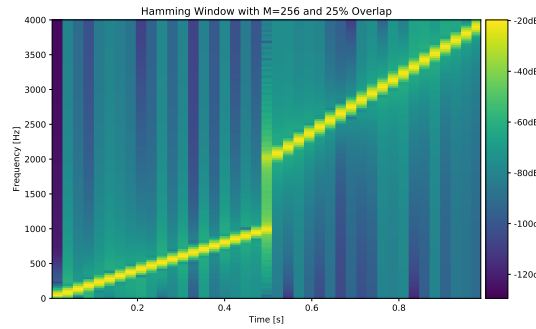
Figure 6.7: Overlapping Hamming windows.

We see on the figure how Hamming windows are plotted with a length- R overlap. Since $L = 2R$ we have a factor 2 or a 50% overlap. This is illustrated with spectrograms in the following example.

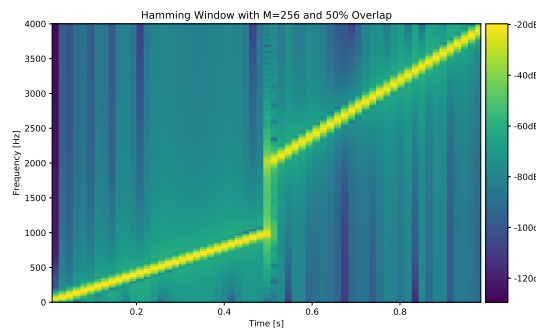
Example 6.6 (Overlapping)

Consider the function defined by (6.2). Using the DSTFT combined with the Hamming window, different overlaps are depicted in Figure 6.6

6.3. Heisenberg's Uncertainty Principle



(a) 25% overlap.



(b) 50% overlap.

Figure 6.8: Spectrograms with a 256-length window.

Comparing the two figures with Figure 6.6b we see that applying an overlap results in a smoother line in the spectrogram. This improves the accuracy when reading the spectrogram.

However, the accuracy of the improved spectrogram comes with a higher computational cost. Consider a 256-length DSTFT, an overlap of 128 (50%) results in double the amount of segments to analyse compared to the amount of segments without any overlap. Therefore, it is important to choose the optimal length of overlap weighted with the computational cost [9, p. 277].

7 Implementation

In this chapter the implementation of the system from Section 1.5 will be described. In order to implement the system, the specifications must be outlined such that it meets the requirements of the system description.

7.1 System Specification

A block diagram of the system, with a Low-pass filter (LP), is depicted on Figure 7.1.

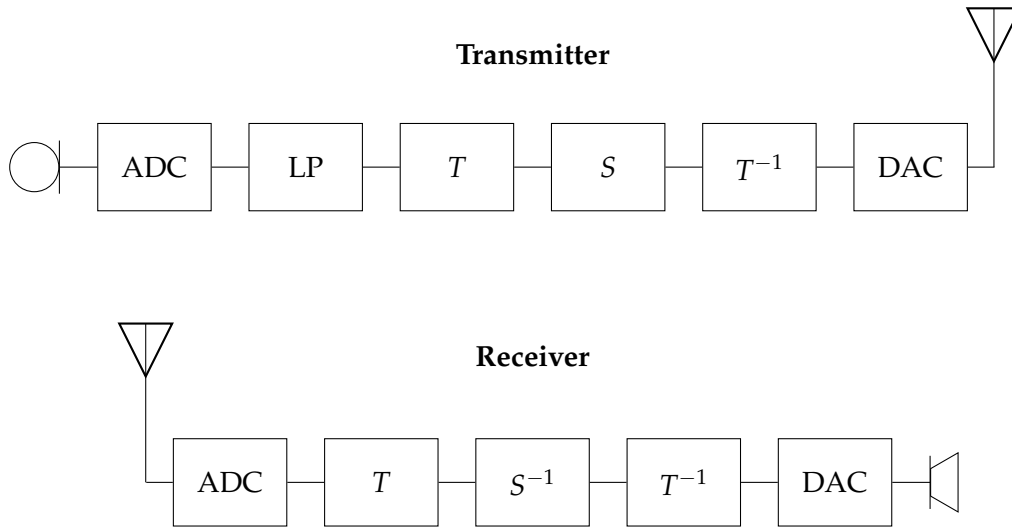


Figure 7.1: A block diagram of the system, where LP is the low-pass filter, T is the transformation, T^{-1} the inverse and S the scrambler.

The whole system has a sampling frequency of 8000 Hz, which is standard for digital telephone communication systems [1, p. 867].

Before processing the input speech signal we have decided to implement a low-pass type 1 FIR filter. The filter will have a cut-off frequency of 3000 Hz. This is because most of the speech signals frequency contents lies below this frequency, as discussed in Section 6.2. In the stopband we desire at least one order of magnitude or -20 dB attenuation, and in the passband a maximum attenuation of -1 dB. Furthermore, the width of the transition band should be 500 Hz. This leads to the following filter specifications:

- cut-off frequency at 3000 Hz,
- maximum of -1 dB attenuation at 2750 Hz,
- minimum of -20 dB attenuation at 3250 Hz.

7.2. Filter

We have decided to use the DFT and DCT as the transformations, and two different methods of scrambling, reversal and shuffle. In the reversal method the order of the coefficients are reversed and in the shuffle method the coefficients are shuffled based on a key.

7.2 Filter

In this section we will describe the implementation of the type 1 FIR filter using the window method described in Section 5.3.

The first objective is to find the desired impulse response, with respect to the filter specifications, described in Section 7.1. The ideal magnitude for a low-pass filter is given by

$$|H_d(e^{j\omega})| = \begin{cases} 1, & |\omega| \leq \omega_c \\ 0, & \omega_c < |\omega| \leq \pi \end{cases}.$$

From the specifications the digital cut-off frequency can be calculated as

$$\omega_c = T2\pi f_c = \frac{1}{8000}2\pi 3000 = \frac{3\pi}{4}.$$

Since the filter is a type 1 FIR filter the phase response is

$$\angle H(e^{j\omega}) = -\omega \frac{M}{2}.$$

Hence, the desired frequency response is

$$H_d(e^{j\omega}) = \begin{cases} e^{-j\omega M/2}, & |\omega| \leq \omega_c \\ 0, & \omega_c < |\omega| \leq \pi \end{cases}.$$

We calculate the desired impulse response by the inverse DTFT

$$\begin{aligned} h_d[n] &= \frac{1}{2\pi} \int_{-\omega_c}^{\omega_c} e^{-j\omega M/2} e^{j\omega n} d\omega \\ &= \frac{1}{2\pi} \int_{-\omega_c}^{\omega_c} e^{j(n-M/2)\omega} d\omega. \end{aligned}$$

Two cases arises from the integral, when $n \neq M/2$ and $n = M/2$. For $n \neq M/2$, Euler's identity can be applied such that

$$\begin{aligned} h_d[n] &= \frac{1}{2\pi} \int_{-\omega_c}^{\omega_c} \cos((n-M/2)\omega) + j \sin((n-M/2)\omega) d\omega \\ &= \frac{1}{2\pi} [\sin((n-M/2)\omega)]_{-\omega_c}^{\omega_c} \cdot \frac{1}{n-M/2} \\ &= \frac{1}{2\pi(n-M/2)} \cdot \{\sin(\omega_c(n-M/2)) - \sin(-\omega_c(n-M/2))\} \\ &= \frac{\sin(\omega_c(n-M/2))}{\pi(n-M/2)}. \end{aligned}$$

7.2. Filter

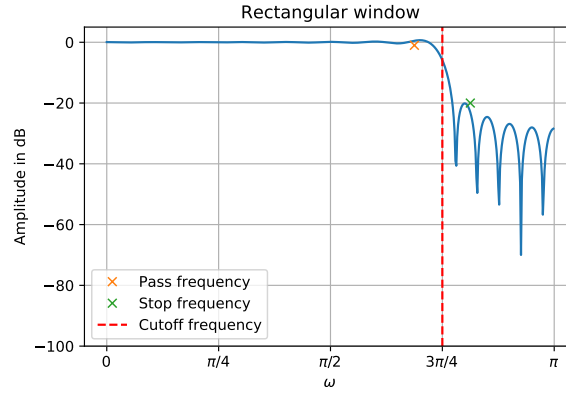
When $n = M/2$

$$\begin{aligned} h_d[M/2] &= \frac{1}{2\pi} \int_{-\omega_c}^{\omega_c} 1 d\omega \\ &= \frac{1}{2\pi} 2\omega_c \\ &= \frac{\omega_c}{\pi}. \end{aligned}$$

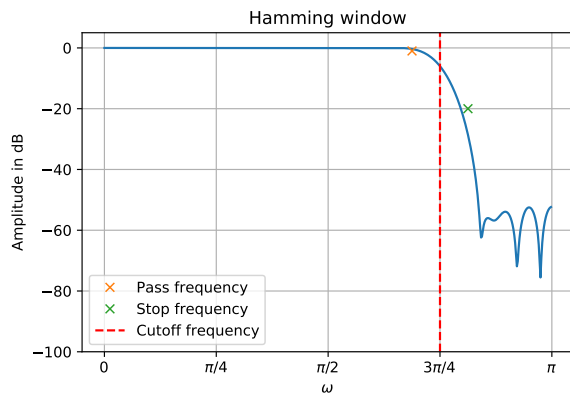
Then the ideal impulse response is made finite by applying a window with the ideal impulse response

$$h[n] = h_d[n]w[n].$$

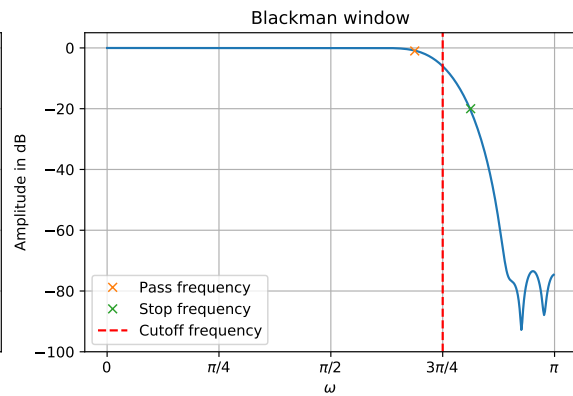
The next step is to choose a window function. On Figure 7.2 the magnitude is plotted with the rectangular, the Hamming and the Blackman window.



(a) Rectangular window with $M = 40$.



(b) Hamming window with $M = 40$.



(c) Blackman window with $M = 40$.

Figure 7.2

Figure 7.2a shows the rectangular window. The slope is narrow which leads to a short

7.2. Filter

transition band, however, the damping in the stopband is low compared to the other filters. Furthermore, there is some ripples in the passband.

Figure 7.2b shows that the Hamming window has a short transition band and few ripples.

Lastly, Figure 7.2c shows a Blackman window. It is quite the opposite to the rectangular window with a large transition band and a high damping in the stopband.

We select the Hamming window since it has a balanced transition band and stopband rippel composition, compared to the rectangular and the Blackman window.

Filter order

When choosing the filter order, it is desirable to have the lowest possible order. On Figure 7.3 the magnitude of the filter with a Hamming window is plotted for different orders.

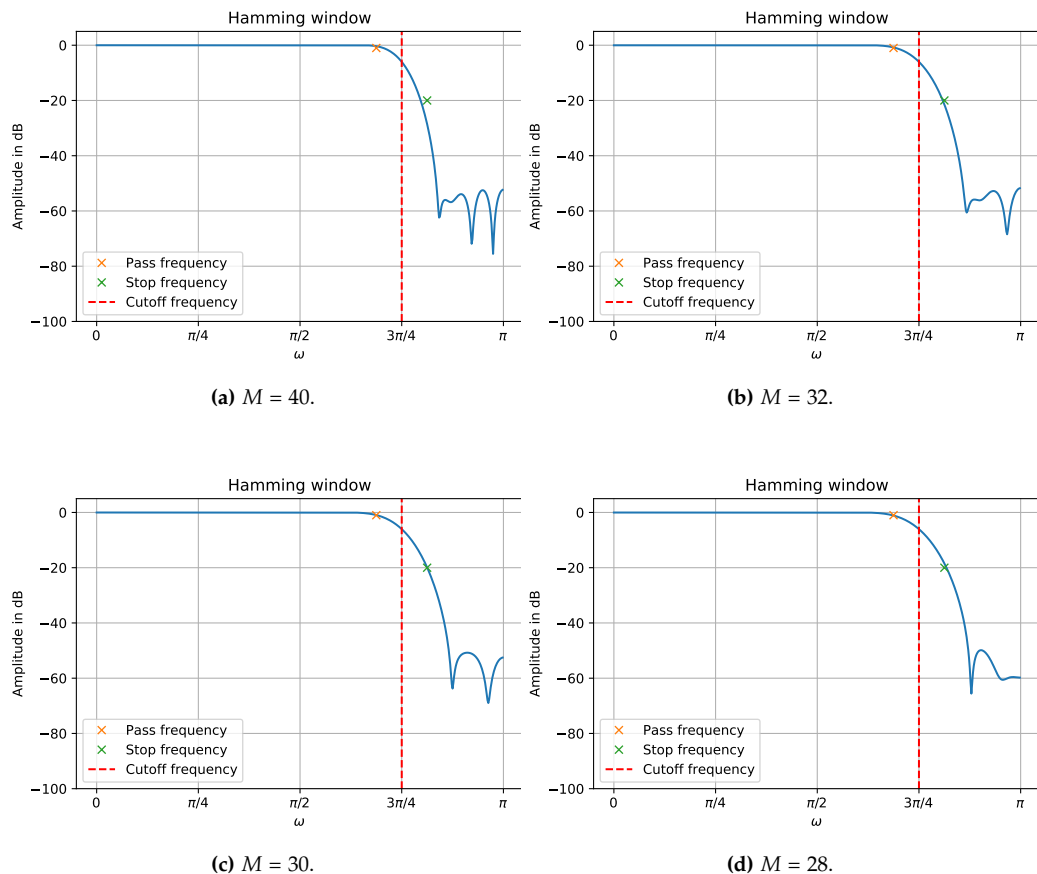


Figure 7.3: Searching for the optimal M by trial and error.

In Figure 7.3a the filter specifications are fulfilled and a lower order is thereby examined. Figure 7.3b shows $M = 32$, which is still within the minimum and maximum attenuation,

7.2. Filter

therefore two lower orders are illustrated. Figure 7.3c, $M = 30$, the magnitude passes below the passband frequency and through the stopband frequency, whereas $M = 28$ is above the stopband frequency. Thus the optimal filter order is $M = 30$.

Validation

In order to validate the designed filter, it is tested on a speech signal. Furthermore, the phase shift is plotted to ensure linear phase.

On Figure 7.4 a spectrogram of a speech signal, both unfiltered and filtered with the above described filter, is shown.

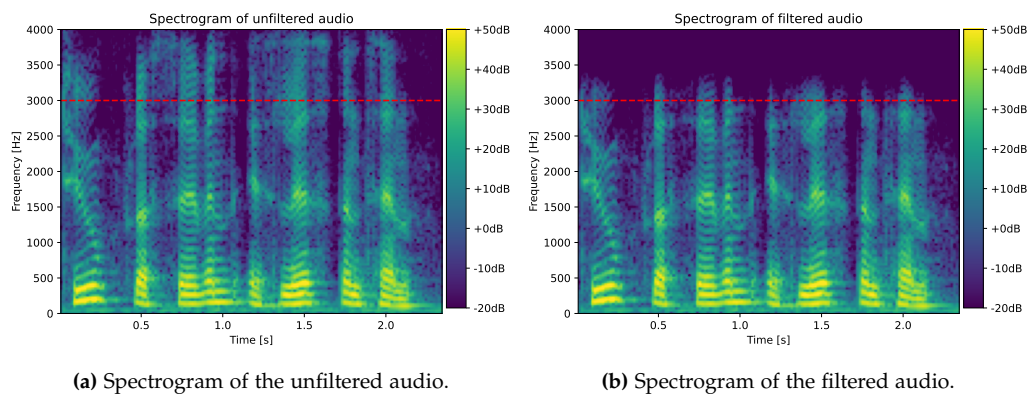


Figure 7.4

It can be seen that most of the frequency content above the cut-off of 3000 Hz is filtered.

The phase shift is plotted in Figure 7.5 showing that the implemented filter has linear phase.

7.3. Transforms and Scrambling

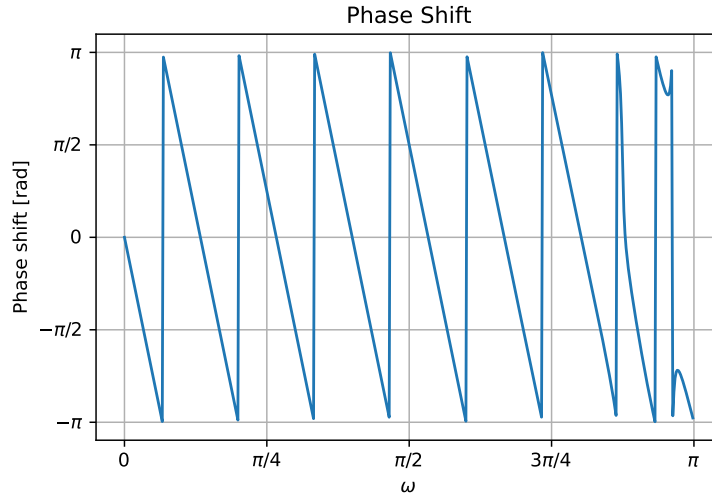


Figure 7.5: Phase shift of the filter with a Hamming window and $M = 30$.

7.3 Transforms and Scrambling

Before transforming the signal, we want to divide the speech signal into segments with lengths being a power of two, such that the FFT can be used to compute the DFT. When choosing a segment length, there are two aspects to be considered, a short contra a long window length. A short segment contains fewer samples compared to a long segment. The number of possible permutations is exponential to the amount of samples, calculated as $n!$. A large amount of samples provides more permutation options, hence the chosen segment length is 2^{11} . The segments must have an equal length, however, it is not guaranteed that an arbitrary signal is equal to an integer when divided with 2^{11} . Therefore the signal must be zero-padded before dividing it into segments as seen on Figure 7.6.

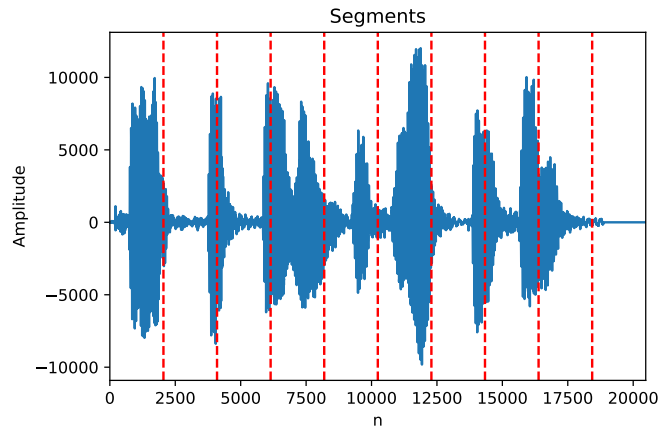


Figure 7.6: The speech signal *"Two plus seven is less than ten"*, with a segment length of 2^{11} . The segments are indicated by the red dashed lines.

7.3. Transforms and Scrambling

The concept about segments can be viewed as vectors, v , with indices of n samples. The vectors can be transformed by either the DFT or DCT which both are considered $N \times N$ matrices denoted T . The matrix-vector product is

$$x = Tv,$$

where the vector x is the transformed vector. Then x can be scrambled by various $N \times N$ permutation matrices, P . We use the two different methods of scrambling, reversal and shuffle, as seen on Figure 7.7.

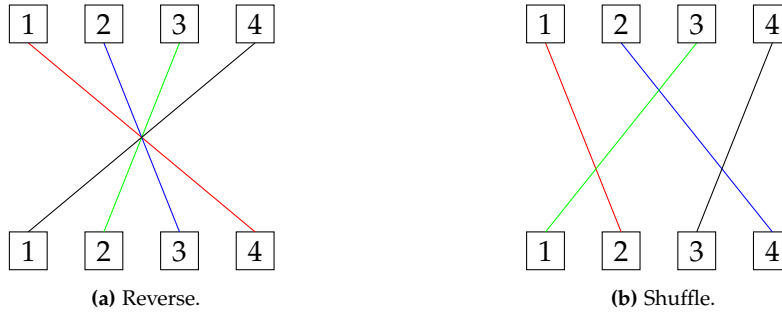


Figure 7.7: Reverse and shuffle permutation.

The reversal method simply reverse the order of the coefficients in each segment. In the shuffle method, the order of the coefficients is randomised according to a key which is needed to invert the permutation. Therefore the matrix-vector product is

$$y = Px,$$

where y is the permuted vector. Afterwards, the reorganised coefficients are transformed back to the time domain by the inverse transformation T^{-1}

$$s = T^{-1}y.$$

The final product of the transmitter from Figure 7.1 is the scrambled vector, s , which passes through the DAC and is send to the receiver. The receiver descrambles s , with an almost identical procedure, the difference being that P is replaced with P^{-1} .

On Figure 7.8 spectrograms of a speech signal are shown both unmodified, reversed scrambled, shuffled scrambled and unscrambled.

7.3. Transforms and Scrambling

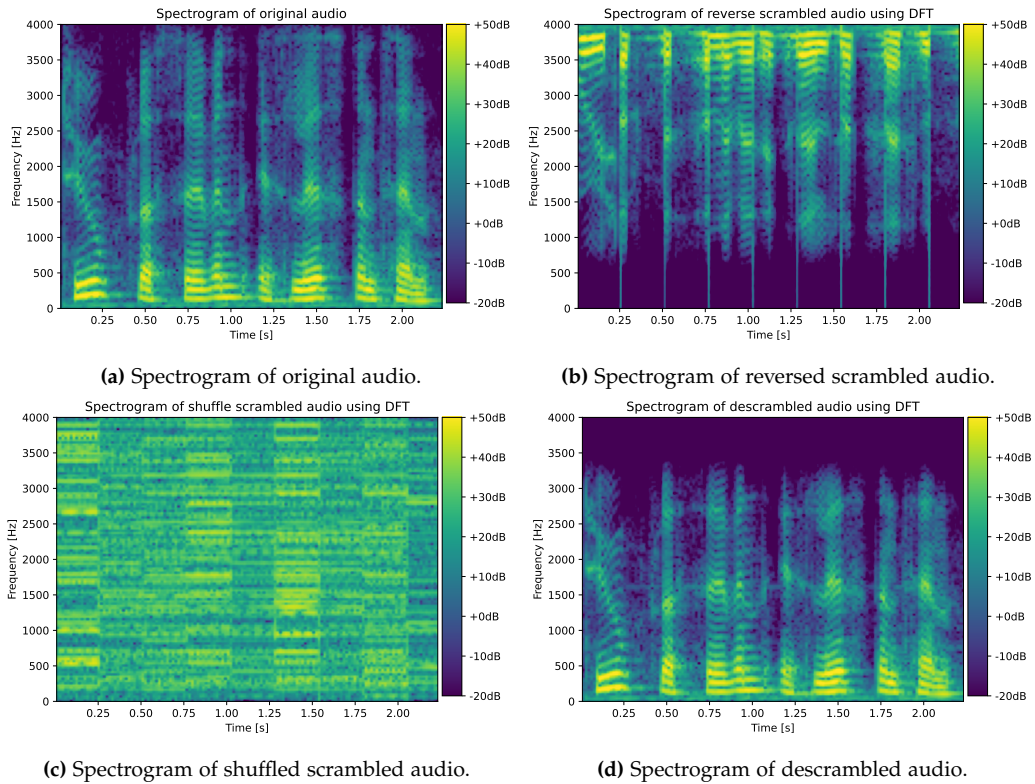


Figure 7.8

On Figure 7.8b of the reversed scrambled audio, it can be seen that the frequency content has been reversed compared to the original audio depicted on Figure 7.8a as desired. On Figure 7.8c of the shuffled scrambled audio the signal is totally unrecognizable, again as desired. Figure 7.8d of the descrambled audio, after descrambling the reversed or shuffled audio, seems identical to the original, except that almost all frequencies over 3000 Hz are damped. This is expected since the audio has been filtered with a 3000 Hz low-pass filter. The spectrogram of the descrambled audio, after descrambling the shuffled audio, were found to be almost identically to Figure 7.8d.

8 Experiment

The purpose of this experiment is to test if the scrambled and descrambled speech signals preserves the intelligibility of speech.

8.1 Test Setup

The test consists of 14 audio sequences which were played to the participants using laptop speakers. The test was performed on 10 of our peers, which was divided into two groups of five. One group for the DCT and another one for the DFT. The 14 audio sequences consists of

- two control audio sequences of speech which was not modified,
- three audio sequences of speech scrambled using the reverse permutation method,
- the same three audio sequences descrambled using the reverse permutation method.
- Three audio sequences of speech scrambled using the shuffle method
- and three audio sequences of speech descrambled using the shuffle method.

After each sequence was played, the participants were asked if they could recognise and repeat the speech signals.

The audio was from the database "Dantale II: Danske Hagerman sætninger" [5]. The data set consists of recordings of sentences with five words in Danish. The sentences consist of a name, a verb, a number, an adjective and a noun in the respectively order. An example of a sentence is "Linda låner seks flotte skabe".

8.2 Results

The results can be seen in Appendix B. Every word in each sentence corresponds to 20%. If the participants recognised the whole sentence, it is noted as 100%, and 0% if none of the words was recognised. Some participants only recognised four out of five words, these were noted as 80%.

For the control tests, all 10 participants recognised every word except one participant, who missed one word in the first control sentence. None of the participants recognised the scrambled sentences. However, the participants had trouble recognising the descrambled sentences. Especially, the sentence "Ulla får fjorten hvide jakker". Five out of ten participants could not recognise the word "hvide". In some cases, the participants misinterprets words that sound similar, for instance "vandt" with "fandt". In other cases, where the participants failed to understand a word, they substituted a word that also made sense in that context, for instance "hvide jakker" became "læder jakker".

8.3. Sources of Errors

The results also showed that the participants had more trouble recognising the descrambled speech signals, which had been shuffled, compared to the reversed. Six out of ten participants had trouble recognising the shuffled speech signals, while four out of ten had trouble recognising the reversed speech signals.

8.3 Sources of Errors

In this section we will discuss some sources of the errors in our experiment.

Some errors in the experiment stems from the equipment which was used. The room is far from sound proof and therefore the participants could get distracted by noise from outside the room. Another error is the quality of the speakers and the reverb from the walls. We used laptop speakers from approximately 1 meter away from the participant, and the participant was seated close to the wall, which could lead to some distortion such that the participant would have trouble recognising the words. All this could have been avoided, if headphones were used instead of laptop speakers.

9 Discussion

The purpose of this project was to implement a system with the ability to scramble and descramble a speech signal, while preserving the intelligibility of speech. An experiment was therefore conducted to test the intelligibility. In this project we focus on comparison between the DCT and DFT as well as the reverse and shuffle method.

An experiment was conducted to test which transformation was the most recognisable the DCT or DFT. Here both transforms were found equally recognisable.

To discuss the efficiency of the two transforms. We found in Section 3.6 that the computational cost of the DCT were the same as for the DFT, if we count the cost of complex arithmetic the same as for real numbers. Therefore, the main difference between the DCT and DFT is the fact that the DCT maps a real sequence to a real sequence compared to the DFT. However, with the DFT we have the possibility to compute DFT using the FFT, which we found in Example 3.28 to be more efficient compared to the DFT and DCT.

Lastly, we experimented with two methods of permutation, the reversed and shuffle method, to test if the scrambled and descrambled speech signals preserves the intelligibility of speech. For both methods, the results showed that the scrambled speech signals was equally unrecognisable. However, for the descrambled speech signals the shuffle method was less recognisable than the reversed method, though the difference is not significant. To conduct a more sufficient experiment, more participants would have resulted in a larger data set, such that the difference between the descrambled speech signals for the two methods could have been investigated further. Another way of comparing the reverse and shuffle method, is to consider the safety of the methods. The reverse method reverses the order of the coefficients compared to the shuffle method, which randomise the order of the coefficients according to a key. Therefore the reversed method lacks the same security as the shuffle method, since the coefficients is ordered in the same way every time.

10 Conclusion

In this project, we have presented the theory of discrete-time systems and Fourier analysis. Applying these theories, we have designed a discrete-time low-pass filter to implement onto our system. The system scrambles and descrambles a speech signal. To test the intelligibility, an experiment with this purpose had been conducted.

The two transforms, the DCT and the DFT, was compared to conclude that both transforms performed equally sufficient. However, we found that the DFT has a lower computational cost than the DCT.

The final results of the experiment, stems from when the two different methods of permutation were compared. For the descrambled speech signals, the shuffle method proved to be slightly less intelligibility when compared to reversed method. However, the shuffle method is considered the safest permutation method, because it permutes according to a key opposed to the reverse method.

Therefore, we conclude that both the DFT and DCT, with either the reverse and shuffle permutation, preserve the intelligibility of speech.

Bibliography

- [1] Ronald W. Schafer Alan v. Oppenheim. Discrete-Time Signal Processing. English. 3. ed. Pearson, 2014.
- [2] Glen Ballou. Handbook for sound engineers. English. 5. ed. Focal Press, 2015.
- [3] Saleh Faruque. Radio frequency modulation made easy. Springer, 2017.
- [4] Gerald B. Folland. Fourier Analysis and Its Applications. English. 4. ed. American Mathematical Society, 1992. ISBN: 978-0-8218-4790-9.
- [5] Martin Hansen and Carl Ludvigsen. Dantale II: Danske Hagerman sætninger. 2001.
- [6] Philip Lieberman and Sheila E Blumstein. Speech physiology, speech perception, and acoustic phonetics. Cambridge University Press, 1988.
- [7] Volker Mehrmann and Jörg Liesen. Linear Algebra. English. Springer, 2015. ISBN: 978-3-319-24344-3.
- [8] John G. Proakis. Digital signal processing : principles, algorithms, and applications. English. 3rd ed. Prentice-Hall International, 1996. ISBN: 0133737624.
- [9] M.W. Trethaway. "Window and overlap processing effects on power estimates from spectra". In: Mechanical Systems and Signal Processing 14.2 (2000), pp. 267–278. ISSN: 0888-3270. DOI: <https://doi.org/10.1006/mssp.1999.1274>. URL: <https://www.sciencedirect.com/science/article/pii/S0888327099912748>.
- [10] Martin Vetterli, Jelena Kovacevic, and Vivek K. Goyal. Foundations of Signal Processing. English. 1. ed. Cambridge Univ. Press, 2014.
- [11] Hugh D. Young and Roger A. Freedman. University Physics: with modern physics. English. 12. ed. Addison Wesley, 2008. ISBN: 9780321501301.

A Permutation

A permutation can be perceived as a rearrangement of the elements in a list.

Definition A.1 (Permutation)

Let $n \in \mathbb{N}$ be given. A permutation of a set $X = \{1, 2, \dots, n\}$ is a bijective map

$$\sigma : X \rightarrow X.$$

The set of all permutations of $X = \{1, 2, \dots, n\}$ is denoted S_n . [7, p. 81]

There is $n!$ permutations of a set X with n elements. The two-rowed notation of a permutation is a list containing all elements of X and their corresponding value after the permutation

$$\sigma = \begin{pmatrix} 1 & 2 & \dots & n \\ \sigma(1) & \sigma(2) & \dots & \sigma(n) \end{pmatrix}.$$

The following example illustrates a permutation of a list X .

Example A.2 (Permutation)

A permutation of the set $X = \{1, 2, 3, 4\}$ where

$$\sigma(1) = 2,$$

$$\sigma(2) = 4,$$

$$\sigma(3) = 1,$$

$$\sigma(4) = 3,$$

is noted by the two-rowed notation as

$$\sigma = \begin{pmatrix} 1 & 2 & 3 & 4 \\ 2 & 4 & 1 & 3 \end{pmatrix}.$$

As seen in Example A.2 a permutation is determined by a rearrangement of the elements in the list X , and the rearrangement thereby determines a permutation σ . Thus, permutation and rearrangement are two perceptions of the same thing. Permutations can also be mapping elements to themselves, hence the identity permutation is presented.

Definition A.3 (Identity Permutation)

The identity permutation is a map that maps every element of a set $X = \{1, 2, \dots, n\}$ to itself

$$\epsilon = \begin{pmatrix} 1 & 2 & \dots & n \\ 1 & 2 & \dots & n \end{pmatrix}.$$

The identity permutation is a fundamental permutation. Since the permutation is a bijective map the inverse exists. To calculate the inverse, composition of permutations is first introduced.

Definition A.4 (Composition of permutations)

The composition of two permutations π and σ on a set $X = \{1, 2, \dots, n\}$ is

$$(\pi \circ \sigma)(X) = \pi(\sigma(X)).$$

And in two-rowed notation

$$\pi \circ \sigma = \begin{pmatrix} 1 & 2 & \dots & n \\ (\pi \circ \sigma)(1) & (\pi \circ \sigma)(2) & \dots & (\pi \circ \sigma)(n) \end{pmatrix}.$$

The application of compositions of permutations can be shown in the following example.

Example A.5 (Composition of Permutations)

Let π and σ be two permutations

$$\pi = \begin{pmatrix} 1 & 2 & 3 \\ 2 & 3 & 1 \end{pmatrix}, \quad \sigma = \begin{pmatrix} 1 & 2 & 3 \\ 1 & 3 & 2 \end{pmatrix}.$$

Then the composition of π and σ is

$$\begin{aligned} \pi \circ \sigma &= \begin{pmatrix} 1 & 2 & 3 \\ 2 & 3 & 1 \end{pmatrix} \begin{pmatrix} 1 & 2 & 3 \\ 1 & 3 & 2 \end{pmatrix} \\ &= \begin{pmatrix} 1 & 2 & 3 \\ 2 & 1 & 3 \end{pmatrix}. \end{aligned}$$

The composition is used to find the inverse permutation.

Definition A.6 (Inverse Permutation)

Let σ be a permutation on the set $X = \{1, 2, \dots, n\}$. The inverse σ^{-1} satisfying

$$\sigma \circ \sigma^{-1} = \sigma^{-1} \circ \sigma = \epsilon.$$

is called the inverse of σ .

[7, p. 82]

In the two-rowed notation, the inverse is obtained by interchanging the rows and then the columns such that the first row is ordered in increasing order. This can be seen in the following example.

Example A.7 (Inverse Permutation)

Take the two-rowed permutation from Example A.2

$$\sigma = \begin{pmatrix} 1 & 2 & 3 & 4 \\ 2 & 4 & 1 & 3 \end{pmatrix}.$$

The inverse permutation is obtained by interchanging the rows

$$\sigma^{-1} = \begin{pmatrix} 2 & 4 & 1 & 3 \\ 1 & 2 & 3 & 4 \end{pmatrix}$$

and then interchanging the columns such that the first row is in increasing order

$$= \begin{pmatrix} 1 & 2 & 3 & 4 \\ 3 & 1 & 4 & 2 \end{pmatrix}.$$

To verify this is correct, we can check that $\sigma\sigma^{-1} = \epsilon$

$$\begin{aligned} \begin{pmatrix} 1 & 2 & 3 & 4 \\ 2 & 4 & 1 & 3 \end{pmatrix} \circ \begin{pmatrix} 1 & 2 & 3 & 4 \\ 3 & 1 & 4 & 2 \end{pmatrix} &= \begin{pmatrix} 1 & 2 & 3 & 4 \\ \sigma(3) & \sigma(1) & \sigma(4) & \sigma(2) \end{pmatrix} \\ &= \begin{pmatrix} 1 & 2 & 3 & 4 \\ 1 & 2 & 3 & 4 \end{pmatrix} \\ &= \epsilon. \end{aligned}$$

Another application method of permutation is the permutation matrix.

Definition A.8 (Permutation Matrix)

A matrix $P \in \mathbb{R}^{n \times n}$ is a permutation matrix, if it has exactly one unit in every row and column while all other entries are zero.

[7, p. 49]

The permutation matrix exchange rows or columns of matrices or vectors. The following example shows the application of the permutation matrix.

Example A.9 (Permutation Matrix)

The corresponding permutation matrix P of the permutation $\sigma = \begin{pmatrix} 1 & 2 & 3 & 4 \\ 2 & 4 & 1 & 3 \end{pmatrix}$ is

$$P = \begin{bmatrix} 0 & 1 & 0 & 0 \\ 0 & 0 & 0 & 1 \\ 1 & 0 & 0 & 0 \\ 0 & 0 & 1 & 0 \end{bmatrix}.$$

It is possible to obtain the permutation from the permutation matrix by calculating the matrix vector product of P and the first row in σ

$$\begin{bmatrix} 0 & 1 & 0 & 0 \\ 0 & 0 & 0 & 1 \\ 1 & 0 & 0 & 0 \\ 0 & 0 & 1 & 0 \end{bmatrix} \begin{bmatrix} 1 \\ 2 \\ 3 \\ 4 \end{bmatrix} = \begin{bmatrix} 2 \\ 4 \\ 1 \\ 3 \end{bmatrix}$$

the resulting column vector transposed equals the second row in σ .

B Result from experiment

| Reverse | Sentences | Person 1 | Person 2 | Person 3 | Person 4 | Person 5 |
|--------------|-------------------------------|----------|----------|----------|----------|----------|
| Control 1 | Ingrid finder syv røde huse | 100% | 100% | 100% | 100% | 100% |
| Control 2 | Mikael ejer tyve pæne ringe | 100% | 100% | 100% | 100% | 100% |
| Scramble 3 | Linda låner seks flotte skabe | 0% | 0% | 0% | 0% | 0% |
| Descramble 3 | Linda låner seks flotte skabe | 100% | 100% | 100% | 100% | 100% |
| Scramble 4 | Ulla får fjorten hvide jakker | 0% | 0% | 0% | 0% | 0% |
| Descramble 4 | Ulla får fjorten hvide jakker | 80% | 80% | 80% | 100% | 100% |
| Scramble 5 | Niels solgte ti store masker | 0% | 0% | 0% | 0% | 0% |
| Descramble 5 | Niels solgte ti store masker | 100% | 100% | 100% | 100% | 100% |

| Shuffle | | | | | | |
|--------------|--------------------------------|------|------|------|------|------|
| Scramble 6 | Henning ser ni smukke planter | 0% | 0% | 0% | 0% | 0% |
| Descramble 6 | Henning ser ni smukke planter | 100% | 80% | 100% | 100% | 100% |
| Scramble 7 | Anders vandt otte sjove gaver | 0% | 0% | 0% | 0% | 0% |
| Descramble 7 | Anders vandt otte sjove gaver | 80% | 100% | 100% | 100% | 80% |
| Scramble 8 | Kirsten købte tre nye blomster | 0% | 0% | 0% | 0% | 0% |
| Descramble 8 | Kirsten købte tre nye blomster | 100% | 80% | 100% | 100% | 100% |

Table B.1: Results from experiment with the DCT.

| Reverse | Sentences | Person 6 | Person 7 | Person 8 | Person 9 | Person 10 |
|--------------|-------------------------------|----------|----------|----------|----------|-----------|
| Control 1 | Ingrid finder syv røde huse | 100% | 100% | 100% | 100% | 80% |
| Control 2 | Mikael ejer tyve pæne ringe | 100% | 100% | 100% | 100% | 100% |
| Scramble 3 | Linda låner seks flotte skabe | 0% | 0% | 0% | 0% | 0% |
| Descramble 3 | Linda låner seks flotte skabe | 100% | 100% | 100% | 100% | 100% |
| Scramble 4 | Ulla får fjorten hvide jakker | 0% | 0% | 0% | 0% | 0% |
| Descramble 4 | Ulla får fjorten hvide jakker | 100% | 80% | 100% | 100% | 100% |
| Scramble 5 | Niels solgte ti store masker | 0% | 0% | 0% | 0% | 0% |
| Descramble 5 | Niels solgte ti store masker | 100% | 100% | 100% | 100% | 100% |

| Shuffle | | | | | | |
|--------------|--------------------------------|------|------|------|------|------|
| Scramble 6 | Henning ser ni smukke planter | 0% | 0% | 0% | 0% | 0% |
| Descramble 6 | Henning ser ni smukke planter | 100% | 100% | 100% | 100% | 100% |
| Scramble 7 | Anders vandt otte sjove gaver | 0% | 0% | 0% | 0% | 0% |
| Descramble 7 | Anders vandt otte sjove gaver | 80% | 100% | 100% | 80% | 100% |
| Scramble 8 | Kirsten købte tre nye blomster | 0% | 0% | 0% | 0% | 0% |
| Descramble 8 | Kirsten købte tre nye blomster | 80% | 100% | 80% | 100% | 0% |

Table B.2: Results from experiment with the DFT.